Numerical Methods for Continuous Time Mean Variance Type Asset Allocation

by

Jian Wang

A thesis
presented to the University of Waterloo
in fulfillment of the
thesis requirement for the degree of
Doctor of Philosophy
in
Computer Science

Waterloo, Ontario, Canada, 2010

I hereby declare that I am the sole author of this thesis. This is a true copy of the thesis, including any required final revisions, as accepted by my examiners.

I understand that my thesis may be made electronically available to the public.

Abstract

Many optimal stochastic control problems in finance can be formulated in the form of Hamilton-Jacobi-Bellman (HJB) partial differential equations (PDEs). In this thesis, a general framework for solutions of HJB PDEs in finance is developed, with application to asset allocation.

The numerical scheme has the following properties: it is unconditionally stable; convergence to the viscosity solution is guaranteed; there are no restrictions on the underlying stochastic process; it can be easily extended to include features as needed such as uncertain volatility and transaction costs; and central differencing is used as much as possible so that use of a locally second order method is maximized.

In this thesis, continuous time mean variance type strategies for dynamic asset allocation problems are studied. Three mean variance type strategies: pre-commitment mean variance, time-consistent mean variance, and mean quadratic variation, are investigated. The numerical method can handle various constraints on the control policy. The following cases are studied: allowing bankruptcy (unconstrained case), no bankruptcy, and bounded control. In some special cases where analytic solutions are available, the numerical results agree with the analytic solutions.

These three mean variance type strategies are compared. For the allowing bankruptcy case, analytic solutions exist for all strategies. However, when additional constraints are applied to the control policy, analytic solutions do not exist for all strategies. After realistic constraints are applied, the efficient frontiers for all three strategies are very similar. However, the investment policies are quite different. These results show that, in deciding which objective function is appropriate for a given economic problem, it is not sufficient to simply examine the efficient frontiers. Instead, the actual investment policies need to be studied in order to determine if a particular strategy is applicable to specific investment problem.

Acknowledgements

First of all, I would like to thank Prof. Peter Forsyth who has been my supervisor since 2003 when I started my MMath. During these years, I am always amazed by his high-quality and high-efficiency work, encouraged by his enthusiasm on research, and inspired by his sharp mind. What has impressed me most is that Professor Forsyth acts not only as a leader or a supervisor, but also as a coworker. He always involves into my research so deeply that he can quickly point out the flaws of my work, give me creative ideas, and direct me to the right trace. No words can fully express my gratitude for his abundant support and flawless guidance. It is so lucky of me to have Prof. Forsyth as my supervisor for my graduate study.

I would like to thank my committee members for the time they have dedicated to reading and reviewing my thesis: Prof. Yuying Li, Prof. Justin Wan, Prof. Ken Vetzal, and my external examiner Prof. Anita Mayo.

I would also like to thank Prof. Yuying Li, Prof. Justin Wan, Prof. Bruce Simpson, and Prof. Jeff Orchard for many discussions and interesting chats.

On the personal side, I owe a lifetime of gratitude to my parents, Xiangyang Wang and Xiaofeng Guo, who are always there ready to encourage me and support me. I owe countless thanks to my wife, Lei Yin, for her care and love. She shared all the joys and sorrows with me in last five years.

My life at UW is a happy journey. I would like to thank all my friends at Waterloo, especially Huaning Nie, Zhuliang Chen, Rong Wang, Stephen Tse, Tiantian Bian, Yi Zhang, Wenjie Xiao, Bo Wang, Dong Han, and Zhirong Li for their friendships and help. Special thanks to Yuli Ye, Yu Guan, Zhenming Jiang, Xun Fan, and Sheng Zhang for fighting together against school work for countless sleepless nights in DC and MC. Many thanks to my colleagues in Scicom lab, both past and present, especially Shannon Kennedy, Amélie Bélanger, Yann d'Halluin, Simon Clift, Amir Memartoluie, Lei Zhu, Ruonan Li, and Lin Xu for their warmhearted help and interesting chats.

Contents

List of Tables

List of Figures

Chapter 1

Introduction

1.1 Overview

There are a number of financial models which result in nonlinear Hamilton-Jacobi-Bellman (HJB) partial differential equations (PDEs). These problems usually arise in the context of optimal stochastic control. Some examples of these HJB type equations include: transaction cost/uncertain volatility models [48, 3, 64], passport options [2, 68], unequal borrowing/lending costs [14], large investor effects [1], risk control in re-insurance [58], pricing options and insurance in incomplete markets using an instantaneous Sharpe ratio [76, 56, 12], minimizing ruin probability in insurance[67, 20], and optimal consumption [13, 23]. A survey article on the theoretical aspects of this topic is given in [63].

In many cases, classical solutions to these nonlinear PDEs do not exist, and we need to solve them numerically. In terms of existing solution methods, Markov chain [46, 19] and PDE [36, 69, 76, 72, 27] based approaches are the two basic threads of literature concerning controlled HJB equations. There are also other approaches including binomial lattice based methods [31] and simulation based methods [34, 22]. A Markov chain approximation is similar to the usual binomial lattice, which is equivalent to an explicit finite difference method. These methods are well-known to suffer from timestep limitations due to stability considerations. Simulation based methods can handle multi-dimensional problems, but they have poor accuracy and have difficulty with non bang-bang type controls.

A more recent approach is based on numerical PDE methods. Since there is usually more than one solution for a nonlinear PDE, a key aspect of this approach is to ensure convergence to the financially relevant solution, which in this case is the viscosity solution [29]. As demonstrated in [64], seemingly reasonable discretization methods can converge to non-viscosity solutions. The theory of viscosity solutions is described in [29]. As pointed out in [10, 5], in order to guarantee convergence to the viscosity solution, the discrete scheme must be pointwise consistent, l_∞ stable and monotone. Unconditionally monotone implicit methods are described in [8]. For optimal stochastic control problems, these methods lead to a nonlinear set of discretized equations which must be solved at each timestep.

It is common in the PDE literature [8] to suggest relaxation type methods for solution of the nonlinear algebraic equations at each timestep. However convergence of relaxation methods can be very slow for fine grids. A Newton-type iteration scheme [65, 36] can also be used to solve this problem. At each iteration, a linear set of equations are solved. Since this scheme can be regarded as a variant of Policy iteration for infinite horizon Markov chains, the convergence proof of the iteration is similar to the proof of convergence for Policy iteration [46]. In practice, this scheme typically converges quickly. As part of our program to solve optimal asset allocation problems, we first develop numerical methods for controlled HJB equations in finance with the following properties:

- The methods are guaranteed to converge to the viscosity solution.
- There should be no timestep limitations due to stability considerations.
- There should be no restrictions on the underlying stochastic process, e.g. geometric Brownian motion, jump diffusion, or regime switching can be easily implemented.
- It should be possible to easily extend the models to include features as needed, for example, uncertain volatility, bid-ask spread, transaction costs and so on.
- The methods should be at least efficient as other existing methods.

In general, there are two types of control for optimal stochastic control problems: bang-bang controls and non bang-bang controls. Controls of bang-bang type can only take values from a finite set. Controls of non bang-bang type take values from an infinite set. Our numerical methods should be able to handle both types of control. To demonstrate the properties of our methods, in Chapter 3, we use two specific examples, passport options and a utility optimization problem for a defined contribution pension plan. These methods are then used as building blocks for solving mean variance type optimal asset allocation strategies for a defined contribution pension plan (see Chapters 4 – 7).

1.2 Contributions

We first develop a general framework to solve HJB PDEs in finance.

Monotonicity is one of important properties which is required to ensure convergence to the viscosity solution. A monotone scheme is usually constructed by using a positive coefficient method [46, 62, 8, 36]. In order to ensure a positive coefficient method, the standard method for discretizing HJB PDEs uses forward/backward differencing for the drift term. The choice of forward or backward differencing depends on the control variable. This has the disadvantage that the truncation error in the space-like direction is only first order.

We develop a positive coefficient method with maximum use of central differencing. Our work in this area makes the following contributions (see Chapter 3):

- We develop a fully implicit finite difference scheme to solve stochastic control problems in finance. Our scheme use central differencing as much as possible, so that use of locally second order method is maximized (for smoothly varying grid sizes).

- We show that our discrete scheme is pointwise consistent, l_∞ stable and monotone so that convergence to viscosity solution is guaranteed.

- Our method can handle both bang-bang controls and non bang-bang controls.

- Our method satisfies the properties listed in Section 1.1.

- In general, when central differencing is used as much as possible, the local objective function at each grid node is now a discontinuous function of the control. We show that convergence of the iterative method for solution of the discrete equations can still be guaranteed, even if the local objective function is a discontinuous function of the control.

- Numerical examples show that the scheme using central differencing as much as possible has a better convergence rate than the standard method (which uses forward/backward differencing only).

We then consider a popular stochastic control problem: optimal dynamic asset allocation. In the existing literature, this problem is usually formulated in terms of a utility function approach [71, 41]. However, in practice, it is not clear how to decide which utility function an individual or an institution would prefer. Moreover, since the tradeoff between the risk and the expected return is implicitly contained in the utility function, the optimal investment decision lacks intuitive interpretation.

In this thesis, we apply the mean variance approach to the optimal dynamic asset allocation problem. We use the defined contribution pension plan problem as a prototypical example. The mean variance approach was first studied by Markowitz in the 1950s [53, 54] for modern portfolio selection analysis in a single period. In Markowitz's model, risk is quantified by using variance, so that investors can maximize their expected return after specifying a risk level, or minimize their risk (variance) after specifying an expected return. Although there are many difficulties [26] in solving variance minimization problems, Markowitz's idea has been extended to multiperiod problems [57, 40, 39, 33, 66, 78, 49]. One advantage of the mean variance approach is that the results can be easily interpreted in terms of an efficient frontier, in which the tradeoff between the risk and the expected return can be clearly demonstrated, so that an investor can intuitively choose her expected return and risk level.

We use three mean variance type strategies to solve this problem (see Chapters 4 – 7): pre-commitment mean variance, time-consistent mean variance, and mean quadratic variation. The mathematical models for these asset allocation problems are in the form of HJB PDEs. We applied the fully implicit method with maximum use of central differencing for solving these HJB PDEs. Our contributions in this area are as follows:

- For time-consistent and mean quadratic variation strategies, dynamic programming can be directly applied in order to construct the efficient frontiers (see Chapters 5 and 6). However, it is well-known that dynamic programming cannot be used in straightforward fashion for the pre-commitment strategy. To avoid this difficulty, we follow the method in [78, 49] which embeds the original optimization problem into a class of auxiliary stochastic linear-quadratic (LQ) problems, which can be solved in terms of dynamic programming (see Chapter 4).

- For the pre-commitment and mean quadratic variation strategies, a fully implicit discretization method is developed for the nonlinear HJB PDE. Under the assumption that the HJB equation satisfies a strong comparison property, our methods are guaranteed to converge to the viscosity solution of the HJB equation. In addition, the policy iteration scheme used to solve the nonlinear algebraic equations at each timestep is globally convergent. Our fully implicit method has no timestep size restrictions due to stability considerations (see Chapters 4 and 6).

- For the time-consistent strategy, our numerical method is based on a piecewise constant policy technique in [45]. In this case, because the time-consistent problem can be formulated as a system of HJB differential algebraic equations, this falls outside the viscosity solution theory in [45]. Hence we have no formal proof of convergence of our method. Nevertheless, our technique does converge to analytic solutions where available (see Chapter 5).

- For all three strategies, by solving the HJB PDE and related linear PDEs, we develop an algorithm for constructing the mean variance type efficient frontiers (see Chapters 4 - 6).

- Our numerical scheme (for all three strategies) can well handle various constraints on the optimal policy. In particular, we consider three types of constraints: allowing bankruptcy (unconstrained case), no bankruptcy and bounded control. We compare the efficient frontiers for various constraints. From a practical point of view, we observe that the addition of realistic constraints can completely alter some of the properties of the mean variance solution compared to the unconstrained control case (see Chapters 4 - 6).

- We make a comparison of the three mean variance type strategies. We compare both their efficient frontier solutions and their control policies. After realistic constraints are applied, the efficient frontiers for all three strategies are very similar. However, the investment policies are quite different. This suggests that the choice among various strategies cannot be made by only examining the efficient frontier, but rather should be based on the qualitative behavior of the optimal policies (see Chapter 7).

To the best of our knowledge, the results for constrained mean variance asset allocation (for all three variants) are new.

1.3 Economic Significance

As stated earlier, mean variance type criteria are popular due to their intuitive interpretation. However, this thesis demonstrates that we now have reliable methods for solution of constrained optimal asset allocation problems using mean variance (pre-commitment, time-consistent and mean quadratic variation) criteria. It is an interesting economic question as to which of these criteria should be used. This is, however, beyond the scope of this thesis.

1.4 Outline

The rest of the thesis is arranged as follows. In Chapter 2, we introduce two examples of stochastic control problems in finance. In Chapter 3, we develop a numerical scheme for solving HJB PDEs in finance, which uses central differencing as much as possible so that use of locally second order method is maximized. In Chapters 4, 5 and 6, we apply the numerical scheme developed in Chapter 3 for solving dynamic asset allocation problems, by using pre-commitment mean variance, time-consistent mean variance, and mean quadratic variation strategies respectively. We make a comparison of the three mean variance type strategies in Chapter 7. Finally, conclusions are drawn in Chapter 8.

Chapter 2

Two Examples of Optimal Stochastic Control Problems

As introduced in Chapter 1, there are many optimal stochastic control problems in finance. In this thesis, in order to demonstrate the properties of our methods, we use two specific problems. These problems are pricing passport options [2], and an optimal dynamic asset allocation strategy for a defined benefit pension plan [21].

2.1 Passport Options

Our first example is pricing passport options. Passport options are financial derivative contracts which allow the holder to take a profit from a trading account while obligating the writer to cover losses [2, 68].

Let S be the underlying asset price which follows the stochastic process

$$dS = \mu S \, dt + \sigma S \, dZ \ , \tag{2.1.1}$$

where dZ is the increment of a Wiener process, σ is volatility, μ is the drift rate. The holder is allowed to hold long and short positions in the underlying asset S at any time during the option life time, say T. Let q denote the number of shares of the underlying the holder holds at time t, $0 \leq t \leq T$. $|q|$ is limited to an amount C, i.e. $|q| \leq C$. At maturity T, the holder keeps any net gain, while any loss is covered by the writer.

2.2 Defined Contribution Pension Plan

The second example in this thesis concerns an optimal dynamic asset allocation strategy for a defined contribution pension plan. A traditional asset allocation strategy for a defined contribution pension plan is *deterministic lifestyling*. Initially, the contributions of the plan are invested entirely in equities. Beginning on a predetermined date, say N

years prior to retirement, the contributions are switched into bonds at a rate of $1/N$ per year. Then, all assets are invested in bonds by the date of retirement. Deterministic lifestyling can reduce the losses of the plan in case of a sudden fall in the stock market just before the date of retirement. This strategy is simple and widely used. However, obviously it is not the optimal strategy.

We will use two main approaches to determine the optimal strategy: the utility function approach (see Chapter 3) and the mean variance approach (see Chapters 4 – 7). For the utility function approach, the strategy is optimal in the sense of maximizing expected utility [71, 41]. For the mean variance approach, the strategy is optimal in the sense of an efficient frontier solution.

For both approaches, the optimal strategy can be determined in terms of the investor's wealth (Section 2.2.1) or her wealth-to-income ratio (Section 2.2.2).

2.2.1 Wealth Case

It is common to determine the optimal strategy in terms of the investor's final wealth. We will refer to this problem in the following as the *wealth* case.

Suppose there are two assets in the market: one is risk free (e.g. a government bond) and the other is risky (e.g. a stock index). The risky asset S follows the stochastic process

$$dS = (r + \xi_1\sigma_1)S\ dt + \sigma_1 S\ dZ_1\ , \tag{2.2.1}$$

where dZ_1 is the increment of a Wiener process, σ_1 is volatility, r is the interest rate, ξ_1 is the market price of risk (or Sharpe ratio) and the stock drift rate can then be defined as $\mu_S = r + \xi_1\sigma_1$. Suppose that the plan member continuously pays into the pension plan at a constant contribution rate π in the unit time. Let $W(t)$ denote the wealth accumulated in the pension plan at time t, let p denote the proportion of this wealth invested in the risky asset S, and let $(1-p)$ denote the fraction of wealth invested in the risk free asset. Then,

$$\begin{aligned} dW &= [(r + p\xi_1\sigma_1)W + \pi]dt + p\sigma_1 W dZ_1\ , \\ W(t=0) &= \hat{w}_0 \geq 0\ . \end{aligned} \tag{2.2.2}$$

Let $p^*(t,w)$ denote the optimal strategy/policy. In the wealth case, we want to determine $p^*(t,w)$ in terms of the investor's final wealth.

Remark 2.1. *The classic multi-period portfolio selection problem can be stated as the following: given some investment choices (assets) in the market, an investor seeks an optimal asset allocation strategy over a period T with an initial wealth $\hat{w}_0$. This problem has been widely studied [55, 78, 49, 51, 15, 50]. We still assume there is one risk free bond and one risky asset in the market. In this case,*

$$\begin{aligned} dW &= (r + p\xi_1\sigma_1)W dt + p\sigma_1 W dZ_1\ , \\ W(t=0) &= \hat{w}_0 > 0\ . \end{aligned} \tag{2.2.3}$$

Clearly, the pension plan problem of the wealth case can be reduced to the classic multi-period portfolio selection problem by simply setting the contribution rate $\pi = 0$.

2.2.2 Wealth-to-income Ratio Case

Many studies have shown that a desirable feature of a pension plan is that the holder's wealth W is large compared to her annual salary Y the year before she retires. Hence, instead of the terminal wealth, we can determine the mean variance efficient strategy in terms of the terminal wealth-to-income ratio $X = \frac{W}{Y}$. We still assume there are two underlying assets in the pension plan: one is risk free and the other is risky. Recall from equation (2.2.1) that the risky asset S follows the Geometric Brownian Motion,

$$dS = (r + \xi_1\sigma_1)S\ dt + \sigma_1 S\ dZ_1\ . \tag{2.2.4}$$

Suppose that the plan member continuously pays into the pension plan at a fraction π of her yearly salary Y, which follows the process

$$dY = (r + \mu_Y)Y\ dt + \sigma_{Y_0}Y\ dZ_0 + \sigma_{Y_1}Y\ dZ_1\ , \tag{2.2.5}$$

where μ_Y, σ_{Y_0} and σ_{Y_1} are constants, and dZ_0 is another increment of a Wiener process, which is independent of dZ_1. Again, let p denote the proportion of this wealth invested in the risky asset S, and let $(1-p)$ denote the fraction of wealth invested in the risk free asset. Then

$$\begin{aligned} dW &= (r + p\xi_1\sigma_1)W\ dt + p\sigma_1 W dZ_1 + \pi Y dt\ , \\ W(t=0) &= \hat{w}_0 \geq 0\ . \end{aligned} \tag{2.2.6}$$

Define a new state variable $X(t) = W(t)/Y(t)$, then by Ito's Lemma, we obtain

$$\begin{aligned} dX &= [\pi + X(-\mu_Y + p\sigma_1(\xi_1 - \sigma_{Y_1}) + \sigma_{Y_0}^2 + \sigma_{Y_1}^2)]dt \\ &\quad -\sigma_{Y_0}X dZ_0 + X(p\sigma_1 - \sigma_{Y_1})dZ_1\ , \\ X(t=0) &= \hat{x}_0 \geq 0\ . \end{aligned} \tag{2.2.7}$$

In the wealth-to-income ratio case, we want to determine the optimal strategy $p^*(t,x)$ in terms of the investor's wealth-to-income ratio.

Remark 2.2. *The wealth case can be seen as a special case of the wealth-to-income ratio case. We can simply set the salary Y to be a constant (let $\sigma_{Y_0} = \sigma_{Y_1} = 0$ and $\mu_Y = -r$), then $X(t)$ is reduced to $W(t)$.*

2.3 Overview for Mean Variance Type Strategies

Continuous time mean variance asset allocation has received considerable attention over the years [78, 49, 61, 47, 15]. Financial applications include hedging futures [32], insurance

[28, 75], pension asset allocation [38, 42] and optimal execution of trades [52]. In its simplest formulation, an investor can choose to invest in a risk free bond or a risky asset, and can dynamically alter the proportion of wealth invested in each asset, in order to achieve a mean variance efficient result.

In this thesis, we consider three mean variance type strategies: pre-commitment mean variance, time-consistent mean variance, and mean quadratic variation. Before we study these strategies in detail in later chapters, we first give a brief overview.

Let us first consider the wealth case for the pension asset allocation problem. Define,

$$\begin{aligned}
E[\cdot] &: \text{ expectation operator,}\\
Var[\cdot] &: \text{ variance operator,}\\
\text{Std}[\cdot] &: \text{ standard deviation operator,}\\
E_{t,w}[\cdot],\ Var_{t,w}[\cdot] \text{ or } \text{Std}_{t,w}[\cdot] &: E[\cdot|W(t)=w],\ Var[\cdot|W(t)=w] \text{ or } \text{Std}[\cdot|W(t)=w]\\
&\quad \text{when sitting at time } t,\\
E^q_{t,w}[\cdot],\ Var^q_{t,w}[\cdot] \text{ or } \text{Std}^q_{t,w}[\cdot] &: E_{t,w}[\cdot],\ Var_{t,w}[\cdot] \text{ or } \text{Std}_{t,w}[\cdot], \text{ with } q(s,W(s)),\ s\geq t,\\
&\quad \text{being the policy along path } W(t) \text{ from stochastic process}\\
&\quad (2.2.2), \text{ where } q \text{ can be } p \text{ (the proportion of the total}\\
&\quad \text{wealth invested in the risky asset), or } pw \text{ (the monetary}\\
&\quad \text{amount invested in the risky asset) .} \qquad (2.3.1)
\end{aligned}$$

Let $W_T = W(t=T)$. An efficient frontier solution can be defined as the solution of the following problem:

$$\begin{aligned}
J(w,t) &= \sup_{q(s\geq t, W(s))} \{E^q_{t,w}[W_T]\}\ ,\\
\text{s.t. } Var^q_{t,w}[W_T] &= v\ , \qquad (2.3.2)
\end{aligned}$$

subject to stochastic process (2.2.2). Given a risk level ($Var^q_{t,w}[W_T] = v$), the solution of problem (2.3.2) gives the best expected terminal wealth.

2.3.1 Pre-commitment Policy

The optimization problem (2.3.2) is equivalent to the following problem,

$$J(w,t) = \sup_{q(s\geq t, W(s))} \{E^q_{t,w}[W_T] - \lambda Var^q_{t,w}[W_T]\}\ , \qquad (2.3.3)$$

subject to stochastic process (2.2.2), and where $\lambda > 0$ is a given Lagrange multiplier. In this thesis, the strategy q can be p (the proportion of the total wealth invested in the risky asset), or pw (the monetary amount invested in the risky asset). We will discuss this in detail in later chapters. The multiplier λ can be interpreted as a coefficient of risk aversion. The optimal policy for (2.3.3) is called a *pre-commitment* policy [11]. Once the initial strategy has been determined (as a function of the state variables) at the initial

time, the investor commits to this strategy, even if the policy computed at a later time would differ from the pre-commitment strategy.

Let $q_t^*(s,w)$, $s \geq t$, be the optimal policy for problem (2.3.3). Then, $q_{t+\Delta t}^*(s,w)$, $s \geq t+\Delta t$, is the optimal policy for

$$J(W(t+\Delta t), t+\Delta t) = \sup_{q(s \geq t+\Delta t, W(s))} \{E^q_{t+\Delta t, W(t+\Delta t)}[W_T] - \lambda Var^q_{t+\Delta t, W(t+\Delta t)}[W_T]\} \ . \quad (2.3.4)$$

However, in general

$$q_t^*(s, W(s)) \neq q_{t+\Delta t}^*(s, W(s)) \ ; \ s \geq t+\Delta t \ , \quad (2.3.5)$$

i.e. the solution of problem (2.3.3) is time inconsistent [11, 16]. Therefore, the dynamic programming principle cannot be directly applied to solve this problem. However, problem (2.3.3) can be embedded into a class of auxiliary stochastic Linear-Quadratic (LQ) problems using the method in [78, 49]. The optimal strategy $q_t^*(s,w)$ can be determined by solving those LQ problems with a dynamic programming principle. Alternatively, equation (2.3.3) can be posed as a convex optimization problem [50, 15, 4, 37]. We will study the pre-commitment policy in detail in Chapter 4.

2.3.2 Time-consistent Policy

Although the pre-commitment strategy is optimal in the sense of maximizing the expected return for a given standard deviation, this may not always be economically sensible. A real world investor experiences only one of many possible stochastic paths [50], hence it is not clear that a strategy which is optimal in an average sense over many paths is appropriate for an individual investor. In addition, the optimal strategy computed from the pre-commitment objective function assumes that the stochastic parameters are known at the beginning of the investment horizon, and do not change over the investment period. In practice, of course, one would normally recompute the investment strategy based on the most recent available data.

For these reasons, a *time-consistent* form of mean variance asset allocation has been suggested recently [16, 11, 73]. We can determine the time-consistent policy by solving problem (2.3.3) with an additional constraint,

$$q_t^*(s,w) = q_{t'}^*(s,w) \ ; \ s \geq t', \ t' \in [t,T] \ . \quad (2.3.6)$$

Hence the mean variance time-consistent problem is

$$\begin{aligned} J(w,t) &= \sup_{q(s \geq t, W(s))} \left\{ E^q_{t,w}[W_T] - \lambda Var^q_{t,w}[W_T] \right\} , \\ \text{s.t. } q_t^*(s,w) &= q_{t'}^*(s,w) \ ; \ s \geq t', \ t' \in [t,T] \ , \end{aligned} \quad (2.3.7)$$

subject to stochastic process (2.2.2).

In other words, we optimize problem (2.3.3) at time t, given that we follow the optimal policy at time t' in the future, which is determined by solving (2.3.3) at each future instant. Obviously, dynamic programming can be applied to the time-consistent problem. We will study the time-consistent policy in detail in Chapter 5.

Remark 2.3. *The solution of problem (2.3.7) may not be efficient in the conventional sense. The pre-commitment problem (2.3.3) is equivalent to problem (2.3.2) by choosing a proper value for λ. However, if we add the time-consistent constraint to problem (2.3.2), there does not exist a constant λ which makes problem (2.3.2) and the time-consistent problem (5.2.2) equivalent. Therefore, strictly speaking, the solution of problem (2.3.7) may not be efficient (in the sense of mean and variance). Nevertheless, we still call the solution of problem (2.3.7) an efficient frontier solution in later sections. This terminology was also used in [11].*

2.3.3 Mean Quadratic Variation

A criticism of both pre-commitment and time-consistent strategies is that the risk is only measured in terms of the standard deviation at the end of trading. In an effort to provide a more direct control over risk during the investment period, a *mean quadratic variation* objective function has been proposed in [18, 35]. Instead of using the variance/standard deviation as the risk measure, we can use the quadratic variation [18], $\int_t^T (dw)^2$. From equation (2.2.2) we have

$$(dw)^2 = (p\sigma_1 w)^2 dt + O(dt^{\frac{3}{2}}) \ . \tag{2.3.8}$$

Ignoring the higher order terms, we obtain,

$$\int_t^T (dw)^2 = \int_t^T (\sigma_1 p(u) w(u))^2 du \ . \tag{2.3.9}$$

In [16], it is pointed out that when bankruptcy is allowed ($w \in (-\infty, +\infty)$ and $p \in (-\infty, +\infty)$, discussed in later chapters), if $\int_t^T (e^{r(T-u)} dw)^2$ is used as the risk measure, the mean quadratic variation strategy has the same solution as the time-consistent strategy. The term $(e^{r(T-u)} dw)^2$ represents the future value of the instantaneous risk due to investing pw (in monetary amount) in the risky asset. Consequently, using this as a risk measure, we have

$$\int_t^T (e^{r(T-u)} dw)^2 = \int_t^T (e^{r(T-u)} \sigma_1 p(u) w(u))^2 du \ . \tag{2.3.10}$$

Then, we want to find the optimal policy which solves the following optimization problem (use p as the control),

$$J(w,t) = \sup_{p(t,w)} \{E^p_{t,w}[W_T] - \lambda \int_t^T (e^{r(T-u)} \sigma_1 p w)^2 du\}, \tag{2.3.11}$$

subject to stochastic process (2.2.2). Let $p_t^*(s, w)$, $s \geq t$, be the optimal policy for problem (2.3.11). Then clearly,

$$p_t^*(s, w) = p_{t'}^*(s, w) \ ; \ s \geq t', \ t' \in [t, T] \ . \tag{2.3.12}$$

Hence, dynamic programming can be directly applied to this problem. We will study the mean quadratic variation policy in detail Chapter 6.

Chapter 3

Maximal Use of Central Differencing for Hamilton-Jacobi-Bellman PDEs in Finance

3.1 Introduction

As introduced in Chapter 1, in many cases, classical solutions to nonlinear HJB PDEs do not exist, and we seek to find the viscosity solution of the HJB equation [29]. In order to guarantee convergence to the viscosity solution, the discrete scheme must be be pointwise consistent, l_∞ stable and monotone [10, 5].

A monotone scheme is usually constructed by using a positive coefficient method [46, 62, 8, 36]. Typically, a positive coefficient method is developed using forward or backward differencing for the drift term. The choice of forward or backward differencing depends on the control variable. This has the disadvantage that the truncation error in the space-like direction is only first order.

If implicit timestepping is used, then the nonlinear discretized algebraic equations are solved by an iterative method. The usual iterative approach [46, 36] requires solution of a local optimization problem for the optimal control at each grid node, at every iteration. Since the discretization at each node is a function of the control variable at that node, the type of discretization (i.e. forward or backward differencing) may change at each iteration. Use of forward/backward differencing means that the local objective function at each node is a continuous function of the control variable, but non-smooth.

In this chapter, we take a slightly different approach compared to the standard technique. We will use a combination of central/forward/backward differencing at each node. Given a value of the control variable at a node, we use the following criteria to select the differencing method

- Central differencing is used if the discretization is a positive coefficient method (for this particular choice of control).

- Forward/backward differencing is used only if central differencing does not result in a positive coefficient method. One of forward or backward differencing must satisfy the positive coefficient condition.

This method has the advantage that central differencing is used as much as possible, so that use of a locally second order method (assuming smoothly varying grids) is maximized. However, in general, the local objective function at each grid node is now a discontinuous function of the control. It would appear that iterative solution of the discretized equations would be problematic in this case.

In this chapter we note that the proof of convergence of the iterative scheme for solution of the discretized algebraic equations does not, in fact, require continuity of the local objective function. Hence, convergence of the iterative method for solution of the discrete equations can be guaranteed, even if the local objective function is a discontinuous function of the control. Nevertheless, it is not clear that, in practice

- the use of a locally second order method as much as possible will result in improved convergence as the mesh is refined, for practical parameter values;
- that the rate of convergence of the nonlinear iteration will be acceptable, if the local objective function is a discontinuous function of the control.

We report the results of several numerical experiments, for passport options [2] (introduced in Chapter 2) and optimal asset allocation for a defined pension plan [21] (introduced in Chapter 2). These experiments show that we can often obtain higher rates of convergence using central differencing as much as possible, although at some additional cost compared to the standard approach.

3.2 General Form for the Example Problems

To avoid repetition, we will carry out our analysis for a general form for the example problems.

As is typically the case with finance problems, we solve backwards in time from the expiry date of the contract $t = T$ to $t = 0$ by use of the variable $\tau = T - t$. Set

$$\mathcal{L}^Q V \equiv a(S,\tau,Q)V_{SS} + b(S,\tau,Q)V_S - c(S,\tau,Q)V \ , \tag{3.2.1}$$

where the control parameter Q is in general a vector, that is, $Q = (q_1, q_2, \ldots)'$. We write our problems in the general form

$$\begin{aligned} V_\tau &= \sup_{Q\in\hat{Q}} \left\{ \mathcal{L}^Q V + d(S,\tau,Q) \right\} \\ &\quad S \in [S_{\min}, S_{\max}] \quad , \quad 0 \le \tau \le T \ , \end{aligned} \tag{3.2.2}$$

where $\hat{Q}$ is the set of admissible controls. Here we include the $d(S,t,Q)$ term in equation (3.2.2) for generality, although in the examples in this chapter, we will always have $d \equiv 0$. We can also replace the sup in equation (3.2.2) by an inf, and all the results of this chapter hold in this case as well.

3.2.1 Boundary Conditions

We assume the boundary and payoff conditions satisfy the following assumptions

Assumption 3.1 (Payoff and Boundary Conditions)**.** At $\tau = 0$, we set $V(S,0)$ to the specified contract payoff. As $S \to S_{\min}, S \to S_{\max}$, we assume that either

- a Dirichlet boundary condition is specified;
- the coefficient $a(S,\tau,Q)$ vanishes, and the sign of $b(S,\tau,Q)$ is such that no boundary condition is required [9].

Note that it may be the case that the original problem has $S_{\max} = +\infty$ or $S_{\min} = -\infty$. In these cases, we will use a finite computational domain, and we assume that financial reasoning can be used to determine an appropriate Dirichlet condition. This is clearly an approximation, and introduces a *localization error*. However, as pointed out in [7], we can expect any errors incurred by imposing approximate boundary conditions at finite values of $S_{\min}, S_{\max}$ to be small in areas of interest if $|S_{\min}|$, $|S_{\max}|$ are selected sufficiently large. We will assume in the following that the original problem has been localized to a finite domain.

An alternative approach is introduced by [79] for handling the infinite domain problem, in which reversion conditions for stochastic models are defined. At $S = S_{\min}$, a reversion condition would be $a(S_{\min},\tau,Q) = 0$ and $b(S_{\min},\tau,Q) \geq 0$. The authors in [79] prove that if the models satisfy reversion conditions, then the financial PDEs have a unique solution and their numerical solutions can be obtained without using any artificial boundary conditions. However, as discussed in [79], in general this may require modification of the PDE coefficients for extreme values of S.

Assumption 3.2 (Assumptions on the HJB PDE.)**.** We make the assumption that the coefficients $a,\ b,\ c,\ d$ are Lipschitz continuous functions of (S,τ,Q), with $a \geq 0$, and $c \geq 0$, and that a,b,c,d, are bounded on $S_{\min} \leq S \leq S_{\max}$ and that the set of admissible controls $\hat{Q}$ is compact.

Remark 3.3. *Since we restrict ourselves to a finite computational domain $S_{\min} \leq S \leq S_{\max}$, we avoid difficulties associated with coefficients that grow with S as $|S| \to \infty$. If Assumptions 3.1, 3.2 hold, then from [24, 9], it follows that solutions to equation (3.2.2) satisfy the strong comparison property. Hence, a unique viscosity solution exists for equation (3.2.2).*

3.3 Implicit Controls

Define a grid $\{S_0, S_1, \ldots, S_p\}$ with $S_0 = S_{\min}$, $S_p = S_{\max}$ and let V_i^n be a discrete approximation to $V(S_i, \tau^n)$. Let $V^n = [V_0^n, \ldots, V_p^n]'$, and let $(\mathcal{L}_h^Q V^n)_i$ denote the discrete form of the differential operator (3.2.1) at node (S_i, τ^n). The operator (3.2.1) can be discretized using forward, backward or central differencing in the S direction to give

$$(\mathcal{L}_h^Q V^{n+1})_i = \alpha_i^{n+1} V_{i-1}^{n+1} + \beta_i^{n+1} V_{i+1}^{n+1} - (\alpha_i^{n+1} + \beta_i^{n+1} + c_i^{n+1}) V_i^{n+1} \ . \quad (3.3.1)$$

Here $\alpha_i,\ \beta_i$ are defined in Appendix A.

It is important that central, forward or backward discretizations be used to ensure that (3.3.3) is a positive coefficient discretization. To be more precise, this condition is

Condition 1. *Positive Coefficient Condition*

$$\alpha_i^{n+1} \geq 0, \quad \beta_i^{n+1} \geq 0, \quad c_i^{n+1} \geq 0. \quad i = 0, .., p-1 \quad . \quad (3.3.2)$$

We will assume that all models have $c_i^{n+1} \geq 0$. Consequently, we choose central, forward or backward differencing at each node to ensure that $\alpha_i^{n+1},\ \beta_i^{n+1} \geq 0$. Note that different nodes can have different discretization schemes.

Equation (3.2.2) can now be discretized using fully implicit timestepping along with the discretization (3.3.1) to give

$$\frac{V_i^{n+1} - V_i^n}{\Delta\tau} = \sup_{Q^{n+1} \in \hat{Q}} \left\{ (\mathcal{L}_h^{Q^{n+1}} V^{n+1})_i + d_i^{n+1} \right\} \ . \quad (3.3.3)$$

Note that $\alpha_i^{n+1} = \alpha_i^{n+1}(Q_i^{n+1})$, $\beta_i^{n+1} = \beta_i^{n+1}(Q_i^{n+1})$, $c_i^{n+1} = c_i^{n+1}(Q_i^{n+1})$ and $d_i^{n+1} = d_i^{n+1}(Q_i^{n+1})$, that is, the discrete equation coefficients are functions of the local optimal control Q_i^{n+1}. This makes equations (3.3.3) highly nonlinear in general. We refer to methods which use an implicit timestepping method where the control is handled implicitly as an *implicit control* method in the following.

3.3.1 Matrix Form of the Discrete Equations

It will be convenient to use matrix notation for equations (3.3.3), coupled with boundary conditions.

If a Dirichlet condition is specified at $S = S_{\min}, \tau = \tau^n$ $(i = 0)$, then we denote this value by G_0^n. If a Dirichlet boundary condition is specified at $S = S_{\max}, \tau = \tau^n$ $(i = p)$, then we denote this value by G_p^n. Set $Q^n = [Q_0^n, Q_1^n, \ldots, Q_p^n]'$, with each Q_i^n a local optimal control. We can write the discrete operator $(\mathcal{L}_h^Q V^n)_i$ as

$$\begin{aligned} (\mathcal{L}_h^Q V^n)_i &= [A^n(Q^n) V^n]_i \\ &= \left[\alpha_i^n V_{i-1}^n + \beta_i^n V_{i+1}^n - (\alpha_i^n + \beta_i^n + c_i^n) V_i^n\right]; \qquad 1 < i < p. \end{aligned} \quad (3.3.4)$$

The first and last rows of A are modified as needed to handle the boundary conditions. The boundary conditions at $S = S_{\min}, S_{\max}$ can be enforced by specifying a boundary condition vector $G^n = [G_0^n, 0, \ldots, 0, G_p^n]'$. If a Dirichlet condition is specified at $i = p$, we set G_p^n to the appropriate value, and set the last row in A^n to be zero. With a slight abuse of notation, we denote this last row in this case as $(A^n)_p \equiv 0$. Conversely, if no boundary condition is required at $i = p$, then we use backward differencing at node $i = p$ (which means that $\beta_p = 0$), and set $G_p^n = 0$. The boundary condition at $S = S_{\min}$, $i = 0$, is handled in a similar fashion. Let D^n be the vector with entries

$$[D^n]_i \;=\; \begin{cases} d_i^n \;, & 1 < i < p \\ 0 \;, & i = 0, p \;; \quad \text{if a Dirichlet condition is specified} \\ d_i^n \;, & i = 0, p \;; \quad \text{if no boundary condition is required} \end{cases}$$

Let

$$\mathcal{F}^n(Q, V^n) = A^n(Q)V^n + D^n(Q) \quad . \tag{3.3.5}$$

As we shall see in Section 3.6.3, $[\mathcal{F}^n(Q, V^n)]_i$, regarded as a function of Q can have a finite number of discontinuities at points where the differencing scheme changes. Recall that an upper semi-continuous ($\mathcal{USC}$) function $g(x)$ has the property that

$$\limsup_{x \to y} g(x) \le g(y) \tag{3.3.6}$$

In particular, we will define a numerical objective function $F^n(Q, V^n)$ so that it is an upper semi-continuous function of Q, i.e.

$$\limsup_{X \to Q} [F^n(X, V^n)]_i \;\le [F^n(Q, V^n)]_i \tag{3.3.7}$$

where

$$F^n(Q, V^n) = A^n(Q, V^n)V^n + D^n(Q) \;, \tag{3.3.8}$$

and we now note that the definition of A^n may depend on V^n. In fact, F is the upper semi-continuous envelope of $\mathcal{F}$. We will give an algorithm for determining $A^n(Q, V^n)$ so that $F^n(Q, V^n)$ is $\mathcal{USC}$ in Section 3.6.2.

Since $F^n(Q, V^n)$ is $\mathcal{USC}$, and $\hat{Q}$ is compact, the discrete equations (3.3.3) can then be written as

$$\begin{aligned} \left[I - \Delta\tau A^{n+1}(Q^{n+1}, V^{n+1})\right] V^{n+1} \;&=\; V^n + \Delta\tau D^{n+1} + (G^{n+1} - G^n) \;, \\ \text{where } Q_i^{n+1} \;&\in\; \underset{Q_i^{n+1} \in \hat{Q}}{\arg\max} \left\{ \left[F^{n+1}(Q^{n+1}, V^{n+1})\right]_i \right\} \;. \end{aligned} \tag{3.3.9}$$

Here the term $(G^{n+1} - G^n)$ enforces possible Dirichlet boundary conditions at $S = S_0, S_p$. Note also that the discrete equations (3.3.9) are nonlinear since $Q^{n+1} = Q^{n+1}(V^{n+1})$.

Remark 3.4. *We could alternatively write the discretized equation as*

$$[V^{n+1}]_i = [V^n]_i + [G^{n+1} - G^n]_i + \sup_{Q_i^{n+1}} \left\{ \Delta\tau \left[\mathcal{F}^{n+1}(Q^{n+1}, V^{n+1}) \right]_i \right\}, \tag{3.3.10}$$

where $\mathcal{F}$ is given in equation (3.3.5). When considering the convergence of the iterative scheme (see Section 3.5), it is convenient to consider the definition (3.3.9), which is our main focus in this chapter. When proving consistency, it is more convenient to consider the form (3.3.10). There is a distinction between these two forms, since the function (3.3.5) is a discontinuous function in general.

3.4 Convergence to the Viscosity Solution

In [64], examples were given in which seemingly reasonable discretizations of nonlinear option pricing PDEs were unstable or converged to the incorrect solution. It is important to ensure that we can generate discretizations which are guaranteed to converge to the viscosity solution [5, 29]. Assuming that equation (3.2.2) satisfies the strong comparison property [6, 9, 24], then, from [10, 5], a numerical scheme converges to the viscosity solution if the method is pointwise consistent, stable (in the l_∞ norm) and monotone.

It is straightforward, using the methods in [8, 36] to show that scheme (3.3.3) is monotone, pointwise consistent, and stable.

Theorem 3.5 (Convergence to the Viscosity Solution)**.** *Provided that the original HJB satisfies Assumptions 3.1, 3.2 and discretization (3.3.10) satisfies the positive coefficient condition (equation (3.3.2)) then scheme (3.3.10) converges to the viscosity solution of equation (3.2.2).*

Proof. Using the methods in [8, 36], this can be shown to follow from results in [10, 5]. We give a brief overview of the proof.
Monotonicity: from the positive coefficient condition (equation (3.3.2)) and following the same method as in [10], we can show that scheme (3.3.10) is monotone.
Pointwise consistency: from Appendix A, a simple Taylor series verifies consistency.
Stability: using the same technique as in [36], we can show that scheme (3.3.10) is l_∞ stable by a maximum analysis.
As shown in [10], if a discretization scheme is monotone, pointwise consistent and l_∞ stable, then that scheme converges to the viscosity solution. □

Remark 3.6 (Rate of Convergence)**.** *If $\Delta S = \max_i(S_{i+1} - S_i)$ and $\Delta\tau = C_1 h$, $\Delta S = C_2 h$, where C_1, C_2 are positive constants, then there has been considerable effort in recent years in attempts to determine rates of convergence for monotone finite difference schemes for HJB equations. Typically, one obtains estimates of the error of the form $O(h^\rho)$ where ρ varies from $1/27$ to $1/2$ depending on assumptions about regularity of the solution and the*

PDE coefficients. See [8] for an overview of recent work along these lines. These results seem generally pessimistic when compared with numerical experiments.

It is also useful to note the following property of the matrix $[I - \Delta\tau A^n(Q,U)]$.

Lemma 3.7 (M-matrix)**.** *If the positive coefficient condition (equation (3.3.2)) is satisfied, and either Dirichlet boundary conditions are specified, or no boundary condition is required, then* $[I - \Delta\tau A^n(Q,U)]$ *is an M-matrix for any* $Q \in \hat{Q}$*, hence* $[I - \Delta\tau A^n(Q,U)]^{-1} \geq 0$*.*

Proof. The positive coefficient condition (equation (3.3.2)) implies that $\alpha_i^n, \beta_i^n, c_i^n$ in equation (3.3.4) are non-negative $\forall Q \in \hat{Q}$. Hence $[I - \Delta\tau A^n(Q,U)]$ has positive diagonals, non-positive off diagonals, and is diagonally dominant. As a result, it is an M-matrix. □

3.4.1 Discretization of the Control

Suppose we have a single control $q \in \hat{Q}$ where $\hat{Q} = [q_{\min}, q_{\max}]$, where $q_{\min}$, $q_{\max}$ are finite. It is sometimes convenient to discretize the control, i.e. we replace $\hat{Q}$ by $\hat{Y}$ where $\hat{Y} = [y_0, y_1, y_2, ..., y_k]$, with $y_0 = q_{\min}, y_k = q_{\max}$. Let $\max_i(y_{i+1} - y_i) = C_3 h$, where C_3 is a positive constant. Then we have the following Lemma.

Lemma 3.8 (Consistency of Discrete Control Approximation)**.** *If the HJB equation satisfies Assumption 3.2, then the discretized control problem with* $\max_i(y_{i+1} - y_i) = C_3 h$

$$V_\tau \;=\; \sup_{Q \in \hat{Y}} \Big\{ \mathcal{L}^Q V + d(S, \tau, Q) \Big\} \tag{3.4.1}$$

is consistent with equation (3.2.2).

Proof. Let $\phi(S,\tau)$ be a smooth test function possessing bounded derivatives of all orders, then, in view of the fact that the coefficients of equation (3.2.2) are assumed to be Lipschitz continuous, bounded functions of Q, then

$$\begin{aligned} &\left| \phi_\tau - \sup_{Q \in \hat{Q}} \Big\{ \mathcal{L}^Q \phi + d(S, \tau, Q) \Big\} - \big(\phi_\tau - \max_{Q \in \hat{Y}} \Big\{ \mathcal{L}^Q \phi + d(S, \tau, Q) \Big\} \big) \right| \\ &= O(h) \quad . \end{aligned} \tag{3.4.2}$$

□

Proposition 3.9 (Discrete Control Approximation: Convergence to the Viscosity Solution)**.** *Let* $\Delta\tau = C_1 h$*,* $\max_i(S_{i+1} - S_i) = C_2 h$*,* $\max_i(y_{i+1} - y_i) = C_3 h$*, with* C_i *being positive constants. Provided the conditions for Theorem 3.5 and Lemma 3.8 are satisfied, then the discretization (3.3.9) with* $\hat{Q}$ *replaced by the discrete control set* $\hat{Y}$ *converges to the viscosity solution of equation (3.2.2) as* $h \to 0$*.*

Proof. This follows immediately from Theorem 3.5 and Lemma 3.8. □

3.5 Solution of Algebraic Discrete Equations

Although we have established that discretization (3.3.9) is consistent, l_∞ stable and monotone, it is not obvious that this is a practical scheme, since the implicit timestepping method requires solution of highly nonlinear algebraic equations at each timestep.

3.5.1 Iterative Method

Recall the definitions of $F^n(Q, V^n)$ and $A^n(Q, V^n)$ in equation (3.3.8). Consider the following iteration scheme:

Iterative Solution of the Discrete Equations

Let $(V^{n+1})^0 = V^n$

Let $\hat{V}^k = (V^{n+1})^k$

For $k = 0, 1, 2, \ldots$ until convergence

Solve

$$\left[I - \Delta\tau A^{n+1}(Q^k, \hat{V}^k)\right] \hat{V}^{k+1} = V^n + (G^{n+1} - G^n) + \Delta\tau D^{n+1}(Q^k)$$

$$Q_i^k \in \arg\max_{Q_i^k \in \hat{Q}} \left\{ \left[F^{n+1}(Q^k, \hat{V}^k)\right]_i \right\}$$

If $(k > 0)$ and $\left(\max_i \dfrac{\left|\hat{V}_i^{k+1} - \hat{V}_i^k\right|}{\max\left(scale, \left|\hat{V}_i^{k+1}\right|\right)} < tolerance \right)$ then quit

EndFor

(3.5.1)

The term *scale* in scheme (3.5.1) is used to ensure that unrealistic levels of accuracy are not required when the value is very small. Typically, $scale = 1$ for options priced in dollars.

Some manipulation of algorithm (3.5.1) results in

$$\begin{aligned}
&\left[I - \Delta\tau A^{n+1}(Q^k, \hat{V}^k)\right] (\hat{V}^{k+1} - \hat{V}^k) \\
&= \Delta\tau \Big[\left(A^{n+1}(Q^k, \hat{V}^k)\hat{V}^k + D^{n+1}(Q^k)\right) \\
&- \left(A^{n+1}(Q^{k-1}, \hat{V}^{k-1})\right)\hat{V}^k + D^{n+1}(Q^{k-1})) \Big]
\end{aligned}$$

. (3.5.2)

The proof of convergence of the iteration scheme (3.5.1) is given in [65, 36]. Since scheme (3.5.1) can be regarded as a variant of Policy iteration for infinite horizon Markov chains, the convergence proof is similar to the proof of convergence for Policy iteration [46]. For the convenience of the reader, we sketch the proof below.

In order to prove the convergence of Algorithm (3.5.1), we first need an intermediate result.

Lemma 3.10 (Sign of RHS of Equation (3.5.2))**.** *If $A^{n+1}(Q^k, \hat{V}^k)\hat{V}^k$ is given by equation (3.3.8, 3.3.9), with the control parameter determined by*

$$Q_i^k \in \arg\max_{Q_i^k \in \hat{Q}} \left\{ \left[F^{n+1}(Q_i^k, \hat{V}^k) \right]_i \right\} , \tag{3.5.3}$$

then every element of the right hand side of equation (3.5.2) is nonnegative, that is,

$$\begin{aligned} &\left[(A^{n+1}(Q^k, \hat{V}^k)\hat{V}^k + D^{n+1}(Q^k)) - (A^{n+1}(Q^{k-1}, \hat{V}^{k-1})\hat{V}^k + D^{n+1}(Q^{k-1})) \right]_i \\ &\geq 0 . \end{aligned} \tag{3.5.4}$$

Proof. Note that from the definitions of $A^n(Q)$ and $A^n(Q, V^n)$, we have

$$A^{n+1}(Q^k, \hat{V}^k)\hat{V}^k + D^{n+1}(Q^k) = \sup_{Q' \in \hat{Q}} \{A^{n+1}(Q')\hat{V}^k + D^{n+1}(Q')\} , \tag{3.5.5}$$

$$A^{n+1}(Q^{k-1}, \hat{V}^{k-1})\hat{V}^k + D^{n+1}(Q^{k-1}) = \limsup_{Q' \to Q^{k-1}} \{A^{n+1}(Q')\hat{V}^k + D^{n+1}(Q')\}. \tag{3.5.6}$$

Clearly,

$$\sup_{Q' \in \hat{Q}} \{A^{n+1}(Q')\hat{V}^k + D^{n+1}(Q')\} \geq \limsup_{Q' \to Q^{k-1}} \{A^{n+1}(Q')\hat{V}^k + D^{n+1}(Q')\} . \tag{3.5.7}$$

The result follows from (3.5.5), (3.5.6) and (3.5.7). □

It is now easy to show that iteration (3.5.1) always converges.

Theorem 3.11 (Convergence of Iteration (3.5.1))**.** *Provided that the conditions for Lemmas 3.7 and 3.10 are satisfied, then the iteration (3.5.1) converges to the unique solution of equation (3.3.9) for any initial iterate $\hat{V}^0$. Moreover, the iterates converge monotonically.*

Proof. Given Lemmas 3.10 and 3.7, the proof of this result is similar to the proof of convergence given in [64]. We give a brief outline of the steps in this proof, and refer readers to [64] for details. A straightforward maximum analysis of scheme (3.5.1) can be used to bound $\|\hat{V}^k\|_\infty$ independent of iteration k. From Lemma 3.10, we have that the right hand side of equation (3.5.2) is non-negative. Noting that $\left[I - \Delta\tau A^{n+1}(Q^k, \hat{V}^k) \right]$ is an M-matrix (from Lemma 3.7) and hence $\left[I - \Delta\tau A^{n+1}(Q^k, \hat{V}^k) \right]^{-1} \geq 0$, it is easily seen that

the iterates form a bounded non-decreasing sequence. Consequently, $\lim_{k\to\infty} \hat{V}^{k+1} = \hat{V}^k$, and manipulation of (3.5.2) shows that the residual goes to zero as $k \to \infty$. Hence the iteration converges to a solution. It follows from the M-matrix property of $\left[I - \Delta\tau A^{n+1}(Q^k, \hat{V}^k)\right]$ that the solution is unique. □

Remark 3.12 (Q Dependent Discretizations)**.** *Note that we obtain convergence of iteration (3.5.1) even if the discrete equations, regarded as a function of the control Q, are discontinuous. We do, however, require that the coefficients a, b, c, d in equations (3.2.1-3.2.2) are bounded functions of the control Q, in order to ensure that A^{n+1}, D^{n+1} are bounded.*

Remark 3.13 (Uniqueness of Solution)**.** *The above argument shows that the solution for V^{n+1} is unique. However, this does not imply that the controls Q^{n+1} are unique. As a trivial counterexample, consider the case where a, b, c, d in equations (3.2.1-3.2.2) are independent of Q, in which case the solution for V is unique for any choice of $Q \in \hat{Q}$.*

3.6 Passport Options

The properties of passport options have been introduced in Chapter 2. In [2], passport option pricing is solved using central weighting and Crank-Nicolson timestepping. While the results appear to converge to the correct solution, convergence to the viscosity solution cannot be guaranteed, since this is a non-monotone method. In [65], it is shown that, for passport options, it is not possible to pre-select central, forward or backward differencing at a node, independent of the control, and guarantee a positive coefficient scheme. In other words, the scheme must depend on the control.

3.6.1 The Pricing Model for Passport Options

Recall from equation (2.1.1) that the underlying asset price follows the stochastic process

$$dS = \mu S\ dt + \sigma S\ dZ\ , \tag{3.6.1}$$

where dZ is the increment of a Wiener process, σ is volatility, μ is the drift rate. Let $V(S, W, t)$ denote the option value at time t with underlying price S and wealth W. Under the process (3.6.1), the pricing PDE for passport options can be written as [70]

$$\begin{aligned} -V_t = &- rV + (r-\gamma)SV_S \\ &+ \sup_{|q|\le 1}\left[-((\gamma - r + r_c)qS - r_t W)V_W + \frac{\sigma^2 S^2}{2}(V_{SS} + 2qV_{SW} + q^2 V_{WW})\right]\ , \end{aligned} \tag{3.6.2}$$

where

W : the accumulated wealth of the underlying trading account.

r : the risk-free interest rate.

γ : the dividend rate on the underlying asset S.

r_c : a cost of carry rate.

r_t : an interest rate for the trading account.

q : the number of shares of S that an investor holds, which is also named as trading strategy. q is limited to $|q| \leq 1$ in equation (3.6.2). Different position limits can be handled by scaling [43].

We consider two types of payoff at $t = T$. The standard payoff is

$$V(S, W, t = T) \quad = \quad \max(W, 0) \ , \tag{3.6.3}$$

and the *asset or nothing* payoff [2]

$$V(S, W, t = T) \quad = \quad \begin{cases} S & \text{if } W \geq 0 \\ 0 & \text{otherwise} \end{cases} \ . \tag{3.6.4}$$

The above payoff can be generalized to specify a non-zero strike, but we assume the form (3.6.4) in this chapter.

For both these payoffs, we can reduce the problem to solving for $V(S, W, t) = Su(x, \tau)$, where $x = W/S$ and $\tau = T - t$ [2], so that equation (3.6.2) can be reduced to a one-dimensional problem for u

$$u_\tau = -\gamma u + \sup_{|q| \leq 1} \left[((r - \gamma - r_c)q - (r - \gamma - r_t)x)u_x + \frac{\sigma^2}{2}(x - q)^2 u_{xx} \right] \ , \tag{3.6.5}$$

where $x \in [-\infty, +\infty]$. Making this simplification, the standard payoff becomes

$$u(x, \tau = 0) = \max(x, 0), \tag{3.6.6}$$

with boundary conditions

$$u(x \to -\infty, \tau) = 0 \quad ; \quad u(x \to \infty, \tau) = x \ , \tag{3.6.7}$$

while the asset or nothing payoff is

$$u(x, \tau = 0) \quad = \quad \begin{cases} 1 & \text{if } x \geq 0 \\ 0 & \text{otherwise} \end{cases} \tag{3.6.8}$$

with boundary conditions

$$u(x \to -\infty, \tau) = 0 \quad ; \quad u(x \to \infty, \tau) = \exp(-\gamma\tau) \ . \tag{3.6.9}$$

For computational purposes, we truncate the domain to $x \in [x_{\min}, x_{\max}]$, and apply the boundary conditions (3.6.7) and (3.6.9) at $x_{\min}, x_{\max}$.

3.6.2 Discretization

Passport option valuation is a special case of the general HJB equation (3.2.2), if we note that in this case

$$\begin{aligned} &Q = (q) \ , \quad \hat{Q} = [-1, +1], \quad a(x, \tau, Q) = \frac{\sigma^2}{2}(x - q)^2 \ , \\ &b(x, \tau, Q) = (r - \gamma - r_c)q - (r - \gamma - r_t)x \ , \quad c(x, \tau, Q) = \gamma \ , \end{aligned} \tag{3.6.10}$$

where $Q,\ \hat{Q},\ a,\ b,\ c$ are defined in Section 3.2. Let the discrete approximation for $u(x_i, \tau^n)$ be denoted by u_i^n with $U^n = [u_0^n, u_1^n, ..., u_{imax}^n]'$. Let $\hat{U}^k$ be the $k'th$ estimate for U^n, then the local objective function which must be maximized in Algorithm (3.5.1) is

$$\begin{aligned} [F^{n+1}(Q, \hat{U}^k)]_i &= [A^{n+1}(Q, \hat{U}^k)\hat{U}^k + D(Q)]_i \\ &= ((r - \gamma - r_c)q - (r - \gamma - r_t)x_i)[(\hat{u}^k)_x]_i + \frac{\sigma^2}{2}(x_i - q)^2[(\hat{u}^k)_{xx}]_i^{n+1} \ , \end{aligned} \tag{3.6.11}$$

where $[\cdot]_i^{n+1}$ refers to the discrete form for $[\cdot]$. We need a positive coefficient scheme to solve the pricing PDE (3.6.5). Given node $x = x_i$, with current solution estimate $\hat{U}^k$, suppose the sets of q's, which give a positive coefficient scheme for central, forward and backward differencing respectively, are $P_i^{cent},\ P_i^{fwd},\ P_i^{bwd}$. Since central differencing is the most accurate, it should be used as much as possible. Consequently, given a q, if central differencing satisfies positive coefficient conditions, central differencing will be used for that q (with the constraint that F^{n+1} is $\mathcal{USC}$). In other words, the proper ranges of q for various differencings are $Range_i^{cent} = P_i^{cent}$, $Range_i^{fwd} = P_i^{fwd} - (P_i^{cent} \cap P_i^{fwd})$ and $Range_i^{bwd} = P_i^{bwd} - (P_i^{cent} \cap P_i^{bwd})$. Note that

$$\begin{aligned} &Range_i^j \cap Range_i^k = \emptyset \ , \text{where } j, k \in \{cent, bwd, fwd\} \text{ and } j \neq k \\ &Range_i^{bwd} \cup Range_i^{fwd} \cup Range_i^{cent} = \hat{Q} \quad . \end{aligned} \tag{3.6.12}$$

Let $\overline{Range_i^j}$ denote the closure of $Range_i^j$. For a given asset grid, and the option values at the current iteration, Algorithm (3.6.13) is used to determine the optimal control and to decide which differencing should be applied. This choice of differencing method uses central differencing as much as possible and determines $A^{n+1}(Q, \hat{U}^k)$ with the constraint that $F^{n+1}(Q, \hat{U}^k)$ is $\mathcal{USC}$, where F is the upper semi-continuous envelope of $\mathcal{F}$.

For a given differencing method, the range of possible values of the control is divided into closed line segments where the objective function is smooth. Standard methods are then used to determine the maximum within each segment. If an analytic form for the local objective function is not available, then an alternate approach is discussed in Section 3.7.4.

3.6.3 Discontinuity of The Objective Function

When we use central differencing as much as possible, the local objective function at each node is in general a discontinuous function of the control q. However, the proof of conver-

gence of the iterative scheme for solution of the discretized algebraic equations (Theorem 3.11) does not require continuity of the local objective function. If forward/backward differencing are applied, the local objective function is continuous but not smooth. Figure 3.1 shows these features, for a given grid and solution values.

Determining the Optimal Control and the Differencing Method

Apply boundary conditions at the first node x_0 and the last node x_p
For each $x_0 < x_i < x_p$
    Compute the positive coefficient sets $Range_i^{cent}$, $Range_i^{fwd}$, $Range_i^{bwd}$
    diff = cent, $q^* = 0$, $F_{\max} = -\infty$
    For j = cent, fwd, bwd
        Compute $[A^{n+1}(q, \hat{V}^k)]_i$ with scheme $= j$
        Solve $q_j^* \in \underset{q \in \overline{Range_i^j}}{\arg\max} \{[F^{n+1}(q, \hat{V}^k)]_i\}$
        If $[F^{n+1}(q_j^*, \hat{V}^k)]_i > F_{\max}$
            diff $= j$, $q^* = q_j^*$
            $F_{\max} = [F^{n+1}(q_j^*, \hat{V}^k)]_i$
        EndIf
    EndFor
EndFor

(3.6.13)

Note that Algorithm (3.6.13) requires determination of the maximum of the local objective function for each set of points where central, forward, or backward differencing is used. For example, as shown in Figure 3.1, central differencing can be used on two disjoint intervals of the control space. On each of the subintervals, the objective function is a smooth function of the control, hence we can use standard methods to maximize the objective function. Determination of the range of controls where central, forward and backward differencing gives rise to a positive coefficient method is generally only possible if we have an analytic expression for the objective function. If this is not available, we can discretize the control, and use a linear search to find the maximum as described in Section 3.7.4. This is, of course, much more computationally expensive compared to analytic maximization.

3.6.4 Numerical Results

In this section, we will examine the convergence as the grid and timesteps are refined for various differencing methods.

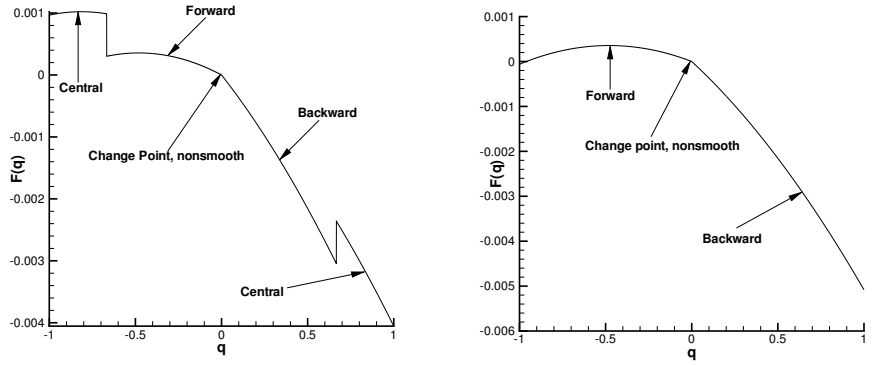

(a) **(b)**

FIGURE 3.1: *Local objective function (3.6.11) for the passport option at* $(x_i = 0)$. *(a) using central differencing as much as possible; (b) using forward/backward differencing only. Parameters:* $r = 0.05,\ \sigma = 0.03,\ \gamma = 0.04,\ r_c = 0.07,\ r_t = 0.03$. *Nodes:* $x_{i-1} = -0.01,\ u_{i-1} = 0.173298$*;* $x_i = 0.,\ u_i = 0.173888$*;* $x_{i+1} = 0.01,\ u_{i+1} = 0.174135$.

We use a convergence tolerance of 10^{-7} in Algorithm (3.5.1), and we truncate the computational domain to $[x_{\min}, x_{\max}] = [-3, 4]$. Numerical experiments show that increasing the size of the computational domain does not affect solution values to six digits.

In [2, 65], input parameters in Table 3.1 are used for testing. An unequally spaced grid in the x direction is used, and a new fine grid node is added between each two coarse grid nodes at each level of refinement. In Table 3.2, *ratio* refers to the ratio of successive changes in the solution as the grid is refined by a factor of two, and the timestep sizes are reduced by a factor of four. Since fully implicit timestepping is used, this allows us to isolate the effect of the use of central weighting as much as possible, compared to forward/backward differencing only. Local second order convergence (in terms of x node spacing) would be consistent with a ratio of four, while first order convergence would be consistent with a ratio of two.

For this particular set of parameters an analytical solution is known [2], $V(S_0, 0, \tau = T) = \$13.1381$ (to six figures). Table 3.2 shows that our numerical solution converges to the analytical solution. The numerical solutions in [2, 65] also converge to that value. However, the discretization schemes in [2, 65] are not monotone so that convergence to the viscosity solution is not guaranteed. As shown in Theorem 3.5, our numerical method guarantees convergence to the viscosity solution.

We now compare the results from two differencing methods — using central differencing as much as possible and using forward/backward differencing only. Using input parameters in Table 3.3, Table 3.4 presents a convergence study, which also reports the actual initial option values, i.e. $V = S_0\ u(x = W_0/S_0, \tau = T)$.

The payoff type is a call (convex payoff). As expected, Table 3.4 indicates that quadratic convergence is obtained by using central differencing as much as possible, and first order convergence is obtained by using forward/backward differencing.

r	0	σ	0.3
γ	0	r_c	0
r_t	0	S_0	\$100
Payoff	Call	Strike	\$ 0
Initial Wealth	0	Time to expiry T	1 year

TABLE 3.1: *Parameters used in [2, 65], passport option.*

Nodes	Timesteps	Nonlinear iterations	Normalized CPU Time	Option value	Ratio
Central Differencing as much as possible					
67	25	52	1	13.0553	
133	100	201	5.72	13.1173	
265	400	801	50.91	13.1329	3.97
529	1600	3201	402.73	13.1368	3.99
1057	6400	12801	3167.27	13.1378	4.03

TABLE 3.2: *Numerical example used in [2, 65], passport option, convex payoff. Fully implicit timestepping is applied, using constant timesteps. On each refinement, a new node is inserted between each two coarse grid nodes, and the timestep is divided by four. Parameters are given in Table 3.1. Ratio is the ratio of successive changes in computed solution as the discretization parameters are reduced. Analytic price is \$13.1381. CPU time is normalized. We take the CPU time used for the first test in this table as one unit of CPU time, which uses 67 nodes and 25 timesteps.*

r	0.08	σ	0.2
dividend	0.035	r_c	0.1
r_t	0.04	S_0	\$100
Payoff	Call	Strike	\$ 0
Initial Wealth	0	Time to expiry T	1 year

TABLE 3.3: *Parameters for the convex payoff, passport option.*

For a convex payoff, it is always optimal to choose $q = -1$ or 1 [65]. But for a non-convex payoff, q can be any value in $[-1, 1]$. Table 3.5 presents a convergence study using the parameters in Table 3.3, but the payoff type is an asset or nothing, non-convex payoff (this is a digital call in terms of u, see equation (3.6.8)). For the asset or nothing payoff, if $W_0 \geq 0$, the option value will be very high (close to the initial stock value) and insensitive to the grid refinement, so it is difficult to carry out a convergence study. In this example, option values are reported at $W_0 = -25$ (initial wealth is $-\$25$). When central differencing as much as possible is applied, the convergence rate is close to second order. First order convergence is obtained by using forward/backward differencing.

From the numerical results, we can conclude that generally we can obtain higher rates of convergence using central weighting as much as possible, compared to forward/backward differencing only. Of course, we cannot guarantee that this will always occur, but we can-

Nodes	Timesteps	Nonlinear iterations	Normalized CPU Time	Option value	Ratio
Central Differencing as much as possible					
133	100	224	1.52	10.6651	
265	400	851	12.73	10.6768	
529	1600	3277	96.06	10.6798	3.95
1057	6400	12848	774.24	10.6805	3.96
2113	25600	51223	5964.55	10.6807	3.95
Forward/backward differencing only					
133	100	224	1	10.6945	
265	400	851	9.70	10.6916	
529	1600	3278	65.75	10.6872	0.66
1057	6400	12849	551.21	10.6842	1.49
2113	25600	51224	3983.94	10.6826	1.77

TABLE 3.4: *Convergence study, passport option, convex payoff. Fully implicit timestepping is applied, using constant timesteps. On each refinement, a new node is inserted between each two coarse grid node, and the timestep is divided by four. Parameters are given in Table 3.3. Ratio is the ratio of successive changes in computed solution as the discretization parameters are reduced. CPU time is normalized. We take the CPU time used for the first test using Forward/backward differencing only in this table as one unit of CPU time, which uses 133 nodes and 100 timesteps.*

not obtain second order convergence using forward/backward differencing. In all our numerical experiments, we have never seen a case where central weighting as much as possible converges at a slower rate compared to forward/backward differencing only.

Note that in both these examples, forward/backward differencing only requires about 60% of the CPU time compared to central differencing as much as possible. This is simply because of the additional tests required to determine the ranges of possible central weighting in Algorithm (3.6.13).

Both Table 3.4 and Table 3.5 show that the number of nonlinear iterations per timestep is about two, indicating that Algorithm (3.5.1) converges rapidly, in spite of the discontinuous objective function that is maximized at each node.

3.7 Defined Contribution Pension Plan

The second example in this chapter concerns an optimal dynamic asset allocation strategy for a defined contribution pension plan, which is introduced in Chapter 2.

In this section, we will follow the utility function approach given in [21] to solve this problem. The objective of the strategy is to maximize the plan member's utility at retirement. It is assumed that the utility is a function of the plan member's wealth to yearly income ratio (wealth-to-income case introduced in Section 2.2.2) [21].

Nodes	Timesteps	Nonlinear iterations	Normalized CPU Time	Option value	Ratio
Central Differencing as much as possible, $W_0 = -25$					
133	100	267	1.54	25.8812	
265	400	865	11.79	26.0794	
529	1600	3300	85.12	26.1315	3.80
1057	6400	12887	661.79	26.1452	3.82
2113	25600	51274	5196.92	26.1488	3.76
Forward/backward differencing only, $W_0 = -25$					
133	100	266	1	26.2905	
265	400	863	7.44	26.2902	
529	1600	3298	55.13	26.2384	.005
1057	6400	12890	446.15	26.1990	1.31
2113	25600	51271	3391.54	26.1758	1.70

TABLE 3.5: *Convergence study, passport option, non-convex payoff. Fully implicit timestepping is applied, using constant timesteps. On each refinement, a new node is inserted between each two coarse nodes, and the timestep is divided by four. Parameters are given in Table 3.3 except that $W_0 = -25$, $K = 0$, and the payoff is an asset or nothing. Ratio is the ratio of successive changes in computed solution as the discretization parameters are reduced. CPU time is normalized. We take the CPU time used for the first test using Forward/backward differencing only in this table as one unit of CPU time, which uses 133 nodes and 100 timesteps.*

We give a brief derivation of the model equations, for details we refer the reader to [21].

3.7.1 Stochastic Model

The stochastic models for the underlying asset S, the plan holder's year salary Y, the wealth W and her wealth-to-income ratio X have been given in equations (2.2.4 - 2.2.7).

Assume the plan member has a power utility function $u(X(T))$ at retirement time T, which is defined as a function of the wealth-to-income ratio,

$$u(X(T)) = \begin{cases} \frac{1}{\gamma}(X(T))^\gamma & \text{where } \gamma < 1 \text{ and } \gamma \neq 0 \\ \log(X(T)) & \text{when } \gamma = 0 \ . \end{cases} \tag{3.7.1}$$

Our goal is to find the optimal asset allocation strategy to maximize the expected terminal utility. Let $J(t, x, p) = E[u(X_p(T))|X(t) = x]$, where $X(t)$ is the path of X given the asset allocation strategy $p = p(t, x)$, and $E[\cdot]$ is the expectation operator. We define

$$V(x, \tau) = \sup_{p \in \hat{P}} E[u(X_p(T))|X(T - \tau) = x] = \sup_{p \in \hat{P}} J(T - \tau, x, p) \ . \tag{3.7.2}$$

where $\hat{P}$ is the set of all admissible asset allocation strategies, and $\tau = T - t$. Then

$V(x,\tau)$ satisfies the HJB equation

$$V_\tau = \sup_{p\in\hat{P}}\{\mu_x^p V_x + \frac{1}{2}(\sigma_x^p)^2 V_{xx}\} \quad ; \quad x\in[0,\infty] \ , \tag{3.7.3}$$

with terminal condition

$$V(x,\tau=0) = \begin{cases} \gamma^{-1}x^\gamma & \text{where } \gamma<1 \text{ and } \gamma\neq 0 \\ \log(x) & \text{when } \gamma = 0 \ , \end{cases} \tag{3.7.4}$$

and where

$$\begin{aligned} \mu_x^p &= \pi + x(-\mu_Y + p\sigma_1(\xi_1 - \sigma_{Y_1}) + \sigma_{Y_0}^2 + \sigma_{Y_1}^2) \\ (\sigma_x^p)^2 &= x^2(\sigma_{Y_0}^2 + (p\sigma_1 - \sigma_{Y_1})^2) \ . \end{aligned} \tag{3.7.5}$$

with boundary conditions

$$V_\tau(x=0,\tau) = \pi V_x \quad ; \quad V(x\to\infty,\tau) = 0 \ . \tag{3.7.6}$$

The boundary condition at $x=0$ can be derived by assuming $\lim_{x\to 0}(px) = 0$, which ensures that total wealth cannot become negative.

For computational purposes, we truncate the domain to $[0, x_{\max}]$, and impose the boundary conditions (3.7.6) on this finite domain. In order to ensure that Assumption 3.2 holds, we define the range of controls to be

$$\hat{P} = [0, p_{\max}] \ . \tag{3.7.7}$$

Note that in the original problem in [21], $\hat{P} = [0,\infty]$. A value of $p>1$ indicates that the holder borrows to invest in risky assets. As a practical matter, it is unlikely that anyone could borrow an unlimited amount relative to her wealth to invest in risky assets. We will choose $p_{\max}$ sufficiently large so that the computed solution is insensitive to $p_{\max}$.

The terminal condition (3.7.1) is undefined for $x=0$, if, for example, $\gamma<0$. We adopt the simple expedient of replacing condition (3.7.1) by

$$V(x,\tau=0) = \begin{cases} \frac{1}{\gamma}\max(x,\epsilon)^\gamma & \text{if } \gamma<0 \\ \log(\max(x,\epsilon)) & \text{if } \gamma = 0 \ , \end{cases} \tag{3.7.8}$$

where $\epsilon>0, \epsilon \ll 1$. We choose ϵ sufficiently small so that the computed results are insensitive to this value. Table 3.6 shows the computational parameters used in our numerical tests.

Note that the HJB equation (3.7.3) becomes independent of p at $x=0$. This non-uniqueness of p does not affect the solution value V. It will be understood in the following that if we refer to a value of, say, $(p\ x)$ at $x=0$, then we are really referring to

$$\lim_{x\to 0}(p\ x) \ . \tag{3.7.9}$$

Convergence Tolerance	10^{-7}
ϵ	10^{-3}
$p_{\max}$	200
$x_{\max}$	80

TABLE 3.6: *Computational parameters, pension plan. Convergence tolerance used in Algorithm (3.5.1).* ϵ *is used to adjust the terminal condition (3.7.8).* $p_{\max}$ *is the maximum value of the equity proportion (3.7.7).* $x_{\max}$ *is the maximum* x *value in the finite computational domain.*

3.7.2 Discretization

The pension plan asset allocation model is a special case of the general HJB equation (3.2.2), if we make the identification

$$\begin{aligned} &Q = (p) \ , \quad \hat{Q} = [0, p_{\max}] \ , \\ &a(x,\tau,Q) = \frac{1}{2}(\sigma_x^p)^2 \ , \quad b(x,\tau,Q) = \mu_x^p, \quad c(x,\tau,Q) = 0 \ , \end{aligned} \tag{3.7.10}$$

where $Q,\ a,\ b,\ c$ are defined in equation (3.2.2). Given node $x = x_i$, with specified solution estimate $\hat{V}^k = [\hat{v}_0^k, ..., \hat{v}_{imax}^k]'$, the objective function which is maximized at each node in Algorithm (3.5.1) is

$$\begin{aligned} [F^{n+1}(Q, \hat{V}^k)]_i &= [A^{n+1}(Q, \hat{V}^k)\hat{V}^k + D(Q)]_i \\ &= [\mu_x^p]_i[(\hat{v}^k)_x]_i + \frac{1}{2}([\sigma_x^p]_i)^2[(\hat{v}^k)_{xx}]_i^{n+1} \ , \end{aligned} \tag{3.7.11}$$

where $\hat{V}^k$ is the vector containing the current estimate of the discrete solution values. Similar to the passport option case, if we want to apply central differencing as much as possible, Algorithm (3.6.13) is used to decide which differencing scheme is used (which depends on Q and $\hat{V}^k$).

3.7.3 Numerical Results

Given parameters in Table 3.7, Table 3.8 shows the numerical results. Recall that as we refine the grid, by inserting a fine grid node between two coarse grid nodes, we reduce the timestep size by four. Since fully implicit timestepping is used (which guarantees a monotone scheme), then the ratio of successive changes in the solution, as the grid is refined, should be four for quadratic convergence, and two for linear convergence. As expected, Table 3.8 shows that quadratic convergence is obtained by using central differencing as much as possible, and first order convergence is obtained by using forward/backward differencing. As for the passport option case, convergence of Algorithm (3.5.1) is rapid.

Numerical tests with the parameters in Table 3.6, indicated that increasing the truncated domain size $x_{\max}$, increasing the maximum value of the control $p_{\max}$, and decreasing

the convergence tolerance and ϵ, resulted in no change to the results in Table 3.8 to six figures.

In the passport option case, particularly with a convex payoff, numerical experiments indicate that using central differencing only does converge to the viscosity solution [2, 65]. However, this cannot be guaranteed. In contrast, in the pension plan case, our experiments show that the numerical scheme does not appear to converge at all using central differencing only. In this respect, the pension plan problem appears to be more challenging than passport option valuation.

μ_Y	0.	ξ_1	0.2
σ_1	0.2	σ_{Y1}	0.05
σ_{Y0}	0.05	π	0.1
T	20 years	γ	-5

TABLE 3.7: *Parameters used in the pension plan examples. The time units in this problem are years, so that the ratio of wealth to salary x has the units of years.*

Given parameters in Table 3.7, Figure 3.2 shows the expected terminal utility at $t = 0$ and the corresponding optimal asset allocation strategy p as a function of the salary to wealth x ratio. Note that as $x \to 0$, the proportion invested in the risky asset becomes very large. However, as noted in [21], the amount actually invested in the risky asset $(p\ x)$, tends to zero as $x \to 0$ (this must be the case in order to ensure non-negative wealth). This is clearly illustrated in Figure 3.2 (d). Moreover, [21] points out that $(p\ x)$ converges to 0 at the same rate as $\sqrt{x}$. Using parameters in Table 3.7, we find that $\lim_{x\to 0} \frac{px}{\sqrt{x}} \simeq 1.59$. In [21], the authors do not give details about their numerical method, and present only graphical results. We can comment only that the results in Figure 3.2 are qualitatively similar to the results in [21].

3.7.4 Discretization of the Control

In some cases, if the form of the HJB equation is complex, then it may be difficult to implement Algorithm (3.6.13). In this case, a simpler approach is desirable. Suppose there is one control q at each node, and we discretize the possible control values as described in Section 3.4.1. From Lemma 3.8, we have that a scheme using discrete controls will converge to the viscosity solution of the original HJB equation. To determine the optimal control at each node, as required in Algorithm (3.5.1), we simply perform a linear search of the discrete control values. For a given q, we use central weighting if this results in a positive coefficient method, otherwise, forward/backward differencing is used.

Note that since we cannot assume that the objective function is a continuous function of the control, linear search is the only way to find the optimal value of q. This method has the obvious advantage that it is very easy to implement, especially in the case where central differencing is used as much as possible.

The numerical results obtained using this method for the pension plan problem are given in Table 3.9. The results are very close to the results reported in Table 3.8. Of

Nodes	Timesteps	Nonlinear iterations	Normalized CPU Time	utility	Ratio
Central Differencing as much as possible, $x = 0$					
87	160	331	1.34	-4.06482×10^{-3}	
173	640	1280	12.04	-3.65131×10^{-3}	
345	2560	5120	91.97	-3.58063×10^{-3}	5.85
689	10240	20480	712.71	-3.56354×10^{-3}	4.13
1377	40960	81920	5621.07	-3.55922×10^{-3}	3.96
Forward/backward differencing only, $x = 0$					
87	160	399	1	-6.73472×10^{-3}	
173	640	1296	7.36	-4.68055×10^{-3}	
345	2560	5135	56.19	-4.04828×10^{-3}	3.25
689	10240	20480	436.79	-3.79150×10^{-3}	2.46
1377	40960	81920	3447.83	-3.67543×10^{-3}	2.21
Central differencing as much as possible, $x = 1$					
87	160	331	1.34	-4.68742×10^{-4}	
173	640	1280	12.04	-4.31528×10^{-4}	
345	2560	5120	91.97	-4.26814×10^{-4}	7.89
689	10240	20480	712.71	-4.25611×10^{-4}	3.92
1377	40960	81920	5621.07	-4.25305×10^{-4}	3.92
Forward/backward differencing only, $x = 1$					
87	160	399	1	-7.14415×10^{-4}	
173	640	1296	7.36	-5.55931×10^{-4}	
345	2560	5135	56.19	-4.87660×10^{-4}	2.32
689	10240	20480	436.79	-4.55786×10^{-4}	2.14
1377	40960	81920	3447.83	-4.40348×10^{-4}	2.06

TABLE 3.8: *Convergence study, pension plan example. Fully implicit timestepping is applied, using constant timesteps. On each refinement, a new node is inserted between each two coarse grid nodes, and the timestep size is reduced by four. Parameters are given in Table 3.7. The utility values are given at $x = 1$ and $x = 0$. Ratio is the ratio of successive changes in computed solution as the discretization parameters are reduced. CPU time is normalized. We take the CPU time used for the first test ($x = 0$) using Forward/backward differencing only in this table as one unit of CPU time, which uses 87 nodes and 160 timesteps.*

course, this method requires much more CPU time compared to Algorithm (3.6.13). This is simply due to the comparatively crude method used to find the optimal control at each grid node.

In an effort to do better than linear search, we experimented with various approximate methods for finding the optimal control (assuming a discrete set of controls). Seemingly reasonable methods based on smooth approximations to the objective function were very unreliable, and Algorithm (3.5.1) typically failed to converge. This is simply because the smooth approximation may not maximize the local objective function, and hence the

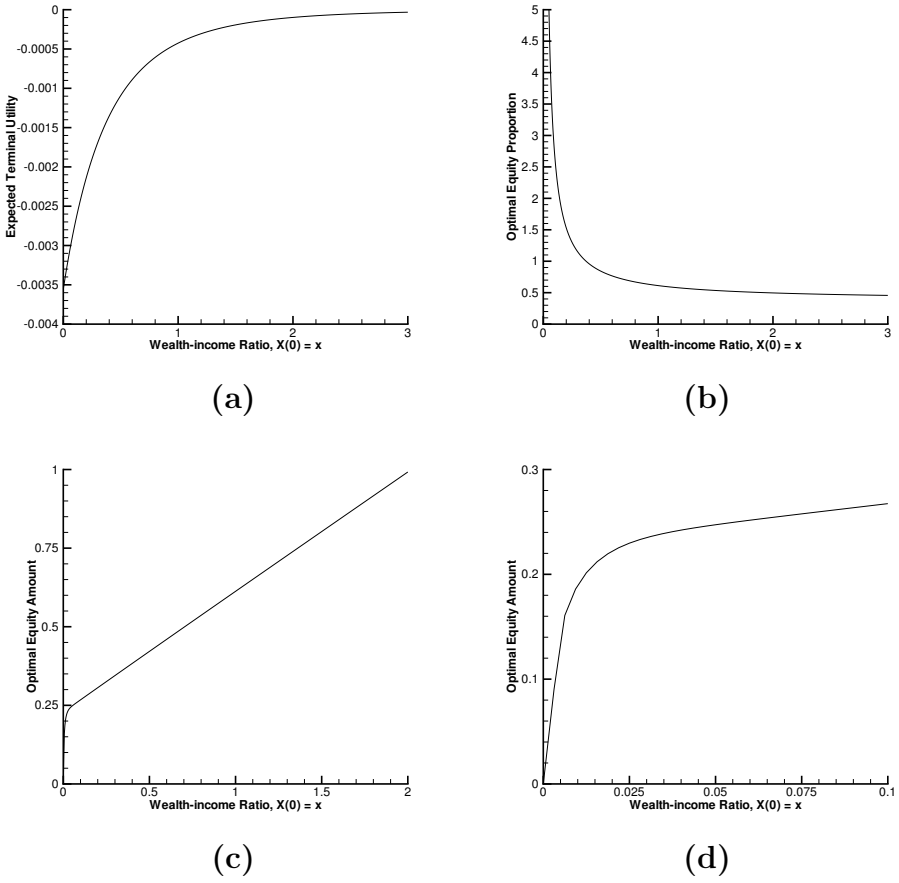

FIGURE 3.2: *Utility and optimal asset allocation strategy at $t = 0$, pension plan example. Parameters are given in Table 3.7. (a) Expected terminal utility; (b) Optimal asset allocation strategy; (c) Optimal equity amount ($p\ x$); (d) Magnified graph of figure (c).*

argument used to prove the convergence of the iteration (Theorem 3.11) breaks down.

3.8 Extension to Multi-dimensional Models

We have fully discussed the solution of one-factor cases. Many financial problems are modelled as multi-factor HJB equations. Our scheme can, in principal, be extended to multi-factor problems. For example, for two-factor models, the operator $\mathcal{L}$ (defined by equation (3.2.1)) changes to

$$\begin{aligned}\mathcal{L}^Q V \equiv\ & a_1(X,Y,\tau,Q)V_{XX} + a_2(X,Y,\tau,Q)V_{YY} + a_3(X,Y,\tau,Q)V_{XY} \\ & + a_4(X,Y,\tau,Q)V_X + a_5(X,Y,\tau,Q)V_Y - a_6(X,Y,\tau,Q)V\ , \end{aligned} \tag{3.8.1}$$

x-Nodes	p-Nodes	Timesteps	Nonlinear iterations	CPU (Sec)	Utility	Ratio
			$x = 0$			
173	113	640	1317	63.5	-3.65307×10^{-3}	
345	225	2560	5146	983.9	-3.58083×10^{-3}	
689	449	10240	20511	15284	-3.56358×10^{-3}	4.19
1377	897	40961	82016	242140	-3.55923×10^{-3}	3.97
			$x = 1.0$			
173	113	640	1317	63.5	-4.31662×10^{-4}	
345	225	2560	5146	983.9	-4.26845×10^{-4}	
689	449	10240	20511	15284	-4.25619×10^{-4}	3.93
1377	897	40961	82016	242140	-4.25306×10^{-4}	3.92

TABLE 3.9: *Convergence study, pension plan example, discretized control. $x-$nodes refers to the number of nodes in the x grid. $p-$nodes refers to the number of nodes in the discretization of the range of control values. Fully implicit timestepping is used with constant timesteps. On each refinement, a new node is inserted between each two coarse grid nodes, and the timestep is reduced by four. Central differencing is used as much as possible. Ratio is the ratio of successive changes in computed solution as the discretization parameters are reduced. CPU time is normalized. We take the CPU time used for the first test ($x = 0$) using Forward/backward differencing only in Table 3.8 as one unit of CPU time, which uses 87 nodes and 160 timesteps. Problem data given in Table 3.7.*

where

$$\begin{bmatrix} a_1 & \frac{a_3}{2} \\ \frac{a_3}{2} & a_2 \end{bmatrix} \tag{3.8.2}$$

is positive semi-definite. Consequently, the general form of our pricing PDE changes to

$$V_\tau = \sup_{Q \in \hat{Q}} \left\{ \mathcal{L}^Q V + d(X, Y, \tau, Q) \right\}$$
$$X \in [X_{\min}, X_{\max}] \ \ , Y \in [Y_{\min}, Y_{\max}] \ \ , 0 \leq \tau \leq T \ . \tag{3.8.3}$$

If we can find a positive coefficient discretization scheme for equation (3.8.3), we can solve this problem using the same methods as described for the single factor case. All the proofs follow without change.

However, the difficulty results from the fact that it is not trivial to find a positive coefficient discretization for the term $a_3 V_{XY}$. One possible approach is discussed in [8], where, if certain grid spacing conditions are satisfied, then a positive coefficient discretization can be obtained if a seven point finite difference method is used to approximate the V_{XY} term (the orientation of the seven point operator depends on the sign of a_3). Note that forward/backward differencing for the first order terms is suggested in [8].

3.9 Summary

Our work in this chapter makes the following contributions:

- We develop a fully implicit finite difference scheme to solve stochastic control problems in finance. Our scheme use central differencing as much as possible, so that use of locally second order method is maximized.
- We prove that our discrete scheme is pointwise consistent, l_∞ stable and monotone so that convergence to viscosity solution is guaranteed.
- Our method satisfies the properties listed in Section 1.1.
- In general, when central differencing is used as much as possible, the local objective function at each grid node is now a discontinuous function of the control. We show that convergence of the iterative method for solution of the discrete equations can be still guaranteed, even if the local objective function is a discontinuous function of the control.
- Numerical examples show that
  (i) the use of a locally second order method as much as possible results in improved convergence as the mesh is refined, for practical parameter values;
  (ii) that the nonlinear iteration converges very quickly, even if the local objective function is a discontinuous function of the control.

Chapter 4

Pre-commitment Strategy

4.1 Introduction

As stated in Section 2.3.1, the continuous time pre-commitment mean variance strategy is time inconsistent. Once the initial strategy has been determined (as a function of the state variables) at the initial time, the investor commits to this strategy, even if the policy computed at a later time would differ from the pre-commitment strategy. Hence, the pre-commitment strategy does not lend itself easily to a dynamic programming formulation. There have been two main approaches to this problem. The original mean variance optimal control problem can be embedded into a class of auxiliary stochastic Linear-Quadratic (LQ) problems, which can then be solved in terms of dynamic programming [78, 49]. Alternatively, Martingale techniques can be used [15]. In the case of the LQ method, previous papers use analytic techniques to solve the nonlinear HJB PDE for special cases. In order to obtain analytic solutions, the authors typically make assumptions which allow for the possibility of unbounded borrowing and infinite negative wealth (bankruptcy). However, some analytic solutions have been developed for handling specific constraints: no stock shorting [51] (but shorting the bond is still allowed) and the no bankruptcy case [15] (but again allowing for shorting the bond).

A popular approach for optimal stochastic control problems in finance is to use utility functions [21, 30, 60, 25, 59]. This approach usually results in financial models in form of HJB PDEs as well. Although investment policy based on mean variance optimization has its critics, an advantage of this approach compared to power-law or exponential utility maximization is that the results can be easily interpreted in terms of an efficient frontier.

The objective of this chapter is to develop a numerical method for solving the continuous time pre-commitment mean variance optimal asset allocation problem. We will use a fully numerical scheme based on solving the HJB equation resulting from the LQ formulation. Our scheme can easily handle any type of constraint (e.g. non-negative wealth, no shorting of stocks, margin requirements).

Although the methods developed in this chapter can be applied to any asset allocation problem, such as those discussed in [61, 15, 28, 75] we will focus on asset allocation

problems which are relevant to the defined contribution pension plan as discussed in [42, 21] (see also Chapter 2). In [42], the objective is to determine the mean variance efficient strategy in terms of final wealth. In [21] and Chapter 3, the problem was formulated in terms of maximizing the utility of the wealth-to-income ratio. Here, we consider the same model, but solve for the optimal continuous time mean variance efficient frontier. Note that by setting the contribution rate to zero, the pension plan problem reduces to the classical continuous time (multi-period) portfolio selection problem [78, 49, 51, 15, 50].

4.2 Pre-commitment Wealth Case

We first consider the problem of determining the pre-commitment strategy for the pension plan asset allocation of the wealth case as introduced in Section 2.2.1. This will allow an explanation of the basic approach for construction of the efficient frontier, without undue algebraic complication. For certain special cases, there are also some analytic solutions available [42] for this problem. This will enable us to compare with the numerical solution.

Recall that we assume there are two assets in the market: one is risk free (e.g. a government bond) and the other is risky (e.g. a stock index). The risky asset S follows the stochastic process (2.2.1), and the investor's wealth W follows the stochastic process (2.2.2).

Recall that p denotes the proportion of this wealth invested in the risky asset S, and $(1-p)$ denotes the fraction of wealth invested in the risk free asset. In general, $p \in (-\infty, +\infty)$. When $p < 0$ this corresponds to shorting the risky asset. When $p > 1$, this corresponds to borrowing (i.e. shorting the risk free asset). In this chapter, we use p as the control.

Given a risk level (defined as the variance of terminal wealth $Var_{t=0,w}[W_T]$), an investor desires her expected terminal wealth $E_{t=0,w}[W_T]$ to be as large as possible. Equivalently, given an expected terminal wealth $E_{t=0,w}[W_T]$, she wishes the risk $Var_{t=0,w}[W_T]$ to be as small as possible. Recall from the pre-commitment optimization problem (2.3.3),

$$\sup_{p(t,w)\in\mathbb{P}} (E^p_{t=0,w}[W_T] - \lambda Var^p_{t=0,w}[W_T]), \tag{4.2.1}$$

subject to stochastic process (2.2.2), where $\mathbb{P}$ is the set of admissible controls. The Lagrange multiplier λ can be interpreted as a coefficient of risk aversion. Varying $\lambda \in [0, \infty)$ allows us to draw an efficient frontier. Note we have emphasized here that the expectations in equation (4.2.1) are as seen at $t = 0$ (the pre-commitment solution).

We would like to use dynamic programming to determine the efficient frontier, given by equation (4.2.1). However, the presence of the variance term causes some difficulty. This can be avoided with the help of the following result [78, 49].

Theorem 4.1. *If $p^*(t,w) \in \mathbb{P}$ is the optimal control of problem (4.2.1), then $p^*(t,w)$ is*

also an optimal control of problem,

$$\sup_{p(t,w)\in\mathbb{P}} E^{p}_{t=0,w}[\mu W_T - \lambda W_T^2] \tag{4.2.2}$$

where

$$\mu = 1 + 2\lambda E^{p^*}_{t=0,w}[W_T] \ . \tag{4.2.3}$$

Proof. See [78, 49]. □

Note that Theorem 4.1 states that the set of controls for the original problem (4.2.1) is a subset of the set of controls for the auxiliary problem (4.2.2). However, if we start with an alternative definition of efficient frontier, then we can show that the two problems are actually equivalent. This equivalence is shown the next section.

4.2.1 Reduction to an LQ Problem

To be more precise here, let

$$\begin{aligned} \mathbb{D} &:= \text{the set of all admissible wealth } W(t), \text{ for } 0 \le t \le T; \\ \mathbb{P} &:= \text{the set of all admissible controls } p(t,w), \text{ for } 0 \le t \le T \text{ and } w \in \mathbb{D}. \end{aligned} \tag{4.2.4}$$

Let $\gamma = \frac{\mu}{\lambda}$, then from equation (4.2.3),

$$\gamma = \frac{1}{\lambda} + 2E^{p^*}_{t=0,w}[W_T] \ . \tag{4.2.5}$$

For a fixed γ, with $\lambda > 0$, equation (4.2.2) is equivalent to

$$\inf_{p(t,w)\in\mathbb{P}} E^{p}_{t=0,w}[(W_T - \frac{\gamma}{2})^2] \ . \tag{4.2.6}$$

Theorem 4.2. *By choosing proper values for λ and γ, $p^*(t,w) \in \mathbb{P}$ is the optimal control of problem (4.2.1), if and only if $p^*(t,w)$ is the optimal control of problem (4.2.6).*

Proof. See Appendix B. □

Corollary 4.3. *By choosing proper values for λ, μ and γ, problems (4.2.1), (4.2.2) and (4.2.6) are equivalent.*

Proof. Problem (4.2.6) is equivalent to problem (4.2.2) by choosing $\gamma = \frac{\mu}{\lambda}$. Problems (4.2.6) and (4.2.1) are equivalent by Theorem 4.2. Hence, the three problems are equivalent. □

Let $K(t,w,p) = E[(W_T - \frac{\gamma}{2})^2 | W(t) = w]$, where $W(t)$ is the path of W given the asset allocation strategy $p = p(t,w)$. We define

$$V(w,\tau) = \inf_{p \in \mathbb{P}} E[(W_T - \frac{\gamma}{2})^2 | W(t = T - \tau) = w] = \inf_{p \in \mathbb{P}} K(t = T - \tau, w, p) \ . \tag{4.2.7}$$

where $\tau = T - t$. Then using equation (2.2.2) and Ito's Lemma, we have that $V(w,\tau)$ satisfies the HJB equation

$$V_\tau \ = \ \inf_{p \in \mathbb{P}} \{ \mu_w^p V_w + \frac{1}{2} (\sigma_w^p)^2 V_{ww} \} \ \ ; \ \ w \in \mathbb{D}, \tag{4.2.8}$$

with terminal condition

$$V(w, \tau = 0) = (w - \frac{\gamma}{2})^2 \ , \tag{4.2.9}$$

and where

$$\begin{aligned} \mu_w^p &= \pi + w(r + p\sigma_1 \xi_1) \\ (\sigma_w^p)^2 &= (p\sigma_1 w)^2 \ . \end{aligned} \tag{4.2.10}$$

In order to trace out the efficient frontier solution of problem (4.2.1), we proceed in the following way. Pick an arbitrary value of γ and solve problem (4.2.6), which determines the optimal control $p^*(t,w)$. We also need to determine $E^{p^*}_{t=0,w}[W_T]$.

Let $U = U(w,\tau) = E[W_T | W(t = T - \tau) = w, p(t = T - \tau, w) = p^*(t = T - \tau, w)]$. Then U is given from the solution to

$$U_\tau = \{ \mu_w^p U_w + \frac{1}{2} (\sigma_w^p)^2 U_{ww} \}_{p(t=T-\tau,w) = p^*(t=T-\tau,w)} \ \ ; \ \ w \in \mathbb{D} \ , \tag{4.2.11}$$

with the payoff

$$U(w, \tau = 0) = w \ . \tag{4.2.12}$$

Since the most costly part of the solution of equation (4.2.8) is the determination of the optimal control p^*, the solution of equation (4.2.11) is very inexpensive, since p^* is known.

Note that $E^{p^*}_{t=0,w}[const.] = const.$. Assume that $W = \hat{w}_0$ at $t = 0$. Then

$$\begin{aligned} V(\hat{w}_0, \tau = T) &= E^{p^*}_{t=0,w}[W_T^2] - \gamma E^{p^*}_{t=0,w}[W_T] + \frac{\gamma^2}{4} \ , \\ U(\hat{w}_0, \tau = T) &= E^{p^*}_{t=0,w}[W_T] \ . \end{aligned} \tag{4.2.13}$$

Assuming $V(\hat{w}_0, \tau = T), U(\hat{w}_0, \tau = T)$ are known, then for a given γ, we can then compute the pair $(Var^{p^*}_{t=0,w}[W_T], E^{p^*}_{t=0,w}[W_T])$ from $Var^{p^*}_{t=0,w}[W_T] = E^{p^*}_{t=0,w}[W_T^2] - (E^{p^*}_{t=0,w}[W_T])^2$.

From equation (4.2.5) we have that

$$\frac{1}{2\lambda} = \frac{\gamma}{2} - E^{p^*}_{t=0,w}[W_T] \ , \tag{4.2.14}$$

which then determines the value of λ in problem (4.2.1). In other words, we have determined the pair $(\text{Std}^{p^*}_{t=0,w}[W_T], E^{p^*}_{t=0,w}[W_T])$ for the optimal control p^* which solves problem (4.2.1), with the value of λ given from equation (4.2.14).

We then pick another value of γ, and obtain another point on the efficient frontier for another value of λ, and so on. Note that we are effectively using the parameter γ to trace out the efficient frontier. Since $\lambda > 0$, we must have (from equation (4.2.14))

$$\frac{\gamma}{2} - E^{p^*}_{t=0,w}[W_T] > 0 \tag{4.2.15}$$

for a valid point on the frontier.

Remark 4.4. *If we allow an unbounded control set $\mathbb{P} = (-\infty, +\infty)$, then the total wealth can become negative (i.e. bankruptcy is allowed). In this case $\mathbb{D} = (-\infty, +\infty)$. If the control set $\mathbb{P}$ is bounded, i.e. $\mathbb{P} = [p_{\min}, p_{\max}]$, then negative wealth is not possible, in which case $\mathbb{D} = [0, +\infty)$. We can also have $p_{max} \to +\infty$, but prohibit negative wealth, in which case $\mathbb{D} = [0, +\infty)$ as well.*

4.3 Localization

Let,

$$\hat{\mathbb{D}} \quad := \quad \text{a finite computational domain which approximates the set } \mathbb{D}. \tag{4.3.1}$$

In order to solve the PDEs (4.2.8), (4.2.11) we need to use a finite computational domain, $\hat{\mathbb{D}} = [w_{\min}, w_{\max}]$. When $w \to \pm\infty$, we assume that

$$\begin{aligned} V(w \to \pm\infty, \tau) &\simeq H_1(\tau)w^2 + H_2(\tau)w + H_3(\tau) \ , \\ U(w \to \pm\infty, \tau) &\simeq J_1(\tau)w + J_2(\tau) \ . \end{aligned} \tag{4.3.2}$$

Then, taking into account the initial conditions (4.2.9), (4.2.12),

$$\begin{aligned} V(w \to \pm\infty, \tau) &\simeq e^{(2k_1+k_2)\tau}w^2 \ , \\ U(w \to \pm\infty, \tau) &\simeq e^{k_1\tau}w \ , \end{aligned} \tag{4.3.3}$$

where $k_1 = r + p\sigma_1\xi_1$ and $k_2 = (p\sigma_1)^2$. We consider three cases.

4.3.1 Allowing Bankruptcy, Unbounded Controls

In this case, we assume there are no constraints on $W(t)$ or on the control p, i.e., $\mathbb{D} = (-\infty, +\infty)$ and $\mathbb{P} = (-\infty, +\infty)$. Since $W(t) = w$ can be negative, bankruptcy is allowed. We call this case the *allowing bankruptcy* case.

Our numerical problem uses

$$\hat{\mathbb{D}} \quad = \quad [w_{\min}, w_{\max}] \ , \tag{4.3.4}$$

where $\hat{\mathbb{D}} = [w_{\min}, w_{\max}]$ is an approximation to the original set $\mathbb{D} = (-\infty, +\infty)$.

As far as the Dirichlet conditions at $w = w_{\min}, w_{\max}$, we can use the asymptotic form of the exact solution (see Section 4.3.4) to note that

$$p^*(t, w \to \pm\infty) \simeq -\frac{\xi_1}{\sigma_1} \ . \tag{4.3.5}$$

At $w = w_{\min}, w_{\max}$ we apply the Dirichlet conditions (4.3.3) with $p = p^*$ from equation (4.3.5).

These artificial boundary conditions will cause some error. However, we can make these errors small by choosing large values for $(|w_{\min}|, w_{\max})$. We will verify this in some subsequent numerical tests. If asymptotic forms of the solution are unavailable, we can use any reasonable estimate for p^* for $|w|$ large, and the error will be small if $(|w_{\min}|, w_{\max})$ are sufficiently large [7].

4.3.2 No Bankruptcy, No Short Sales

In this case, we assume that bankruptcy is prohibited and the investor cannot short the stock index, i.e., $\mathbb{D} = [0, +\infty)$ and $\mathbb{P} = [0, +\infty)$. We call this case the *no bankruptcy* (or *bankruptcy prohibition*) case.

Our numerical problem uses,

$$\hat{\mathbb{D}} \ = \ [0, w_{\max}] \ . \tag{4.3.6}$$

We make the assumption that $p^*(t, w_{\max}) \simeq 0$ (i.e. once the investor's wealth is very large, she prefers the riskless asset). The boundary conditions for V, U at $w = w_{\max}$ are given by equations (4.3.3) with $p = 0, w = w_{\max}$. We prohibit the possibility of bankruptcy $(W(t) < 0)$ by requiring that (see Remark 4.5) $\lim_{w\to 0}(pw) = 0$, so that equations (4.2.8), (4.2.11) reduce to (at $w = 0$)

$$\begin{aligned} V_\tau(0, \tau) &= \pi V_w \ , \\ U_\tau(0, \tau) &= \pi U_w \ . \end{aligned} \tag{4.3.7}$$

4.3.3 No Bankruptcy, Bounded Control

This is a realistic case, in which we assume that bankruptcy is prohibited and infinite borrowing is not allowed. As a result, $\mathbb{D} = [0, +\infty)$ and $\mathbb{P} = [0, p_{\max}]$. We call this case the *bounded control* case.

Our numerical problem uses,

$$\hat{\mathbb{D}} \ = \ [0, w_{\max}] \ , \tag{4.3.8}$$

where $w_{\max}$ is an approximation to the infinity boundary. Other assumptions and the boundary conditions for V and U are the same as those of no bankruptcy case introduced in Section 4.3.2.

We summarize the various cases in Table 4.1

Case	$\hat{\mathbb{D}}$	$\mathbb{P}$
Bankruptcy	$[w_{\min}, w_{\max}]$	$(-\infty, +\infty)$
No Bankruptcy	$[0, w_{\max}]$	$[0, +\infty)$
Bounded Control	$[0, w_{\max}]$	$[0, p_{\max}]$

TABLE 4.1: *Summary of cases.*

4.3.4 Analytic Solution: Unconstrained Control

Suppose that the control $p(t, w)$ is unbounded, i.e. $\mathbb{P} = (-\infty, +\infty)$. This allows infinite shorting of the risky asset and the bond. This also allows for bankruptcy, which means that $\mathbb{D} = (-\infty, +\infty)$. This is the case of *allowing bankruptcy* introduced in Section 4.3.1.

The analytic solution to this problem is given in [42],

$$\begin{cases} Var^{p}_{t=0,w}[W_T] = \frac{e^{\xi_1^2 T}-1}{4\lambda^2} \\ E^{p}_{t=0,w}[W_T] = \hat{w}_0 e^{rT} + \pi \frac{e^{rT}-1}{r} + \sqrt{e^{\xi_1^2 T}-1}\text{Std}(W_T) \ , \end{cases} \tag{4.3.9}$$

and the optimal control at any time $t \in [0, T]$ is

$$p^*(t, w) = -\frac{\xi_1}{\sigma_1 w}[w - (\hat{w}_0 e^{rt} + \frac{\pi}{r}(e^{rt} - 1)) - \frac{e^{-r(T-t)+\xi_1^2 T}}{2\lambda}] \ . \tag{4.3.10}$$

Note that when $|w| \to 0$, from equation (4.3.10), $p^*(t, w)w$, the monetary amount invested in the risky asset, is a positive finite number, and that $|p^*(t, w)| \to \infty$ as $|w| \to 0$.

We can then see directly from the SDE (2.2.2), that $W(t)$ can be negative in this case. Hence, $\mathbb{D} = (-\infty, +\infty)$. From equation (4.3.10), when w is negative, $p^*(t, w)$ is negative. As a result, $p^*(t, w)w$ is positive, i.e., the total monetary amount invested in stock is still positive (the investor is long stock).

The efficient frontier $(\text{Std}^{p^*}_{t=0,w}[W_T], E^{p^*}_{t=0,w}[W_T])$ in this case is a straight line (equation (4.3.9)). We will use this analytic result to check our numerical solution.

Remark 4.5. *It is important to know the behaviour of p^*w as $w \to 0$, since it helps us determine whether negative wealth is admissible or not. As shown above, negative wealth is admissible for the case of allowing bankruptcy. In the case of no bankruptcy, although $p \in \mathbb{P} = [0, +\infty)$, we must have $\lim_{w\to 0}(pw) = 0$ so that $W(t) \geq 0$ for all $0 \leq t \leq T$. In particular, we need to make sure that the optimal strategy never generates negative wealth, i.e., Probability$(W(t) < 0|p^*) = 0$ for all $0 \leq t \leq T$. We will see from the*

numerical solutions that boundary condition (4.3.7) does in fact result in $\lim_{w\to 0}(p^*w) = 0$. *Hence, negative wealth is not admissible under the optimal strategy. More discussion of this issue is given in Section 4.7. For the bounded control case, the control is finite, thus* $\lim_{w\to 0}(pw) = 0$ *and negative wealth is not admissible.*

4.3.5 Special Case: Reduction to the Classic Multi-period Portfolio Selection Problem

As discussed in Remark 2.1, the wealth case of the pension plan problem can be reduced to the classic multi-period portfolio selection problem by simply setting the contribution rate $\pi = 0$. All equations and boundary conditions stay the same.

The authors of [15] study the case with bankruptcy prohibition, i.e., $W(t)$ is forced to be nonnegative for all $t \in [0, T]$. In this case, $\mathbb{D} = [0, +\infty)$ and $\mathbb{P} = [0, +\infty)$. An analytic solution for this case is given in [15]. Note that the stochastic control used in [15] is not the proportion of the total wealth invested in the stock, but the monetary amount invested in the stock. The authors of [15] point out that their strategy cannot be expressed as a finite proportional strategy. However, we will see later in Section 4.7 that the efficient frontier given by our approach (using the proportion as the control) converges to the analytic solution given in [15] (using the monetary amount as the control).

4.4 Pre-commitment Wealth-to-income Ratio Case

We then consider the wealth-to-income ratio case introduced in Section 2.2.2. The stochastic models for the underlying asset S, the plan holder's year salary Y, the wealth W and her wealth-to-income ratio X have been given in equations (2.2.4 - 2.2.7).

The control problem is then to determine the control $p(t, X(t) = x)$ such that $p(t, x)$ maximizes

$$\max_{p(t,x)\in\mathbb{P}} (E^p_{t=0,x}[X_T] - \lambda Var^p_{t=0,x}[X_T]) \ , \tag{4.4.1}$$

subject to stochastic process (2.2.7). Similar to problem (4.2.1), we can use Theorem 4.1 and 4.2 to embed problem (4.4.1) into the following LQ stochastic optimal control problem

$$\min_{p(t,x)\in\mathbb{P}} E^p_{t=0,x}[(X_T - \frac{\gamma}{2})^2] \ . \tag{4.4.2}$$

Let $K(t, x, p) = E[(X_T - \frac{\gamma}{2})^2 | X(t) = x]$, where $X(t)$ is the path of X given the asset allocation strategy $p = p(t, x)$. We define

$$V(x, \tau) = \inf_{p\in\mathbb{P}} E[(X_T - \frac{\gamma}{2})^2 | X(t = T - \tau) = x] = \inf_{p\in\mathbb{P}} K(t = T - \tau, x, p) \ . \tag{4.4.3}$$

where $\tau = T - t$. Then $V(x,\tau)$ satisfies the HJB equation

$$V_\tau = \inf_{p\in\mathbb{P}}\{\mu_x^p V_x + \frac{1}{2}(\sigma_x^p)^2 V_{xx}\} \;\; ; \;\; x \in [0,+\infty) \; , \tag{4.4.4}$$

with terminal condition

$$V(x,\tau=0) = (x - \frac{\gamma}{2})^2 \; , \tag{4.4.5}$$

and where

$$\begin{aligned} \mu_x^p &= \pi + x(-\mu_Y + p\sigma_1(\xi_1 - \sigma_{Y_1}) + \sigma_{Y_0}^2 + \sigma_{Y_1}^2) \\ (\sigma_x^p)^2 &= x^2(\sigma_{Y_0}^2 + (p\sigma_1 - \sigma_{Y_1})^2) \; . \end{aligned} \tag{4.4.6}$$

We also solve for $U(x,\tau) = E[X_T | X(t = T-\tau) = x, p(t = T-\tau, x) = p^*(t = T-\tau, x)]$ using

$$U_\tau = \{\mu_x^p U_x + \frac{1}{2}(\sigma_x^p)^2 U_{xx}\}_{p(t=T-\tau,x)=p^*(t=T-\tau,x)} \;\; ; \;\; x \in [0,+\infty) \; , \tag{4.4.7}$$

with terminal condition

$$U(x,\tau=0) = x \; . \tag{4.4.8}$$

We can then use the method described in Section 4.2.1 to trace out the efficient frontier solution of problem (4.4.1).

We consider the cases: allowing bankruptcy ($\mathbb{D} = (-\infty,+\infty)$, $\mathbb{P} = (-\infty,+\infty)$), no bankruptcy ($\mathbb{D} = [0,+\infty)$, $\mathbb{P} = [0,+\infty)$), and bounded control ($\mathbb{D} = [0,+\infty)$, $\mathbb{P} = [0, p_{\max}]$). For computational purposes, we localize the problem to to $\hat{\mathbb{D}} = [x_{\min}, x_{\max}]$, and apply boundary conditions as in Section 4.3. More precisely, if $x = 0$ is a boundary, with $X < 0$ prohibited, then $\lim_{w\to 0}(px) = 0$, and hence

$$\begin{aligned} V_\tau(0,\tau) &= \pi V_x \; , \\ U_\tau(0,\tau) &= \pi U_x \; . \end{aligned} \tag{4.4.9}$$

The boundary conditions at $x \to \pm\infty$ are given in equation (4.3.3), but using x instead of w with $k_1 = -\mu_Y + p\sigma_1(\xi_1 - \sigma_{Y_1}) + \sigma_{Y_0}^2 + \sigma_{Y_1}^2$ and $k_2 = \sigma_{Y_0}^2 + (p\sigma_1 - \sigma_{Y_1})^2$.

Remark 4.6. *Although the pension plan account contains the risk free bond, the stochastic process for dX does not contain the risk free rate r. As a result, there is no risk free rate r in the HJB PDE (4.4.4). The drift rate (mean growth rate) for the yearly salary Y is $r + \mu_Y$ in equation (2.2.5). If Y grows faster than the risk free rate, then $\mu_Y > 0$; otherwise $\mu_Y \leq 0$. Normally, we assume that the salary Y grows at the risk free rate, so $\mu_Y = 0$.*

Remark 4.7. *As discussed in Remark 2.2 that the wealth case can be seen as a special case of the wealth-to-income ratio case. We can simply set the salary Y to be a constant*

(let $\sigma_{Y_0} = \sigma_{Y_1} = 0$ and $\mu_Y = -r$), then $X(t)$ is reduced to $W(t)$ and PDE (4.4.4) is reduced to PDE (4.2.8).

4.5 Discretization of the HJB PDE

The pension plan asset allocation model is a special case of the general HJB equation (3.2.2), if we make the identification

$$\begin{aligned} &Q = (p) \ , \quad \hat{Q} = \mathbb{P} \ , \quad d(z,\tau,0) = 0 \ , \\ &a(z,\tau,Q) = \frac{1}{2}(\sigma_z^p)^2 \ , \quad b(z,\tau,Q) = \mu_z^p, \quad c(z,\tau,Q) = 0 \ , \end{aligned} \tag{4.5.1}$$

where $z = w$ for the wealth case, $z = x$ for the wealth-to-income ratio case, and $Q,\ a,\ b,\ c$ are defined in equation (3.2.2). Then equation (4.2.8)/(4.4.4) can be written as,

$$V_\tau = \inf_{Q \in \hat{Q}} \{\mathcal{L}^Q V\} \ , \tag{4.5.2}$$

and equation (4.2.11)/(4.4.7) can be written as,

$$U_\tau = \{\mathcal{L}^Q U\}_{Q=Q^*} \ . \tag{4.5.3}$$

where the operator $\mathcal{L}$ is defined in equation (3.2.1). Note that we use inf in this chapter instead of sup in Chapter 3. We can directly apply the numerical scheme developed in Chapter 3 to solve equations (4.5.2) and (4.5.3).

Given node $z = z_i$, with specified solution estimate $\hat{V}^k = [\hat{v}_0^k, ..., \hat{v}_{imax}^k]'$, the objective function which is maximized at each node in Algorithm (3.5.1) is

$$\begin{aligned} [F^{n+1}(Q,\hat{V}^k)]_i &= [A^{n+1}(Q,\hat{V}^k)\hat{V}^k + D(Q)]_i \\ &= [\mu_z^p]_i[(\hat{v}^k)_z]_i + \frac{1}{2}([\sigma_z^p]_i)^2[(\hat{v}^k)_{zz}]_i^{n+1} \ , \end{aligned} \tag{4.5.4}$$

where $\hat{V}^k$ is the vector containing the current estimate of the discrete solution values, and $D(Q) = 0$. Similar to the passport option case in Chapter 3, if we want to apply central differencing as much as possible, Algorithm (3.6.13) is used to decide which differencing scheme is used (which depends on Q and $\hat{V}^k$).

Remark 4.8. *As mentioned in Remark 4.4, for the wealth case with allowing bankruptcy, we have $\mathbb{D} = (-\infty, +\infty)$ and $\mathbb{P} = (-\infty, +\infty)$. In this case, our W grid contains*

$$\begin{aligned} &[w_{min}, \ldots, w_{-2}, w_{-1}, w_1, w_2, \ldots, w_{max}] \\ &w_{min} < \cdots < w_{-2} < w_{-1} < 0 < w_1 < w_2 < \cdots < w_{max} \end{aligned} \tag{4.5.5}$$

with large $|w_{min}|$ and w_{max}. Note that our W grid does not contain the node $w = 0$, because if $w = 0$ is in the grid, no information can be passed between the negative value nodes and positive value nodes. We set $|w_{-1}|$ and w_1 to be small values close to zero. As

Figure 4.1 shows, when the W grid is refined, a new node is inserted in between each two consecutive nodes, except for the pair w_{-1} and w_1. Since $w = 0$ cannot be in the grid, we add two nodes at $w_{-1}^{new} = \frac{w_{-1}}{2}$ and $w_1^{new} = \frac{w_1}{2}$ into the grid.

Note that we could avoid this problem (near $w = 0$) by defining the control to be amount invested in the risky asset ($a = pw$) instead of p. This would result in a control problem of the form

$$\begin{aligned} V_\tau &= \inf_{a\in\mathbb{A}}\{\mu_w^a V_w + \frac{1}{2}(\sigma_w^a)^2 V_{ww}\} \quad ; \quad w \in \mathbb{D}, \\ &\quad \mu_w^a = \pi + wr + a\sigma_1\xi_1 \\ &\quad (\sigma_w^a)^2 = (a\sigma_1)^2 \quad , \end{aligned} \tag{4.5.6}$$

where $\mathbb{A}$ is the set of admissible controls for the amount invested in the risky asset. However, in the more realistic case of bounded p, it is more natural to impose constraints on p, rather than on (pw), hence we prefer to formulate the control (and constraints) in terms of the variable p.

Remark 4.9. *We use a fully implicit method to solve equation (4.5.2). Since $p \to \infty$ in some cases, it would be a challenging task to determine the maximum stable timestep for an explicit method.*

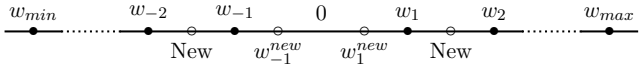

FIGURE 4.1: *Node insertion in W grid.*

4.5.1 Convergence to the Viscosity Solution

Assumption 4.10 (Strong Comparison)**.** We assume that equation (4.5.2) satisfies the strong comparison property, hence a unique continuous viscosity solution to equation (4.5.2) exists.

PDE (4.5.3) is linear, since the optimal control is pre-computed. We can then obtain a classical solution of the linear PDE (4.5.3). However, PDE (4.5.2) is highly nonlinear, so the classical solution may not exist in general. Provided that the original HJB satisfies Assumption 4.10, Theorem 3.5 shows that our numerical scheme converges to the viscosity solution.

Remark 4.11. *If the control p is bounded, then from the results in [24, 9] we can deduce that Equation (4.5.2) satisfies the strong comparison property on the localized computational domain $\hat{\mathbb{D}}$ (see Remark 3.3). In the unbounded control case, we violate one of the assumptions in [9] used in the proof of the strong comparison property. However, our*

numerical results indicate that (pw) is always bounded. Hence, in the unbounded control case, we could reformulate the problem in terms of a control (pw), and solve the problem with assumed bounds on (pw), which would then satisfy the conditions in [9]. However, it is not obvious how to obtain a priori *bounds for (pw). In practical cases, we are more interested in bounded controls, so in this case we have that strong comparison holds.*

4.6 Algorithm for Construction of the Efficient Frontier

Given an initial value $\hat{z}_0$, Algorithm (4.6.1) is used to obtain the efficient frontier. Since the grid for Z is discretized over the interval $[z_{min}, z_{max}]$, we can use Algorithm (4.6.1) to obtain the efficient frontier for any initial wealth $\hat{z}_0 \in [z_{min}, z_{max}]$ by interpolation. Of course, if we choose $\hat{z}_0$ to be a node in the discretized Z grid, then there is no interpolation error.

Algorithm for Constructing the Efficient Frontier

For $\gamma = \gamma_{min}, \gamma_1, \ldots, \gamma_{max}$
  For timestep $n = 1, \ldots, N$
    Solve equation (3.3.9) by using policy iteration (3.5.1)
    Solve PDE (4.5.3) // Q^* is given from the solution of equation (3.3.9)
  EndFor
  Given the initial $\hat{z}_0$, use interpolation to get the value of

$$(E^{p^*}_{t=0,z}[Z_T], E^{p^*}_{t=0,z}[(Z_T - \frac{\gamma}{2})^2])_\gamma \text{ at } Z(t=0) = \hat{z}_0$$

  If $(\frac{\gamma}{2} - E^{p^*}_{t=0,z}[Z_T]_\gamma > 0)$ // possible valid point $\lambda > 0$
    Solve equations (4.2.13) to get $(E^{p^*}_{t=0,z}[Z_T], E^{p^*}_{t=0,z}[Z_T^2])_\gamma$
    Calculate the pair $(\mathrm{Std}^{p^*}_{t=0,z}[Z_T], E^{p^*}_{t=0,z}[Z_T])_\gamma$
  EndIf
EndFor
Construct the efficient frontier from the set of points

$$(\mathrm{Std}^{p^*}_{t=0,z}[Z_T], E^{p^*}_{t=0,z}[Z_T])_\gamma, \gamma \in [\gamma_{\min}, \gamma_{\max}] \tag{4.6.1}$$

In Algorithm (4.6.1), we trace out the efficient frontier by varying $\gamma \in [\gamma_{min}, \gamma_{max}]$. Heuristic methods can be used to estimate $\gamma_{min}, \gamma_{max}$. These choices are not crucial, since we will detect invalid values of γ from the condition that $\lambda > 0$. For example, in the wealth case, to determine γ_{min}, we consider the left most point on the efficient frontier.

If $\lambda \to \infty$, then the investor seeks to minimize risk. Obviously, in this case, the investor would invest all her wealth in the risk free bond at all times. In this case, her terminal wealth would be $\hat{w}_0 e^{rT} + \pi \frac{e^{rT}-1}{r}$ with zero standard deviation. Then theoretically,

$$\gamma_{min} = 2(\hat{w}_0 e^{rT} + \pi \frac{e^{rT}-1}{r}) \ . \tag{4.6.2}$$

There is no upper bound for γ. In particular, if there is no upper bound for the control p, there are no upper bounds for $\text{Std}^{p^*}_{t=0,w}[W_T]$ and $E^{p^*}_{t=0,w}[W_T]$ either. From our numerical tests, we find that $\gamma_{max} = 50$ is large enough to plot the efficient frontier over a reasonable range of interest.

4.7 Numerical Results

In this section, we carry out numerical tests for the defined contribution pension plan problem. We examine both the wealth case (addressed in Section 4.2) and the wealth-to-income ratio case (addressed in Section 4.4).

4.7.1 Wealth Case

4.7.1.1 Allowing Bankruptcy

r	0.03	ξ_1	0.33
σ_1	0.15	π	0.1
T	20 years	$W(t=0)$	1

TABLE 4.2: *Parameters used in the pension plan examples.*

We first examine the wealth case with bankruptcy allowed. Parameters in Table 4.2 are used for numerical tests. We use $w_{\max} = |w_{\min}| = 5925$ and $tolerance = 10^{-6}$ (see Algorithm (3.5.1)). We test a special case first, in which the variance is zero ($\lambda \to +\infty$). From equation (4.3.9), the analytic solution is $(\text{Std}^{p^*}_{t=0,w}[W_T], E^{p^*}_{t=0,w}[W_T]) = (0, 4.5625)$. Moreover, in this case, $\gamma = 2E^{p^*}_{t=0,w}[W_T]$, so $E^{p^*}_{t=0,w}[(W_T - \frac{\gamma}{2})^2] = 0$. We use a finite difference method with fully implicit timestepping to solve this problem numerically. We analytically determine the local optimal control at each node (as required in Algorithm 3.5.1).

Table 4.3 and 4.4 show the numerical results. Table 4.3 reports the value of $E^{p^*}_{t=0,w}[(W_T - \frac{\gamma}{2})^2]$, which is the viscosity solution of nonlinear HJB PDE (4.2.8). Table 4.4 reports the value of $E^{p^*}_{t=0,w}[W_T]$, which is the solution of the linear PDE (4.2.11). Given $E^{p^*}_{t=0,w}[(W_T - \frac{\gamma}{2})^2]$ and $E^{p^*}_{t=0,w}[W_T]$, the standard deviation is can be easily computed, which is also reported in Table 4.4. The results show that the numerical solutions of $E^{p^*}_{t=0,w}[(W_T - \frac{\gamma}{2})^2]$

and $E^{p^*}_{t=0,w}[W_T]$ converge to the analytic values at a first order rate as mesh and timestep size tends to zero. Let

$$\max_i(w_{i+1} - w_i) = O(h) \quad ; \quad \Delta\tau \quad = \quad O(h) \tag{4.7.1}$$

where h is the discretization parameter, then from Table 4.4, we see that the standard deviation converges at a rate $O(h^{1/2})$. The total number of nonlinear iterations shown in Table 4.3 is about two or three times of the number of timesteps. Hence, the iteration scheme (3.5.1) converges rapidly.

Nodes (W)	Timesteps	Nonlinear iterations	Normalized CPU Time	$E^{p^*}_{t=0,w}[(W_T - \frac{\gamma}{2})^2]$	Ratio
728	160	480	1	0.0818318	
1456	320	960	4.42	0.0409428	
2912	640	1295	13.21	0.0204766	1.998
5824	1280	2561	52.82	0.0102394	1.999
11648	2560	5120	213.98	0.0051200	2.000
23296	5120	10240	888.49	0.0025601	2.000

TABLE 4.3: *Convergence study. Use analytic solution for the optimal control at each node. Fully implicit timestepping is applied, using constant timesteps. Parameters are given in Table 4.2, with* $\gamma = 9.125$. *Values of* $E^{p^*}_{t=0,w}[(W_T - \frac{\gamma}{2})^2]$ *are reported at* $(W = 1, t = 0)$. *Ratio is the ratio of successive changes in the computed values for decreasing values of the discretization parameter* h. *Analytic solution is* $E^{p^*}_{t=0,w}[(W_T - \frac{\gamma}{2})^2] = 0$. *CPU time is normalized. We take the CPU time used for the first test in this table as one unit of CPU time, which uses 728 nodes for the* W *grid and 160 timesteps.*

Nodes (W)	Timesteps	$\text{Std}^{p^*}_{t=0,w}[W_T]$	$E^{p^*}_{t=0,w}[W_T]$	Ratio for $\text{Std}^{p^*}_{t=0,w}[W_T]$	Ratio for $E[W_T]$
728	160	0.285617	4.54653		
1456	320	0.202202	4.55494		
2912	640	0.143039	4.55845	1.410	2.396
5824	1280	0.101166	4.56031	1.413	1.887
11648	2560	0.071547	4.56148	1.414	1.590
23296	5120	0.050595	4.56200	1.414	2.250

TABLE 4.4: *Convergence study. Use analytic solution for the optimal control at each node. Fully implicit timestepping is applied, using constant timesteps. Parameters are given in Table 4.2, with* $\gamma = 9.125$. *Values of* $Std^{p^*}_{t=0,w}[W_T]$ *and* $E^{p^*}_{t=0,w}[W_T]$ *are reported at* $(W = 1, t = 0)$. *Ratio is the ratio of successive changes in the computed values for decreasing values of the discretization parameter* h. *Analytic solution is* $(Std^{p^*}_{t=0,w}[W_T], E^{p^*}_{t=0,w}[W_T]) = (0.0, 4.5625)$.

For another example, let $\lambda = 1.72646$ in problem (4.2.1). The analytic solution given by equation (4.3.9) is $(\text{Std}^{p^*}_{t=0,w}[W_T], E^{p^*}_{t=0,w}[W_T]) = (0.8307, 6.9454)$. Tables 4.5 and 4.6

show the numerical results. The numerical solutions for $E^{p^*}_{t=0,w}[(W_T-\frac{\gamma}{2})^2]$ and $E^{p^*}_{t=0,w}[W_T]$ converge to the analytic solution at a first order rate as $h \to 0$. We also carried out a convergence study using Crank-Nicholson timestepping. In this case, convergence cannot be guaranteed, since Crank-Nicholson is not monotone in general. The numerical results are shown in Table 4.7 and 4.8. Tables 4.5 and 4.7 show that the value function appears to converge more rapidly using Crank-Nicholson. Figure 4.2 shows an efficient frontier at $(W = 1, t = 0)$, which is a straight line as expected.

Nodes (W)	Timesteps	Nonlinear iterations	Normalized CPU Time	$E^{p^*}_{t=0,w}[(W_T-\frac{\gamma}{2})^2]$	Ratio
728	160	480	1.11	0.934593	
1456	320	855	4.05	0.852331	
2912	640	1280	12.95	0.812095	2.045
5824	1280	2560	54.16	0.792530	2.057
11648	2560	5120	222.56	0.783030	2.059

TABLE 4.5: *Convergence study. Use analytic solution for the optimal control at each node. Fully implicit timestepping is applied, using constant timesteps. Parameters are given in Table 4.2, with* $\lambda = 1.72646$ *(*$\gamma = 14.47$*). Values of* $E^{p^*}_{t=0,w}[(W_T-\frac{\gamma}{2})^2]$ *are reported at* $(W = 1, t = 0)$*. Ratio is the ratio of successive changes in the computed values for decreasing values of the discretization parameter* h*. CPU time is normalized. We take the CPU time used for the first test in Table 4.3 as one unit of CPU time, which uses 728 nodes for the* W *grid and 160 timesteps.*

Nodes (W)	Timesteps	$\text{Std}^{p^*}_{t=0,w}[W_T]$	$E^{p^*}_{t=0,w}[W_T]$	Ratio for $\text{Std}^{p^*}_{t=0,w}[W_T]$	Ratio for $E[W_T]$
728	160	0.915441	6.92426		
1456	320	0.872917	6.93442		
2912	640	0.851483	6.93992	1.975	1.847
5824	1280	0.840821	6.94251	2.007	2.124
11648	2560	0.835612	6.94383	2.045	1.962

TABLE 4.6: *Convergence study. Use analytic solution of the optimal control at each node. Fully implicit timestepping is applied, using constant timesteps. Parameters are given in Table 4.2, with* $\lambda = 1.72646$ *(*$\gamma = 14.47$*). Values of* $\text{Std}^{p^*}_{t=0,w}[W_T]$ *and* $E^{p^*}_{t=0,w}[W_T]$ *are reported at* $(W = 1, t = 0)$*. Ratio is the ratio of successive changes in the computed values for decreasing values of the discretization parameter* h*. Analytic solution:* $(\text{Std}^{p^*}_{t=0,w}[W_T], E^{p^*}_{t=0,w}[W_T]) = (0.8307, 6.9454)$*.*

Note that according to equation (4.3.9), if the market price of risk ξ_1 is fixed, the value of stock volatility σ_1 has no effect on the efficient frontier. When we reproduce Table 4.3, 4.4, 4.5 and 4.6 by using parameters in Table 4.2 but with different volatilities σ_1, we obtain the same solutions. Hence, our numerical solutions agree with this property. However, we will see in later sections that this property may not hold when additional constraints are added to the optimal policy.

Nodes (W)	Timesteps	Nonlinear iterations	Normalized CPU Time	$E^{p^*}_{t=0,w}[(W_T - \frac{\gamma}{2})^2]$	Ratio
728	160	480	1.37	0.806889	
1456	320	727	3.86	0.786974	
2912	640	1280	14.48	0.778982	2.492
5824	1280	2560	58.45	0.775851	2.553
11648	2560	5120	236.27	0.774658	2.624

TABLE 4.7: *Convergence study. Use analytic solution for the optimal control at each node. Crank-Nicholson timestepping with Rannacher smoothing is applied, using constant timesteps. Parameters are given in Table 4.2, with* $\lambda = 1.72646$ *(*$\gamma = 14.47$*). Values of* $E^{p^*}_{t=0,w}[(W_T - \frac{\gamma}{2})^2]$ *are reported at* $(W = 1, t = 0)$*. Ratio is the ratio of successive changes in the computed values for decreasing values of the discretization parameter* h*. CPU time is normalized. We take the CPU time used for the first test in Table 4.3 as one unit of CPU time, which uses 728 nodes for the* W *grid and 160 timesteps.*

Nodes (W)	Timesteps	$\text{Std}^{p^*}_{t=0,w}[W_T]$	$E^{p^*}_{t=0,w}[W_T]$	Ratio for $\text{Std}^{p^*}_{t=0,w}[W_T]$	Ratio for $E[W_T]$
728	160	0.847680	6.93780		
1456	320	0.837022	6.94112		
2912	640	0.833002	6.94330	2.651	1.523
5824	1280	0.831430	6.94418	2.557	2.477
11648	2560	0.830873	6.94464	2.822	1.913

TABLE 4.8: *Convergence study. Use analytic solution of the optimal control at each node. Crank-Nicholson timestepping with Rannacher smoothing is applied, using constant timesteps. Parameters are given in Table 4.2, with* $\lambda = 1.72646$ *(*$\gamma = 14.47$*). Values of* $\text{Std}^{p^*}_{t=0,w}[W_T]$ *and* $E^{p^*}_{t=0,w}[W_T]$ *are reported at* $(W = 1, t = 0)$*. Ratio is the ratio of successive changes in the computed values for decreasing values of the discretization parameter* h*. Analytic solution:* $(\text{Std}^{p^*}_{t=0,w}[W_T], E^{p^*}_{t=0,w}[W_T]) = (0.8307, 6.9454)$*.*

As mentioned in Section 4.3.1, some error is introduced using the artificial boundaries $w_{\min}$ and w_{max}, which approximate infinite boundaries. However, we can make these errors small by choosing large values for $(|w_{\min}|, w_{\max})$. Table 4.9 shows the values of $E^{p^*}_{t=0,w}[(W_T - \frac{\gamma}{2})^2]$ and $E^{p^*}_{t=0,w}[W_T]$ for different large boundaries. We can see that once $(|w_{\min}|, w_{\max})$ are large enough, the values of $E^{p^*}_{t=0,w}[(W_T - \frac{\gamma}{2})^2]$ and $E^{p^*}_{t=0,w}[W_T]$ are insensitive to the location of these large boundaries. Recall that we use an unequally spaced grid, with a large grid spacing as $|w| \to \infty$. Hence use of large values for $|w_{min}|$ and w_{max} is inexpensive.

4.7.1.2 Bounded Control

In this section, we examine the wealth case with bounded control $\mathbb{P} = [0, 1.5]$. There is no analytic solution in this case. The efficient frontier is shown in Figure 4.3, with $(W(t = 0) = 1, t = 0)$. We also show the efficient frontiers for $\mathbb{D} \in [0, +\infty)$ and $\mathbb{P} = [0, +\infty)$, the

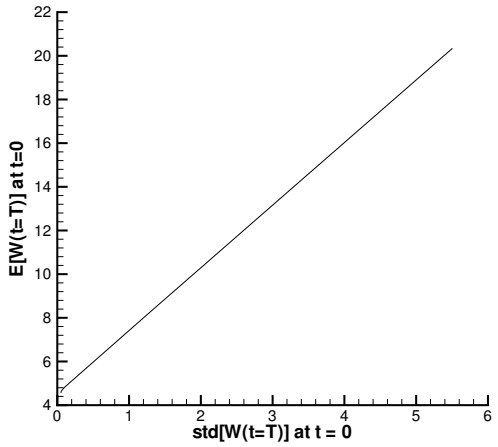

FIGURE 4.2: *Pre-commitment efficient frontier. Parameters are given in Table 4.2. Values are reported at* $(W = 1, t = 0)$.

Nodes (W)	$(w_{\min}, w_{\max})$	$E^{p^*}_{t=0,w}[(W_T - \frac{\gamma}{2})^2]$	$E^{p^*}_{t=0,w}[W_T]$
11648	(-5925, 5925)	0.783030	6.94383
11904	(-11953, 11953)	0.783030	6.94383
12160	(-23906, 23906)	0.783030	6.94383
12672	(-47869, 47869)	0.783030	6.94383

TABLE 4.9: *Effect of finite boundary. Parameters are given in Table 4.2, with* $\gamma = 14.47$. *There are 2560 timesteps for each test.*

no bankruptcy case, and for the case where bankruptcy is allowed, $\mathbb{D} = (-\infty, +\infty)$ and $\mathbb{P} = (-\infty, +\infty)$. Clearly, the strategy given by the allowing bankruptcy case is the most efficient, and the strategy given by the bounded control case is the least efficient.

As discussed in Section 4.7.1.1, in the case of allowing bankruptcy, if the market price of risk ξ_1 is fixed, the value of stock volatility σ_1 has no effect on the efficient frontier. However, this property may not hold when additional constraints are added on the optimal policy. For example, in the case of bounded control, the efficient frontier will move upward, if the value of σ_1 increases with ξ_1 fixed (this makes the stock drift rate $\mu_S = r + \xi_1\sigma_1$ increase). This result is illustrated in Figure 4.4 (a). However, if the value of σ_1 increases with μ_S fixed (this makes ξ_1 decrease), the efficient frontier will move downward. This result is illustrated in Figure 4.4 (b).

4.7.1.3 Multi-period Portfolio Selection Problem

In Section 4.3.5, we show that the pension plan problem can be reduced to the classic multi-period portfolio selection problem by simply setting the contribution rate $\pi = 0$. Of course, when $\pi = 0$, the efficient frontier is still a straight line in this case from equation

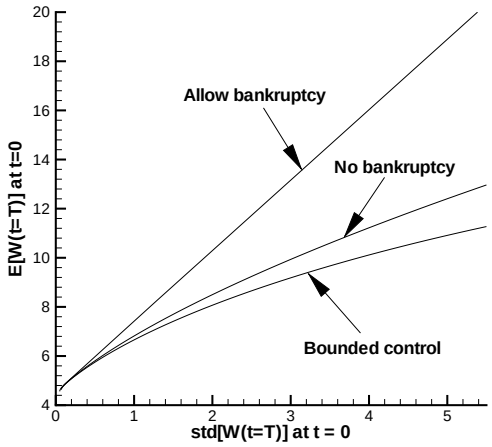

FIGURE 4.3: *Pre-commitment efficient frontiers (wealth case) for allowing bankruptcy ($\mathbb{D} = (-\infty, +\infty)$ and $\mathbb{P} = (-\infty, +\infty)$), no bankruptcy ($\mathbb{D} = [0, +\infty)$ and $\mathbb{P} = [0, +\infty)$) and bounded control ($\mathbb{D} = [0, +\infty)$ and $\mathbb{P} = [0., 1.5]$) cases. Parameters are given in Table 4.2. Values are reported at $(W = 1, t = 0)$.*

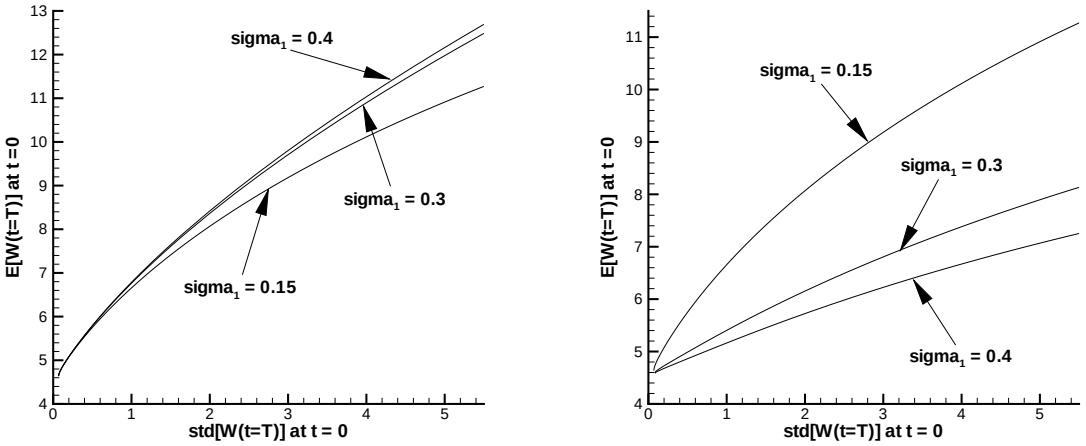

(a) Fix $\xi_1 = 0.15$ **(b) Fix $\mu_S = 0.08$**

FIGURE 4.4: *Pre-commitment efficient frontiers for various values of stock volatilities. Parameters are given in Table 4.2, in particular $W(t = 0) = 1$, $\mathbb{D} = [0, +\infty)$ and $\mathbb{P} = [0, 1.5]$. Figure (a) shows the efficient frontiers for different volatilities with a fixed market price of risk $\xi_1 = 0.15$. Figure (b) shows the efficient frontiers for different volatilities with a fixed stock drift rate $\mu_S = 0.08$.*

(4.3.9) for the case of allowing bankruptcy. In this section, we examine the case of no bankruptcy, where $\mathbb{D} = [0, +\infty)$ and $\mathbb{P} = [0, +\infty)$. An analytic solution is given for the no bankruptcy case in [15]. We can show numerically that the efficient frontier given by

our approach converges to the analytic solutions given in [15]. Using the parameters in [15, 78] ($r = 0.06$, $\sigma_1 = 0.15$, $\xi_1 = 0.4$, $T = 1$ and $W(t = 0) = 1$), Figure 4.5 shows the efficient frontiers. The straight line is for the case of unbounded control, allowing bankruptcy, which is obtained from equation (4.3.9). The curves below the straight line are actually two overlapping curves. One of them is obtained from the analytic solution given in [15], and the other is obtained from the numerical solutions using our approach. Figure 4.5 clearly shows that our numerical solutions converge to the analytic curve. Note that as discussed in Section 4.3.5, the approach given in [15] uses the monetary amount as the control, but our method uses the proportion as the control. Figure 4.5 shows that the two methods produce the same solutions in terms of efficient frontier.

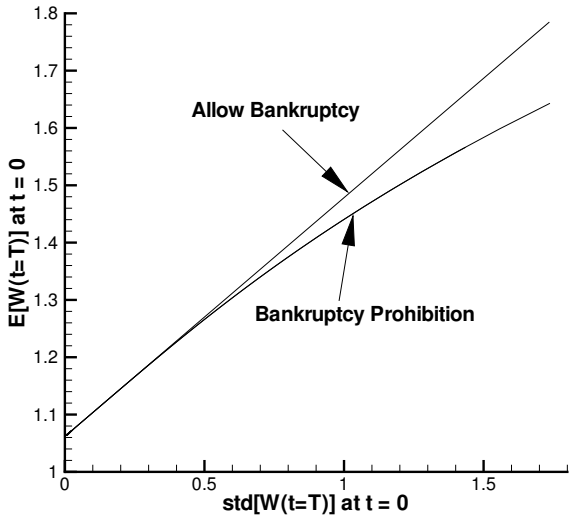

FIGURE 4.5: *Pre-commitment efficient frontiers for the multi-period portfolio selection problem. The straight line is for the case of allowing bankruptcy, which is obtained from equation (4.3.9). The curve below the straight line is actually two overlapping curves. One of them is obtained from the analytic solution given in [15], and the other is obtained from the numerical solutions by our approach. Parameters are* $r = 0.06$, $\sigma_1 = 0.15$, $\xi_1 = 0.4$, $T = 1$ *and* $W(t = 0) = 1$. *Values are reported at* $(W = 1, t = 0)$.

The 80% Rule [50]

In [50], the authors discuss an 80% rule for continuous time mean variance efficiency. This rule states that in the case of allowing bankruptcy ($\mathbb{D} = (-\infty, +\infty)$ and $\mathbb{P} = (-\infty, +\infty)$), given any target terminal wealth, say $\hat{g}$ ($> W(t = 0)e^{rT}$), where $\hat{g} = E^{p^*}_{t=0,w}[W_T]$, there is at least an 80% probability that the optimal strategy will reach the target over the time horizon $[0, T]$. This result may be surprising at first glance. The cost of this surprising rule is the high probability of bankruptcy when the target terminal wealth is high. We use Monte-Carlo simulations to examine this rule. Using the same parameters as used

to construct Figure 4.5, we solve the stochastic optimal control problem (4.2.1) with Algorithm (4.6.1) (we choose a γ such that $E^{p^*}_{t=0,w}(W_T) = \hat{g}$), and store the optimal strategies for each $(W = w, t)$). We then carry out Monte-Carlo simulations based on the stored strategies with $W(t = 0) = 1$ initially. As mentioned in [50], at any time $t \in [0, T]$, once the investor's wealth $W(t) \geq \hat{g}e^{-r(T-t)}$, the investor will switch all her wealth into bonds, so that her final wealth $W_T \geq \hat{g}$. Note that this simulation strategy is slightly different from the pre-commitment strategy. With a pre-commitment strategy, the investor commits to the pre-computed strategy until $t = T$ irregardless of reaching the investment target. Table 4.10 shows the result of Monte-Carlo simulations. We see that no matter how large the target wealth, the probability of success (hitting the target wealth) is higher than 80%. However, when the target wealth is high, the probability of bankruptcy is also very high. Note that at any time $t \in [0, T]$, if $W(t) \leq 0$, bankruptcy occurs. But since bankruptcy is allowed, the investor can still borrow money and continue investing. This may result in positive wealth at some later time. The last column in Table 4.10 shows the probability of bankruptcy at time T, which is much lower than the probability of bankruptcy at any time $t \in [0, T]$.

Table 4.10 also examines the probability of hitting the target for the bankruptcy prohibition case and the bounded control case. The results show that the 80% rule does not hold for these two cases. When the target wealth increases, the probability of hitting the target decreases, but the probability of bankruptcy is zero.

$E^{p^*}_{t=0,w}[W_T] = \hat{g}$	$\text{Std}^{p^*}_{t=0,w}[W_T]$	Success investment	Bankruptcy at any time t	Bankruptcy at time T
Bankruptcy is allowed: $\mathbb{D} = (-\infty, +\infty)$ and $\mathbb{P} = (-\infty, +\infty)$				
1.19979	0.33123	82.3984%	1.3063%	0.5297%
2.00060	2.25380	82.2125%	38.7344%	10.6656%
4.60097	8.49677	82.3922%	69.7328%	14.1094%
Bankruptcy prohibition: $\mathbb{D} = [0, +\infty)$ and $\mathbb{P} = [0, +\infty)$				
1.19994	0.33348	82.7866%	0	0
2.00199	3.69090	63.8516%	0	0
3.06641	20.66430	43.9625%	0	0
Bounded control: $\mathbb{D} = [0, +\infty)$ and $\mathbb{P} = [0, 1.5]$				
1.08225	0.04908	82.5922%	0	0
1.16185	0.26486	74.9141%	0	0

TABLE 4.10: *80% rule study. Parameters used as in [15, 78] ($r = 0.06$, $\sigma_1 = 0.15$, $\xi_1 = 0.4$, $T = 1$ and $W(t = 0) = 1$). 64,000 Monte-Carlo simulations for each test. 512 Monte-Carlo timesteps are used for allowing bankruptcy case and bounded control case, and 25600 timesteps are used for no bankruptcy case. Success is defined as $W(t) \geq E^{p^*}_{t=0,w}[W_T]e^{-r(T-t)}$, $t \leq T$.*

Remark 4.12. *In the case of bankruptcy prohibition,* $\lim_{w\to 0}(p^*w) = 0$. *Our numerical tests show that as w goes to zero, $p^*w = O(w^\beta)$. For a reasonable range of parameters, $\beta \simeq 0.95 \pm 0.02$. Hence, this verifies that the boundary condition (4.3.7) ensure that*

negative wealth is not admissible under the optimal strategy. This property also holds for the wealth case and the wealth-to-income ratio case.

We apply an explicit Milstein method [44] when carrying out Monte-Carlo simulations to ensure that negative wealth is unattainable. The explicit Milstein method requires some timestep size restrictions. As a result, we use a small timestep size ($\frac{1}{25600}$ year) for the no bankruptcy case in simulations. Although negative wealth is unattainable for the bounded control case, we do not have to use the Milstein method. Since the control p is capped at 1.5, as $w \to 0$, $p^* w$ goes to zero as the same rate as w. We do not observe any difficulties in this case using the standard explicit Euler scheme.

4.7.2 Wealth-to-income Ratio Case

μ_Y	0.	ξ_1	0.2
σ_1	0.2	σ_{Y1}	0.05
σ_{Y0}	0.05	π	0.1
T	20 years	γ	15
$\mathbb{P}$	$[0, 1.5]$	$\mathbb{D}$	$[0, +\infty)$

TABLE 4.11: *Parameters used in the pension plan examples.*

In this Section, we examine the wealth-to-income ratio case. We use parameters in Table 4.11, and our finite difference method for solution of the optimal stochastic control problem (4.4.1). We set $x_{\max}, |x_{\min}| = 1000$ in this case, and *tolerance* $= 10^{-6}$ in Algorithm 3.5.1. Increasing $x_{\max}$ had no effect on the solution to six digits. There is no known analytic solution for this case. A convergence study is shown in Tables 4.12 and 4.13. Table 4.12 reports the values of $E^{p^*}_{t=0,x}[(X_T - \frac{\gamma}{2})^2]$, and Table 4.13 reports the values of $\text{Std}^{p^*}_{t=0,x}[X_T]$ and $E^{p^*}_{t=0,x}[X_T]$. Both tables show a first order convergence rate as $h \to 0$.

Nodes (X)	Timesteps	Nonlinear iterations	Normalized CPU Time	$E^{p^*}_{t=0,x}[(X_T - \frac{\gamma}{2})^2]$	Ratio
89	40	100	1	15.9197	
177	80	166	4.08	15.7498	
353	160	320	13.27	15.6682	2.082
705	320	640	53.06	15.6272	1.990
1409	640	1280	205.10	15.6066	1.990
2817	1280	2560	841.84	15.5963	2.000

TABLE 4.12: *Convergence study. Fully implicit timestepping is applied, using constant timesteps. Parameters are given in Table 4.11. Values of $E^{p^*}_{t=0,x}[(X_T - \frac{\gamma}{2})^2]$ are reported at $(X = 0.5, t = 0)$. Ratio is the ratio of successive changes in computed values as $h \to 0$. CPU time is normalized. We take the CPU time used for the first test in this table as one unit of CPU time, which uses 89 nodes for the X grid and 40 timesteps.*

Nodes (X)	Timesteps	$\text{Std}^{p^*}_{t=0,x}[X_T]$	$E^{p^*}_{t=0,x}[X_T]$	Ratio for $\text{Std}^{p^*}_{t=0,x}[X_T]$	Ratio for $E^{p^*}_{t=0,x}[X_T]$
89	40	1.80509	3.94173		
177	80	1.77167	3.94881		
353	160	1.75521	3.95213	2.030	2.133
705	320	1.74692	3.95381	1.986	1.976
1409	640	1.74276	3.95467	1.993	1.953
2817	1280	1.74068	3.95509	2.000	2.048

TABLE 4.13: *Convergence study. The optimal control at each node is computed using analytic methods. Fully implicit timestepping is applied, using constant timesteps. Parameters are given in Table 4.11. Values of* $E^{p^*}_{t=0,x}[X_T]$ *and* $Std^{p^*}_{t=0,x}[X_T]$ *are reported at* $(X = 0.5, t = 0)$*. Ratio is the ratio of successive changes in computed values as* $h \to 0$*.*

In order to solve the HJB PDE (4.4.4), the optimal control p^* needs to be determined to minimize the objective function at each node. This objective function is a piecewise quadratic function of p. Hence, it is not difficult to determine the analytic solution for the control p. Values in Table 4.12 and 4.13 are obtained by using the analytic method for optimal p^* at each node. However, in some cases, it is not easy to determine the analytic solution for the control. In such cases, the control set $\mathbb{P}$ can be discretized to a set $\hat{\mathbb{P}}$, and the optimal control can be determined by linear search. The convergence to viscosity solution of this method is proven in [72] (see Chapter 3). Table 4.14 and 4.15 show a convergence study with the discretized control. Again, a first order convergence rate is obtained in both tables. Of course, this method requires much more CPU time compared to the method used by Table 4.12 and 4.13. This is simply due to the comparatively crude method used to find the optimal control at each grid node.

Nodes $(X \times \hat{\mathbb{P}})$	Timesteps	Nonlinear iterations	Normalized CPU Time	$E^{p^*}_{t=0,x}[(X_T - \frac{\gamma}{2})^2]$	Ratio
89×21	40	101	4.08	15.9242	
177×41	80	166	22.45	15.7509	
353×81	160	320	161.22	15.6684	2.101
705×161	320	640	1276.53	15.6272	2.002
1409×321	640	1280	9917.35	15.6066	2.000
2817×641	1280	2560	76102.04	15.5963	2.000

TABLE 4.14: *Convergence study. Use discretized control set* $\hat{\mathbb{P}}$ *and linear search to find the optimal control. Fully implicit timestepping is applied, using constant timesteps. Parameters are given in Table 4.11. Values of* $E^{p^*}_{t=0,x}[(X_T - \frac{\gamma}{2})^2]$ *are reported at* $(X = 0.5, t = 0)$*. Ratio is the ratio of successive changes in computed values as* $h \to 0$*. CPU time is normalized. We take the CPU time used for the first test in Table 4.12 as one unit of CPU time, which uses 89 nodes for X grid and 40 timesteps.*

Figure 4.6 shows the efficient frontiers for the allowing bankruptcy, no bankruptcy and bounded control cases. Again, the strategy given by the allowing bankruptcy case is the

Nodes ($X \times \hat{\mathbb{P}}$)	Timesteps	$\text{Std}^{p^*}_{t=0,x}[X_T]$	$E^{p^*}_{t=0,x}[X_T]$	Ratio for $\text{Std}^{p^*}_{t=0,x}[X_T]$	Ratio for $E^{p^*}_{t=0,x}[X_T]$
89×21	40	1.80701	3.94206		
177×41	80	1.77144	3.94854		
353×81	160	1.75529	3.95213	2.202	1.805
705×161	320	1.74693	3.95381	1.932	2.137
1409×321	640	1.74276	3.95466	2.005	1.976
2817×641	1280	1.74068	3.95509	2.005	1.977

TABLE 4.15: *Convergence study. Use discretized control set $\hat{\mathbb{P}}$ and linear search to find the optimal control. Fully implicit timestepping is applied, using constant timesteps. Parameters are given in Table 4.11. Values of $E^{p^*}_{t=0,x}[X_T]$ and $\text{Std}^{p^*}_{t=0,x}[X_T]$ are reported at $(X = 0.5, t = 0)$. Ratio is the ratio of successive changes in computed values as $h \to 0$.*

most efficient, and the strategy given by the bounded control case is the least efficient.

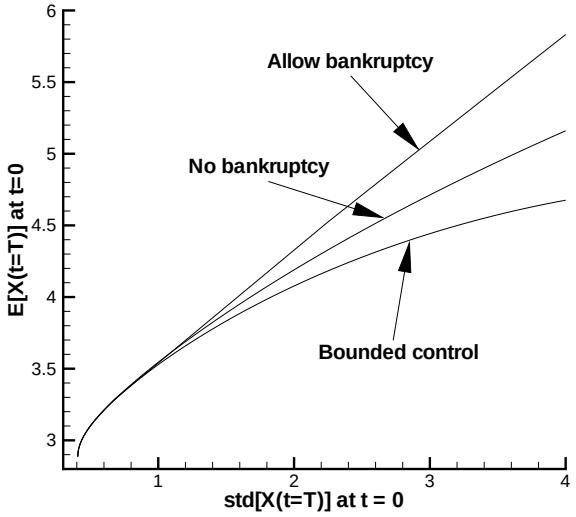

FIGURE 4.6: *Pre-commitment efficient frontiers (wealth-to-income ratio case) for allowing bankruptcy ($\mathbb{D} = (-\infty, +\infty)$ and $\mathbb{P} = (-\infty, +\infty)$), no bankruptcy ($\mathbb{D} = [0, +\infty)$ and $\mathbb{P} = [0, +\infty)$) and bounded control ($\mathbb{D} = [0, +\infty)$ and $\mathbb{P} = [0., 1.5]$) cases. Parameters are given in Table 4.11. Values are reported at $(X = 0.5, t = 0)$.*

In Section 4.7.1, we have discussed the effects of changing the value of σ_1 on the efficient frontier solution. We obtain similar results for the wealth-to-income case. For a fixed ξ_1, different values of σ_1 give the same efficient frontier solution in the case of allowing bankruptcy. However, this property does not hold for the bounded control case. Figure 4.7 (a) illustrates that for a fixed ξ_1, increasing σ_1 moves the efficient frontier

upward in the case of bounded control. Figure 4.7 (b) illustrates that for a fixed μ_S, increasing σ_1 moves the efficient frontier downward.

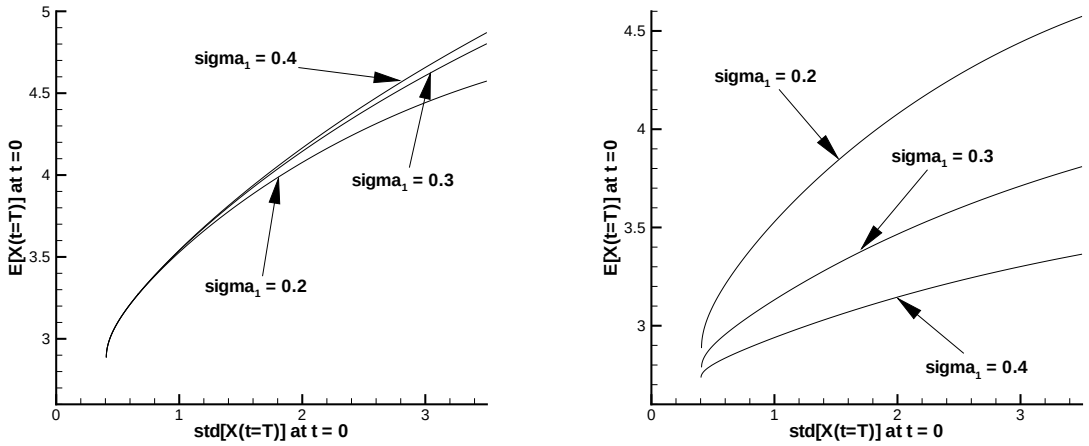

(a) Fix $\xi_1 = 0.2$ **(b) Fix $\mu_S = 0.04$**

FIGURE 4.7: *Pre-commitment efficient frontiers for various values of stock volatilities. Parameters are given in Table 4.11, in particular $X(t=0) = 0.5$, $\mathbb{D} = [0, +\infty)$ and $\mathbb{P} = [0, 1.5]$. Figure (a) shows the efficient frontiers for different volatilities with a fixed market price of risk $\xi_1 = 0.2$. Figure (b) shows the efficient frontiers for different volatilities with a fixed stock drift rate $\mu_S = 0.04$.*

Figure 4.8 shows the values of the optimal control (the investment strategies) at different time t for a fixed $T = 20$ and $\gamma = 15$. Under these inputs, if $X(t=0) = 0.5$, $(\text{Std}^{p^*}_{t=0,x}[X_T], E^{p^*}_{t=0,x}[X_T]) = (1.7407, 3.9551)$ from the finite difference solution. From this figure, we can see that the control p is an increasing function of time t for a fixed X. This is a bit counterintuitive, since one may imagine that the investor should become more conservative (switch to bonds) as time goes on. However, if total wealth-to-income ratio remains fixed as time increases, then the investor must take on more risk to have a higher probability of hitting the investment target. This behaviour of the optimal strategy is also seen in the analytic solution for the wealth case with bankruptcy allowed (Equation (4.3.10)).

Using the parameters in Table 4.11, we solve the stochastic optimal control problem (equation (4.4.1)) and store the optimal strategies for each $(X = x, t)$. We then carry out Monte-Carlo simulations based on the stored strategies for $X(t=0) = 0.5$ initially. The value for $(\text{Std}^{p^*}_{t=0,x}[X_T], E^{p^*}_{t=0,x}[X_T])$ is $(1.7407, 3.9551)$ (from the finite difference solution). Table 4.16 shows a convergence study for Monte-Carlo simulations, and Figure 4.9 shows a plot of the convergence study. As the number of simulations increases and the timestep size decreases, the results given by Monte-Carlo simulation converge to the values given by solving the finite difference solution.

Figure 4.10 shows the probability density function of Monte-Carlo simulations (500000 simulations). Figure 4.10 (a) uses $\gamma = 15$ ($(\text{Std}^{p^*}_{t=0,x}[X_T], E^{p^*}_{t=0,x}[X_T]) = (1.7407, 3.9551)$),

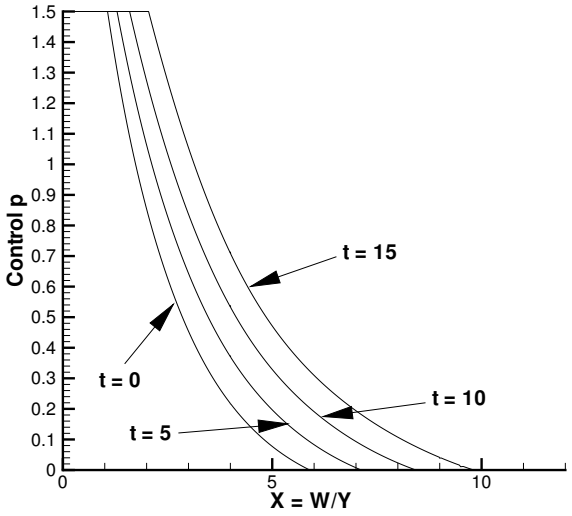

FIGURE 4.8: *Pre-commitment optimal control as a function of* (X, t)*. Parameters are given in Table 4.11. Under these inputs, if* $X(t=0) = 0.5$*,* $(Std^{p^*}_{t=0,x}[X_T], E^{p^*}_{t=0,x}[X_T]) = (1.7407, 3.9551)$ *from finite difference solution.*

# of Simulations	MC Timestep	$E^{p^*}_{t=0,x}[X_T]$	$\text{Std}^{p^*}_{t=0,x}[X_T]$
1000	0.25	3.9840	1.7233
4000	0.125	3.9396	1.7305
16000	0.0625	3.9656	1.7366
64000	0.03125	3.9566	1.7381
256000	0.015625	3.9559	1.7390

TABLE 4.16: *Convergence study for the Monte-Carlo Simulations. Parameters are given in Table 4.11. Values for* $E^{p^*}_{t=0,x}[X_T]$ *and* $Std^{p^*}_{t=0,x}[X_T]$ *are reported at* $(X = 0.5, t = 0)$*. The finite difference values are:* $E^{p^*}_{t=0,x}[X_T] = 3.9551$ *and* $Std^{p^*}_{t=0,x}[X_T] = 1.7407$*.*

while Figure 4.10 (b) uses $\gamma = 8$ $((\text{Std}^{p^*}_{t=0,x}[X_T], E^{p^*}_{t=0,x}[X_T]) = (0.6627, 3.2647))$. The shape of the probability density function depends on input parameters (γ in this example). Note the double peak in Figure 4.10(a). For this case, when the control is unconstrained ($\mathbb{P} = (-\infty, +\infty)$), the probability density function (which is not shown in this thesis) has a single peak near $E^{p^*}_{t=0,x}[X_T]$.

However, when $\gamma = 15$, $p_{\max} = 1.5$, then the control hits the constraint (see Figure 4.8) for small X. Hence the investor has to choose a strategy with less than optimal (compared to the unbounded control case) expected return. As a result, there is another peak to the left of the value of $E^{p^*}_{t=0,x}[X_T]$ in the probability density function. If γ is small enough, the optimal strategy does not hit the constraints, and the probability density function reverts to a single peak. As shown in Figure 4.10 (b), there is only one peak in

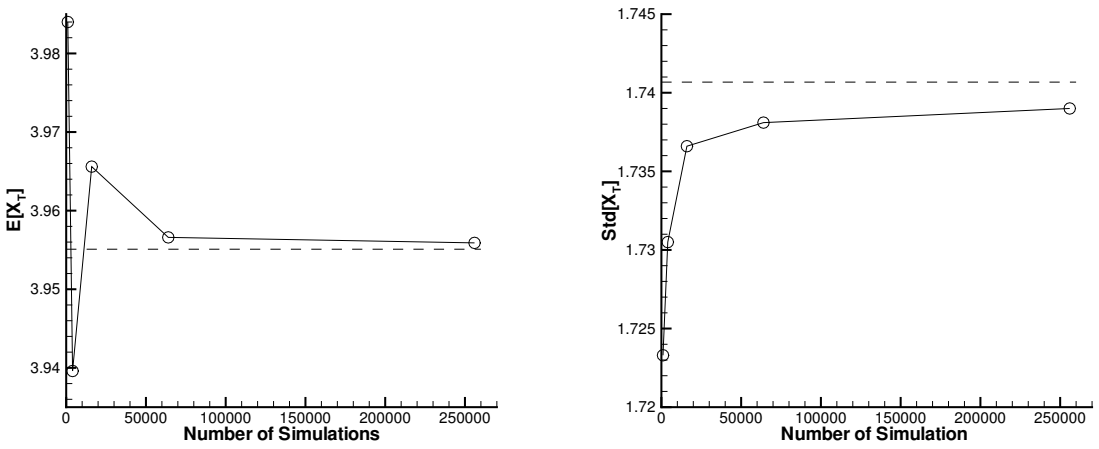

(a) **(b)**

FIGURE 4.9: *Convergence study for the Monte-Carlo Simulations, pre-commitment strategy. Parameters are given in Table 4.11. Figure (a) shows the plot of* $E^{p^*}_{t=0,x}[X_T]$. *Figure (b) shows the plot for* $Std^{p^*}_{t=0,x}[X_T]$. $E^{p^*}_{t=0,x}[X_T]$ *and* $Std^{p^*}_{t=0,x}[X_T]$ *are written as* $E[X_T]$ *and* $Std[X_T]$ *in the figure. Values for* $E^{p^*}_{t=0,x}[X_T]$ *and* $Std^{p^*}_{t=0,x}[X_T]$ *are reported in Table 4.16. The finite difference values are* $(Std^{p^*}_{t=0,x}[X_T], E^{p^*}_{t=0,x}[X_T]) = (1.7407, 3.9551)$.

the probability density function for $\gamma = 8$.

Figure 4.11 shows the mean and standard deviation for the strategy $p(t,x)$ as time changes. Figure 4.11 (a) uses $\gamma = 15$ $((\text{Std}^{p^*}_{t=0,x}[X_T], E^{p^*}_{t=0,x}[X_T]) = (1.7407, 3.9551))$, while Figure 4.11 (b) uses $\gamma = 8$ $((\text{Std}^{p^*}_{t=0,x}[X_T], E^{p^*}_{t=0,x}[X_T]) = (0.6627, 3.2647))$. Both of these Figures show that the mean of $p(t,x)$ is a decreasing function of time t, i.e., as time goes on, the investor switches into the less risky strategy (on average). Since the value of $E^{p^*}_{t=0,x}[X_T]$ in Figure 4.11 (a) is higher than the one in Figure 4.11 (b), the mean strategy in Figure 4.11 (a) is more risky compared to Figure 4.11 (b).

4.8 Summary

The main results of this chapter are

- Based on the methods in Chapter 3, we develop a fully implicit method for solving the nonlinear HJB PDE, which arises in the LQ formulation of the pre-commitment mean variance problem. Under the assumption that the HJB equation satisfies a strong comparison property, our methods are guaranteed to converge to the viscosity solution of the HJB equation. In addition, the policy iteration scheme used to solve the nonlinear algebraic equations at each timestep is globally convergent. Note that

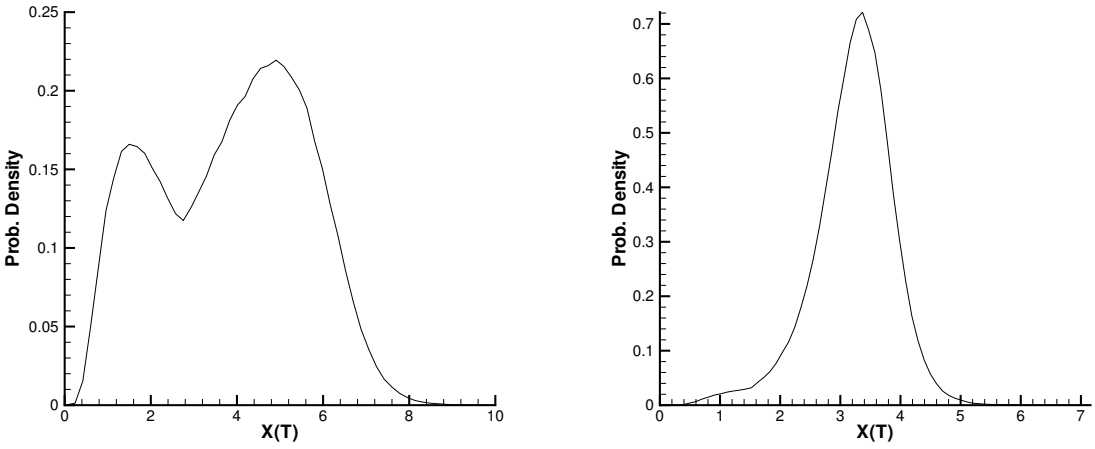

(a) $\gamma = 15$ **(b)** $\gamma = 8$

FIGURE 4.10: *Probability density function for Monte-Carlo Simulation,* $500,000$ *simulations and 1280 simulation timesteps. Parameters are given in Table 4.11. Values for* $(E^{p^*}_{t=0,x}[X_T], Std^{p^*}_{t=0,x}[X_T])$ *are reported at* $(X = 0.5, t = 0)$*. Figure (a) uses* $\gamma = 15$*, while Figure (b) uses* $\gamma = 8$*. For Figure (a),* $(Std^{p^*}_{t=0,x}[X_T], E^{p^*}_{t=0,x}[X_T]) = (1.7407, 3.9551)$ *from finite difference solution; For Figure (b),* $(Std^{p^*}_{t=0,x}[X_T], E^{p^*}_{t=0,x}[X_T]) = (0.6627, 3.2647)$ *from finite difference solution.*

an explicit method would have timestep restrictions due to stability considerations. In the case of an unbounded control, the maximum stable timestep would be difficult to estimate. This problem does not arise if an implicit method is used.

- By solving the HJB PDE and a related linear PDE, we develop a numerical method for constructing the mean variance efficient frontier (in continuous time). Any type of constraint can be applied to the investment policy. To the best of our knowledge, this scheme for numerical computation of the pre-commitment efficient frontier is new.

- We pay particular attention to handling various constraints on the optimal policy. In particular, in order to compare the numerical solution with the known analytic solution in special cases, it is necessary to allow for negative wealth and unbounded controls. This requires careful attention to the grid construction and form of the control as the mesh and timesteps shrink to zero.

- From a practical point of view, we observe that the addition of realistic constraints can completely alter some of the properties of the mean variance solution compared to the unconstrained control case [50].

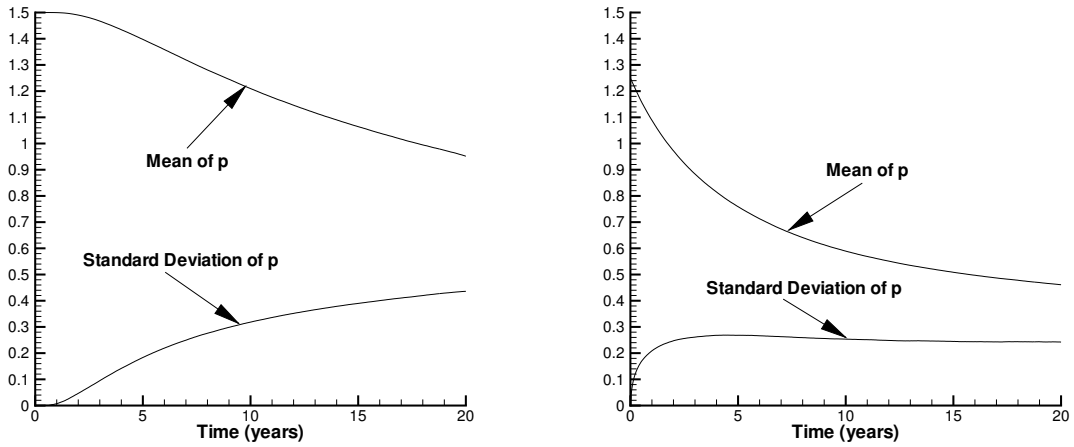

(a) $\gamma = 15$ **(b)** $\gamma = 8$

FIGURE 4.11: *Mean and standard deviation for the control* $p(t,x)$*. There are 64000 simulations and 1280 simulation timesteps. Parameters are given in Table 4.11. Figure (a) uses* $\gamma = 15$*, while Figure (b) uses* $\gamma = 8$*. For Figure (a),* $(Std^{p^*}_{t=0,x}[X_T], E^{p^*}_{t=0,x}[X_T]) = (1.7407, 3.9551)$ *from finite difference solution; For Figure (b),* $(Std^{p^*}_{t=0,x}[X_T], E^{p^*}_{t=0,x}[X_T]) = (0.6627, 3.2647)$ *from finite difference solution.*

Chapter 5

Time-consistent Strategy

5.1 Introduction

In Chapter 4, we studied the mean variance pre-commitment strategy. Recall the pre-commitment strategy, for time $t + \Delta t$, computed at time t will not necessarily agree with the strategy for time $t+\Delta t$, computed at time $t+\Delta t$. Hence, the pre-commitment strategy is time inconsistent. This time inconsistent property may be problematic in practice as discussed in Section 2.3.2.

A time-consistent form of mean variance asset allocation has been suggested recently [16, 11, 73]. We may view the time-consistent strategy as a pre-commitment policy with a time-consistent constraint (equation (2.3.6)). We will study the time-consistent strategy in this chapter.

5.2 Time-consistent Wealth Case

We first consider the wealth case for the pension asset allocation problem. Let,

$$\begin{aligned} \mathbb{D} &:= \text{the set of all admissible wealth } W(t), \text{ for } 0 \le t \le T; \\ \mathbb{Q} &:= \text{the set of all admissible controls } q(t,w), \text{ for } 0 \le t \le T \text{ and } w \in \mathbb{D}. \end{aligned} \tag{5.2.1}$$

Recall from equation (2.3.7) that the mean variance time-consistent problem is

$$J(w,t) = \sup_{\substack{q(s\ge t, W(s)) \\ q\in\mathbb{Q}}} \left\{ E^q_{t,w}[W_T] - \lambda Var^q_{t,w}[W_T] \right\} , \tag{5.2.2}$$

$$\text{s.t. } q^*_t(s,w) = q^*_{t'}(s,w) \ ; \ s \ge t', \ t' \in [t,T] \ , \tag{5.2.3}$$

subject to stochastic process (2.2.2), and where q^* denotes the optimal control. In this chapter, the control q can be p (the proportion of the total wealth invested in the risky

asset), or pw (the monetary amount invested in the risky asset). Varying $\lambda \in (0, \infty)$ allows us to draw an efficient frontier.

We can now drop the subscript "t" from $q_t^*(s, w)$, since we will impose constraint (2.3.6) and the optimal policy at time $t + \Delta t$ does not depend on the policy at time t. Note we are following here time consistency as defined in [11]. There are other possibilities, as discussed in [16].

Define,

$$U(w,t) = E_{t,w}^{q^*(s \geq t, W(s))}[W_T] \ , \tag{5.2.4}$$

$$V(w,t) = E_{t,w}^{q^*(s \geq t, W(s))}[W_T^2] \ , \tag{5.2.5}$$

with terminal condition

$$\begin{aligned} U(w, t = T) &= w, \\ V(w, t = T) &= w^2 \ . \end{aligned} \tag{5.2.6}$$

Note that

$$U(w,t) = E_{t,w}^{q^*(t \leq s \leq t+\Delta t, W(s))}[U(W(t+\Delta t), t+\Delta t)] \ , \tag{5.2.7}$$

$$V(w,t) = E_{t,w}^{q^*(t \leq s \leq t+\Delta t, W(s))}[V(W(t+\Delta t), t+\Delta t)] \ . \tag{5.2.8}$$

Then, $J(w,t)$ can be rewritten as

$$\begin{aligned} J(w,t) &= \sup_{\substack{q(s \geq t, W(s)) \\ q \in \mathbb{Q} \\ q \text{ satisfies (5.2.3)}}} \left\{ E_{t,w}^{q(s \geq t, W(s))}[W_T] - \lambda \{ E_{t,w}^{q(s \geq t, W(s))}[W_T^2] - (E_{t,w}^{q(s \geq t, W(s))}[W_T])^2 \} \right\} \\ &= \sup_{\substack{q(t \leq s \leq t+\Delta t, W(s)), W(s)) \\ q \in \mathbb{Q} \\ q \text{ satisfies (5.2.3)}}} \Bigg\{ E_{t,w}^{q(t \leq s \leq t+\Delta t, W(s))}[E_{t+\Delta t, W(t+\Delta t)}^{q^*(s \geq t+\Delta t, W(s))}(W_T)] \\ &\quad -\lambda E_{t,w}^{q(t \leq s \leq t+\Delta t, W(s))}[E_{t+\Delta t, W(t+\Delta t)}^{q^*(s \geq t+\Delta t, W(s))}(W_T^2)] \\ &\quad +\lambda (E_{t,w}^{q(t \leq s \leq t+\Delta t, W(s))}[E_{t+\Delta t, W(t+\Delta t)}^{q^*(s \geq t+\Delta t, W(s))}(W_T)])^2 \Bigg\} \\ &= \sup_{\substack{q(t \leq s \leq t+\Delta t, W(s)) \\ q \in \mathbb{Q} \\ q \text{ satisfies (5.2.3)}}} \Bigg\{ E_{t,w}^{q}[U(W(t+\Delta t), t+\Delta t)] \\ &\quad -\lambda (E_{t,w}^{q}[V(W(t+\Delta t), t+\Delta t)] - \{E_{t,w}^{q}[U(W(t+\Delta t), t+\Delta t)]\}^2) \Bigg\} \ . \end{aligned} \tag{5.2.9}$$

Assume that the set of all controls $\mathbb{Q}$ is compact, and that $E_{t,w}^q[\cdot]$ is a bounded, upper semi-continuous function of the control q. Given $q^*(s \geq t + \Delta t, W(s))$, suppose we can

determine $(U(W(t+\Delta t),t+\Delta t),V(W(t+\Delta t),t+\Delta t))$. Then,

$$q^*(t\le s\le t+\Delta t,W(s)) \in \underset{\substack{q(t\le s\le t+\Delta t,W(s))\\ q\in\mathbb{Q}}}{\arg\max}\Big\{E^q_{t,w}[U(W(t+\Delta t),t+\Delta t)] - \lambda(E^q_{t,w}[V(W(t+\Delta t),t+\Delta t)] - \{E^q_{t,w}[U(W(t+\Delta t),t+\Delta t)]\}^2)\Big\} . \tag{5.2.10}$$

Equations (5.2.7-5.2.10) can be used as the basis for a recursive algorithm to determine $V(w,t),U(w,t)$ for any t (see later Algorithm (5.4.10)). Assuming $V(w,t=0),U(w,t=0)$ are known, then for a given λ, we can compute the pair $(Var^{q^*}_{t=0,w}[W_T],E^{q^*}_{t=0,w}[W_T])$ from $Var^{q^*}_{t=0,w}[W_T]=V(w,t=0)-[U(w,t=0)]^2$.

5.3 Time-consistent Wealth-to-income Ratio Case

We then consider the wealth-to-income ratio case introduced in Section 2.2.2. The stochastic models for the underlying asset S, the plan holder's year salary Y, the wealth W and her wealth-to-income ratio X have been given in equations (2.2.4 - 2.2.7).

The time-consistent control problem is then to determine the strategy $q(t,X(t)=x)$ such that $q(t,x)$ maximizes

$$J(x,t) = \sup_{\substack{q(s\ge t,X(s))\\ q\in\mathbb{Q}}}\left\{E^q_{t,x}[X_T]-\lambda Var^q_{t,x}[X_T]\right\} , \tag{5.3.1}$$

$$\text{s.t. } q^*_t(s,x) = q^*_{t'}(s,x)\ ;\ s\ge t',\ t'\in[t,T] . \tag{5.3.2}$$

subject to stochastic process (2.2.7). Similar to the wealth case, let

$$\begin{aligned} U(x,t) &= E^{q^*(s\ge t,X(s))}_{t,x}[X_T] , \\ V(x,t) &= E^{q^*(s\ge t,X(s))}_{t,x}[X^2_T] , \end{aligned} \tag{5.3.3}$$

with,

$$q^*(t\le s\le t+\Delta t,X(s)) \in \underset{\substack{q(t\le s\le t+\Delta t,X(s))\\ q\in\mathbb{Q}}}{\arg\max}\Big\{E^q_{t,x}[U(X(t+\Delta t),t+\Delta t)] - \lambda(E^q_{t,x}[V(X(t+\Delta t),t+\Delta t)] - \{E^q_{t,x}[U(X(t+\Delta t),t+\Delta t)]\}^2)\Big\} . \tag{5.3.4}$$

Then, $J(x,t)$ can be rewritten as

$$J(x,t) = \sup_{\substack{q(t\le s\le t+\Delta t,X(s))\\ q\in\mathbb{Q}\\ q \text{ satisfies (5.3.2)}}} \Big\{ E^q_{t,x}[U(X(t+\Delta t),t+\Delta t)] \tag{5.3.5}$$
$$-\lambda(E^q_{t,x}[V(X(t+\Delta t),t+\Delta t)] - \{E^q_{t,x}[U(X(t+\Delta t),t+\Delta t)]\}^2)\Big\} .$$

5.4 Discretization

In this section, we develop a discretization scheme to solve the mean variance time-consistent problem numerically. Let $z = w$ for the wealth case, and $z = x$ for the wealth-to-income ratio case. The optimal control problem in both cases is then

$$U(z,t) = E^{q^*(t\le s\le t+\Delta t,Z(s))}_{t,z}[U(Z(t+\Delta t),t+\Delta t)] , \tag{5.4.1}$$
$$V(z,t) = E^{q^*(t\le s\le t+\Delta t,Z(s))}_{t,z}[V(Z(t+\Delta t),t+\Delta t)] , \tag{5.4.2}$$
$$q^*(t\le s\le t+\Delta t,Z(s)) \in \arg\max_{\substack{q(t\le s\le t+\Delta t,Z(s))\\ q\in\mathbb{Q}}} \Big\{ E^q_{t,z}[U(Z(t+\Delta t),t+\Delta t)] \tag{5.4.3}$$
$$-\lambda(E^q_{t,z}[V(Z(t+\Delta t),t+\Delta t)] - \{E^q_{t,z}[U(Z(t+\Delta t),t+\Delta t)]\}^2)\Big\} ,$$

with terminal condition

$$U(z,t=T) = z,$$
$$V(z,t=T) = z^2 . \tag{5.4.4}$$

The form of constraints applied to the control will dictate a choice of $q = p$ or $q = pz$. This will be discussed in later Sections.

5.4.1 Piecewise Constant Timestepping

For general constraints, we cannot find an analytic solution for the time-consistent strategy. Therefore, the control has to be to determined numerically. One possible approach for solution of problem (5.4.1-5.4.3) is to use piecewise constant policy timestepping [45].

We can replace the set of admissible controls $\mathbb{Q}$ by an approximation $\hat{\mathbb{Q}}$. Define

$$\hat{\mathbb{Q}} = [q_0, q_1, ..., q_m] \quad , \quad \text{with } q_0 = q_{\min} \ ; \ q_m = q_{\max} \ ,$$
$$\max_{0\le j\le m-1}(q_{j+1} - q_j) = C_1 h \ , \tag{5.4.5}$$

where C_1 is a positive constant. Let $\Delta t = \frac{T}{N}$. Define a set of discrete times,

$$\begin{aligned} \{t_n \quad | \quad t_n = n\Delta t \ , \ 0 \leq n \leq N\} \ , \\ \Delta t \quad = \quad C_2 h \ , \end{aligned} \tag{5.4.6}$$

where C_2 is a positive constant. We assume the control is a constant over the period $[t_n, t_{n+1}]$. Set

$$q^n(z) = q(t_n, z) \ ; \ U^n(z) = U(t_n, z) \ ; \ V^n(z) = V(t_n, z) \tag{5.4.7}$$

$$U_j^n(z) = E_{t_n,z}^{q_j}[U^{n+1}(Z(t_{n+1}))] \ , \tag{5.4.8}$$

$$V_j^n(z) = E_{t_n,z}^{q_j}[V^{n+1}(Z(t_{n+1}))] \ , \tag{5.4.9}$$

We compute the solutions of equations (5.4.8) and (5.4.9) for each control q_j, $0 \leq j \leq m$, then find the optimal control q_{j^*} according to the objective function, and update the values for U^n and V^n. This gives us the following algorithm.

Piecewise Constant Timestepping Algorithm

$U_j^N(z) = z \ , \ V_j^N(z) = z^2 \ ,$ for all $0 \leq j \leq m$
For timestep $n = N-1, \ldots, 0$
  For $j = 0, \ldots, m$
    $U_j^n(z) = E_{t_n,z}^{q_j}[U^{n+1}(Z(t+\Delta t))]$
    $V_j^n(z) = E_{t_n,z}^{q_j}[V^{n+1}(Z(t+\Delta t))]$
  EndFor
  $j^* \in \arg\max_{0 \leq j \leq m} \{U_j^n(z) - \lambda(V_j^n(z) - (U_j^n(z))^2)\}$
  $(q^n(z))^* = q_{j^*} \ ; \ U_j^n(z) = U_{j^*}^n(z) \ ; \ V_j^n(z) = V_{j^*}^n(z) \ ,$ for all $0 \leq j \leq m$
EndFor

(5.4.10)

Remark 5.1. *In [45], the authors applied the piecewise constant timestepping to a scalar HJB equation, and proved that the solution given by the piecewise constant timestepping method converges to the viscosity solution as $h \to 0$. However, the problem we study in this chapter is more complex, since we solve a system set of expectations and a nonlinear algebraic equation. We have no proof that Algorithm (5.4.10) converges to the solutions of equations (5.2.7-5.2.10), although we will see in Section 5.6 that our numerical solutions converge to the analytic solutions where available.*

5.4.2 PDE Formulation

Formally, we can formulate this problem in the limit as $\Delta t \to 0$ (equation (5.4.6)) as

$$\begin{aligned} -U_t &= \mu_z^q U_z + \frac{1}{2}(\sigma_z^q)^2 U_{zz} \ , \\ -V_t &= \mu_z^q V_z + \frac{1}{2}(\sigma_z^q)^2 V_{zz} \ , \\ q &\in \arg\max_q \left\{ U - \lambda(V - U^2) \right\} \ , \end{aligned} \tag{5.4.11}$$

where

$$\begin{aligned} \mu_z^q &= \mu_w^q = \pi + w(r + p\sigma_1\xi_1) \\ (\sigma_z^q)^2 &= (\sigma_w^q)^2 = (p\sigma_1 w)^2 \ . \end{aligned} \tag{5.4.12}$$

for the wealth case introduced in Section 5.2; and

$$\begin{aligned} \mu_z^q &= \mu_x^q = \pi + x(-\mu_Y + p\sigma_1(\xi_1 - \sigma_{Y_1}) + \sigma_{Y_0}^2 + \sigma_{Y_1}^2) \\ (\sigma_z^q)^2 &= (\sigma_x^q)^2 = x^2(\sigma_{Y_0}^2 + (p\sigma_1 - \sigma_{Y_1})^2) \ . \end{aligned} \tag{5.4.13}$$

for the wealth-to-income ratio case introduced in Section 5.3. Note that in equations (5.4.12) and (5.4.13), we set $q = p$ (use p as the control). If we want to use pw (the monetary amount invested in the risky asset) as the control, we can set $q = pw$ (px) and replace pw (px) by q in equation (5.4.12) ((5.4.13)).

Equation (5.4.11) is a coupled system of nonlinear differential algebraic equations (DAEs) which appears to be beyond the scope of present day viscosity solution theory.

5.4.3 Computing the Expectations

Algorithm (5.4.10) gives a piecewise constant timestepping method for solution of the optimal stochastic control problem. However, it is not clear how we can compute $U_j^n(z)$ and $V_j^n(z)$. Recall that

$$\begin{aligned} U_j^n(z) &= E_{t_n,z}^{q_j}[U^{n+1}(Z(t_{n+1}))] \ , \\ V_j^n(z) &= E_{t_n,z}^{q_j}[V^{n+1}(Z(t_{n+1}))] \ . \end{aligned}$$

According to [45], given a constant control q_j, we can determine $U_j^n(z)$ and $V_j^n(z)$ by solving (dropping the subscript from q to avoid notational clutter)

$$-U_t = \mu_z^q U_z + \frac{1}{2}(\sigma_z^q)^2 U_{zz} \quad ; \quad z \in \mathbb{D} \ , \tag{5.4.14}$$

$$-V_t = \mu_z^q V_z + \frac{1}{2}(\sigma_z^q)^2 V_{zz} \quad ; \quad z \in \mathbb{D}, \tag{5.4.15}$$

over the interval $[t_{n+1}, t_n]$ (we solve backward in time) with $U(z, t = t_{n+1})$, $V(z, t = t_{n+1})$ computed from the previous step of Algorithm (5.4.10), and at $t = t_N$ $(t = T)$,

$$\begin{aligned} U(z, t = T) &= z, \\ V(z, t = T) &= z^2 \ . \end{aligned} \tag{5.4.16}$$

Since we solve PDEs (5.4.14) and (5.4.15) backward in time, in order to derive the discretization of the PDEs using conventional notations, let $\tau = T - t$. Then, $\tau_n = T - t_{N-n}$ for $0 \leq n \leq N$. We define

$$\hat{U}(\tau, z) = U(T - t, z) \ , \tag{5.4.17}$$

$$\hat{V}(\tau, z) = U(T - t, z) \ . \tag{5.4.18}$$

Then equations (5.4.14) and (5.4.15) become

$$\hat{U}_\tau \ = \ \mu_z^q \hat{U}_z + \frac{1}{2}(\sigma_z^q)^2 \hat{U}_{zz} \ \ ; \ \ z \in \mathbb{D} \ , \tag{5.4.19}$$

$$\hat{V}_\tau \ = \ \mu_z^q \hat{V}_z + \frac{1}{2}(\sigma_z^q)^2 \hat{V}_{zz} \ \ ; \ \ z \in \mathbb{D}, \tag{5.4.20}$$

with terminal condition

$$\begin{aligned} \hat{U}(z, \tau = 0) &= z \ , \\ \hat{V}(z, \tau = 0) &= z^2 \ , \end{aligned} \tag{5.4.21}$$

We then can find the values for $\hat{U}_j^n(z)$ and $\hat{V}_j^n(z)$ by solving PDEs (5.4.19) and (5.4.20), over the interval $[\tau_n, \tau_{n+1}]$ in Algorithm (5.4.10), with q replaced by q_j as appropriate.

5.4.4 Localization

Let,

$$\begin{aligned} \hat{\mathbb{D}} \ &:= \ \text{a finite computational domain which approximates the set } \mathbb{D}. \\ \hat{\mathbb{Q}} \ &:= \ \text{a finite computational set which approximates the set } \mathbb{Q}. \end{aligned} \tag{5.4.22}$$

In order to solve PDEs (5.4.19) and (5.4.20) we need to use a finite computational domain, $\hat{\mathbb{D}} = [z_{\min}, z_{\max}]$. When $z \to \pm\infty$, we assume that

$$\begin{aligned} \hat{U}(z \to \pm\infty, \tau) \ &\simeq \ A_1(\tau) z \ , \\ \hat{V}(z \to \pm\infty, \tau) \ &\simeq \ B_1(\tau) z^2 \ . \end{aligned} \tag{5.4.23}$$

Then, taking into account the initial conditions (5.2.6),

$$\begin{aligned} \hat{U}(z \to \pm\infty, \tau) \ &\simeq \ e^{k_1 \tau} z \ , \\ \hat{V}(z \to \pm\infty, \tau) \ &\simeq \ e^{(2k_1 + k_2)\tau} z^2 \ , \end{aligned} \tag{5.4.24}$$

If $q = p$ (use p as the control), then $k_1 = r + q\sigma_1\xi_1$ and $k_2 = (q\sigma_1)^2$ for the wealth case; $k_1 = -\mu_Y + q\sigma_1(\xi_1 - \sigma_{Y_1}) + \sigma_{Y_0}^2 + \sigma_{Y_1}^2$ and $k_2 = \sigma_{Y_0}^2 + (q\sigma_1 - \sigma_{Y_1})^2$ for the wealth-to-income ratio case. If $q = pz$ (use pw or px as the control), then $k_1 = r + \frac{q}{w}\sigma_1\xi_1$ and $k_2 = \frac{(q\sigma_1)^2}{w^2}$ for the wealth case; $k_1 = -\mu_Y + \frac{q}{x}\sigma_1(\xi_1 - \sigma_{Y_1}) + \sigma_{Y_0}^2 + \sigma_{Y_1}^2$ and $k_2 = \sigma_{Y_0}^2 + (\frac{q}{x}\sigma_1 - \sigma_{Y_1})^2$ for the wealth-to-income ratio case.

Since in Algorithm (5.4.10), we update the values for U and V at the end of each timestep according to the optimal strategy, it is more appropriate to compute $\hat{U}$ and $\hat{V}$ at $z \to \pm\infty$ by using the updated values. Rewriting equation (5.4.24) gives

$$\begin{aligned} \hat{U}(z \to \pm\infty, \tau + \Delta\tau) &\simeq e^{k_1\Delta\tau}\hat{U}(z \to \pm\infty, \tau) \ , \\ \hat{V}(z \to \pm\infty, \tau + \Delta\tau) &\simeq e^{(2k_1+k_2)\Delta\tau}\hat{V}(z \to \pm\infty, \tau) \ . \end{aligned} \tag{5.4.25}$$

Note that the optimal control at $z \to \pm\infty$ is also determined by Algorithm (5.4.10), i.e. we compute equation (5.4.25) for each $q \in \hat{\mathbb{Q}}$, then determine the optimal q according to the objective function. More discussion of these boundary conditions is given in Section 5.5.

5.4.5 Discretization of PDEs

The discretization method for PDEs (5.4.19) and (5.4.20) is the same as the method developed in Chapter 3, if we make the identification

$$\begin{aligned} &Q = (q) \ , \quad \hat{Q} = \hat{\mathbb{Q}} \ , \quad d(z, \tau, 0) = 0 \ , \\ &a(z, \tau, Q) = \frac{1}{2}(\sigma_z^q)^2 \ , \quad b(z, \tau, Q) = \mu_z^q, \quad c(z, \tau, Q) = 0 \ , \end{aligned} \tag{5.4.26}$$

where $Q,\ a,\ b,\ c$ are defined in equation (3.2.2). Then,

$$\hat{U}_\tau = \mathcal{L}^Q\hat{U} \ , \tag{5.4.27}$$

$$\hat{V}_\tau = \mathcal{L}^Q\hat{V} \ . \tag{5.4.28}$$

where the operator $\mathcal{L}$ is defined in equation (3.2.1). From equation (3.3.9), we can see that equation (5.4.27) can be discretized into (in matrix form),

$$\left[I - \Delta\tau A^{n+1}(Q^{n+1}, \hat{U}^{n+1})\right]\hat{U}^{n+1} = \hat{U}^n + (G_U^{n+1} - G_U^n) \ , \tag{5.4.29}$$

and equation (5.4.28) can be discretized into

$$\left[I - \Delta\tau A^{n+1}(Q^{n+1}, \hat{V}^{n+1})\right]\hat{V}^{n+1} = \hat{V}^n + (G_V^{n+1} - G_V^n) \ . \tag{5.4.30}$$

5.4.6 Algorithm for Construction of the Efficient Frontier

Given a positive value for λ, by solving PDEs (5.4.19) and (5.4.20) over each period $[\tau_n, \tau_{n+1}]$, we can compute the numerical solutions of equations (5.4.1), (5.4.2) and (5.4.3).

For the convenience of the reader, we rewrite Algorithm (5.4.10) in terms of $\tau = T - t$, where the expectations are given by solving equations (5.4.30) and (5.4.29). The algorithm is given below. Note that $\hat{U}^n_{i,j}$ and $\hat{V}^n_{i,j}$ are the values for $\hat{U}$ and $\hat{V}$ at node (z_i, q_j, τ_n) respectively.

Algorithm for the Time-consistent Policy

$\hat{U}^0_{i,j} = z_i$, $\hat{V}^0_{i,j} = z_i^2$, for all $0 \le i \le l$ and $0 \le j \le m$
For timestep $n = 0, \ldots, N-1$
  For each $j = 0, \ldots, m$
    Solve equations (5.4.29) and (5.4.30)
      // Note that $[Q^{n+1}]_i = q_j$, for all $0 \le i \le l$
  EndFor
  For $i = 0, \ldots, l$
    $j^* \in \arg\max_{0 \le j \le m} \{\hat{U}^{n+1}_{i,j} - \lambda(\hat{V}^{n+1}_{i,j} - (\hat{U}^{n+1}_{i,j})^2)\}$
    $(q_i^{n+1})^* = q_{j^*}$; $\hat{U}^{n+1}_{i,k} = \hat{U}^{n+1}_{i,j^*}$; $\hat{V}^{n+1}_{i,k} = \hat{V}^{n+1}_{i,j^*}$, for all $0 \le k \le m$,
  EndFor
EndFor

(5.4.31)

Given an initial value $\hat{z}_0$, Algorithm (5.4.32) is used to obtain the efficient frontier. Since the Z grid is discretized over the interval $[z_{\min}, z_{\max}]$, we can use Algorithm (5.4.32) to obtain the efficient frontier for any initial wealth $\hat{z}_0 \in [z_{\min}, z_{\max}]$ by interpolation. Of course, if we choose $\hat{z}_0$ to be a node in the discretized Z grid, then there is no interpolation error.

Algorithm for Constructing the Efficient Frontier

For $\lambda = \lambda_{\min}, \lambda_1, \ldots, \lambda_{\max}$

Compute solutions of equations (5.4.1), (5.4.2) and (5.4.3) by Algorithm (5.4.31)

Given the initial $\hat{z}_0$, use interpolation to get the numerical values of

$$(\hat{U}(\hat{z}_0, t=0), \hat{V}(\hat{z}_0, t=0))_\lambda \text{ at } Z(t=0) = \hat{z}_0$$

Then $E^{q^*}_{t=0,\hat{z}_0}[Z_T] = \hat{U}(\hat{z}_0, t=0)$

and $\text{Std}^{q^*}_{t=0,\hat{z}_0}[Z_T] = \sqrt{\hat{V}(\hat{z}_0, t=0) - [\hat{U}(\hat{z}_0, t=0)]^2}$

EndFor

Construct the efficient frontiers from the points

$$(\text{Std}^{q^*}_{t=0,\hat{z}_0}[Z_T], E^{q^*}_{t=0,\hat{z}_0}[Z_T])_\lambda, \lambda \in [\lambda_{\min}, \lambda_{\max}] \tag{5.4.32}$$

5.5 Various Constraints

In this section, we apply various constraints to the control policy q. As for the pre-commitment strategy, we consider three cases: allowing bankruptcy, no bankruptcy (no shorting stocks) and bounded control. We will see later that these constraints have different effects on boundary conditions and dramatically change the properties of the efficient frontiers.

We summarize the various cases in Table 5.1 below.

Case	Control q	Original Domain: $\mathbb{D}$, $\mathbb{Q}$	Localized Domain: $\hat{\mathbb{D}}$, $\hat{\mathbb{Q}}$
Bankruptcy	pz	$(-\infty, +\infty)$, $(-\infty, +\infty)$	$[z_{\min}, z_{\max}]$, $[q_{\min}, q_{\max}]$
No Bankruptcy	p or pz	$[0, +\infty)$, $[0, +\infty)$	$[0, z_{\max}]$, $[0, q_{\max}]$
Bounded Control	p	$[0, +\infty)$, $[0, q_{\max}]$	$[0, z_{\max}]$, $[0, q_{\max}]$

TABLE 5.1: *Summary of cases.*

5.5.1 Allowing Bankruptcy, Unbounded Controls

We have defined this case in Section 4.3.1. We solve this problem by using the monetary amount invested in the risky asset as the control ($q = pz$). Note that the amount invested in the risky asset was also used as the control in [15] to determine analytic solution for the pre-commitment policy.

Our numerical problem uses

$$\hat{\mathbb{D}} = [z_{\min}, z_{\max}] \ , \ \hat{\mathbb{Q}} = [q_{\min}, q_{\max}] \ , \tag{5.5.1}$$

where $\hat{\mathbb{D}} = [z_{\min}, z_{\max}]$ and $\hat{\mathbb{Q}} = [q_{\min}, q_{\max}]$ are approximations to the original set $\mathbb{D} = (-\infty, +\infty)$ and $\mathbb{Q} = (-\infty, +\infty)$. For each $q \in \hat{\mathbb{Q}}$, we apply the Dirichlet conditions (5.4.25) at $z = z_{\min}, z_{\max}$.

As discussed in previous chapters, the artificial boundary conditions will cause some error. However, we can make these errors small by choosing large values for $(|z_{\min}|, z_{\max})$ and $(|q_{\min}|, q_{\max})$. The error will be small if $(|z_{\min}|, z_{\max})$ and $(|q_{\min}|, q_{\max})$ are sufficiently large [7]. We will verify this in some subsequent numerical tests.

An analytic solution exists for the wealth case [11]. The efficient frontier solution is

$$\begin{cases} Var_{t=0,\hat{w}_0}[W_T] = \frac{\xi_1^2}{4\lambda^2} T \\ E_{t=0,\hat{w}_0}[W_T] = \hat{w}_0 e^{rT} + \pi \frac{e^{rT}-1}{r} + \xi \sqrt{T} \mathrm{Std}(W_T) \ , \end{cases} \tag{5.5.2}$$

and the optimal control ($q = pw$) at any time $t \in [0, T]$ is

$$q^*(t, w) = \frac{\xi_1}{2\lambda\sigma_1} e^{-r(T-t)} \ . \tag{5.5.3}$$

We can then see directly from the SDE (2.2.2), that $W(t)$ can be negative in this case. Hence, $\mathbb{D} = (-\infty, +\infty)$. From equation (5.5.3), given a time t, the optimal monetary amount $q^* = p^* w$ invested in the risky asset is a positive constant. Hence the investor is always long stock.

The efficient frontier $(\mathrm{Std}^{q^*}_{t=0,w}[W_T], E^{q^*}_{t=0,w}[W_T])$ in this case is a straight line. We will use this analytic result to check our numerical solution.

Remark 5.2. *For the wealth case, from equation (5.5.3), we can see that if we use p as the control, then*

$$p^*(t, w) = \frac{\xi_1}{2\lambda\sigma_1 w} e^{-r(T-t)} \ . \tag{5.5.4}$$

Clearly, this will cause some difficulties near $w = 0$, as discussed in [74] (see also Chapter 4). We can avoid these problems in this case by using the control $q = pw$, which is always finite from equation (5.5.3).

Remark 5.3. *The authors of [16] argue that the optimal control (equation (5.5.3)) is not economically meaningful. Since equation (5.5.3) suggests that the investment strategy (in monetary amount) is independent of the level of wealth, a wealthy investor would have the same investment strategy as a less wealthy investor if she uses the same value for λ. [16] suggests letting the risk aversion coefficient λ depend on current wealth, i.e. a function $\lambda(w)$ instead of a constant λ. Our numerical method can easily handle this (use $\lambda(z_i)$ instead of λ in Algorithm (5.4.31) without any further change). We show a numerical test for a particular function of $\lambda(w)$ suggested in [16], in Appendix C.*

5.5.2 No Bankruptcy, No Short Sales

We have defined this case in Section 4.3.2. We can solve this problem by either using the proportion p as the control ($q = p$) or using the monetary amount pw as the control ($q = pw$).

Our numerical problem uses,

$$\hat{\mathbb{D}} \;=\; [0, z_{\max}] \;,\; \hat{\mathbb{Q}} = [0, q_{\max}] \;. \tag{5.5.5}$$

Similar to the pre-commitment strategy, we prohibit the possibility of bankruptcy ($Z(t) < 0$) by requiring that (see Remark 4.5) the optimal monetary amount $\lim_{z\to 0}(p^* z) = 0$, so that PDEs (5.4.19) and (5.4.20) reduce to (at $z = 0$)

$$\begin{aligned} \hat{U}_\tau(0,\tau) &= \pi \hat{U}_z \;, \\ \hat{V}_\tau(0,\tau) &= \pi \hat{V}_z \;. \end{aligned} \tag{5.5.6}$$

5.5.3 No Bankruptcy, Bounded Control

We have defined this case in Section 4.3.3. Since the borrowing upper bound $q_{\max}$ is usually based on the investor's total wealth (e.g, the investor can borrow at most 50% of her total wealth), we use the proportion of the total wealth invested in the risky asset as the control ($q = p$) for this case.

Our numerical problem uses,

$$\hat{\mathbb{D}} \;=\; [0, z_{\max}] \;,\; \hat{\mathbb{Q}} = \mathbb{Q} = [0, q_{\max}] \;. \tag{5.5.7}$$

where $z_{\max}$ is an approximation to the infinity boundary. In this case we also specify that $q \geq 0$ (no shorting the risky asset). Other assumptions and the boundary conditions for V and U are the same as those of no bankruptcy case introduced in Section 5.5.2.

5.6 Numerical Results

In this section, we carry out numerical tests for the defined contribution pension plan problem. We examine both the wealth case (addressed in Section 5.2) and the wealth-to-income ratio case (addressed in Section 5.3).

5.6.1 Wealth Case

We first consider the wealth case introduced in Section 5.2. When bankruptcy is allowed, analytic solutions exist. We use the monetary amount pw as the control. Table 5.2 and 5.3 show the numerical results. Table 5.2 reports the value of $E^{q^*}_{t=0,w}[W_T^2]$, which is the solution of equation (5.4.9). Table 5.3 reports the value of $E^{q^*}_{t=0,w}[W_T]$, which is the

solution of equation (5.4.8). Given $E^{q^*}_{t=0,w}[W_T^2]$ and $E^{q^*}_{t=0,w}[W_T]$, the standard deviation can be easily computed, which is also reported in Table 5.3. The results show that the numerical solutions of $E^{q^*}_{t=0,w}[W_T^2]$ and $E^{q^*}_{t=0,w}[W_T]$ converge to the analytic values at a first order rate as mesh and timestep size tends to zero.

Nodes $(W \times Q)$	Timesteps	Normalized CPU Time	$E^{q^*}_{t=0,w}[W_T^2]$	Ratio
180 × 105	40	1	43.0211	
360 × 209	80	7.24	40.3870	
720 × 417	160	56.16	41.4764	-2.418
1440 × 833	320	437.04	42.0794	1.807
2880 × 1665	640	3445.49	42.3825	1.989
5760 × 3329	1280	31277.09	42.5347	1.991

TABLE 5.2: *Convergence study for the wealth case, allowing bankruptcy. The monetary amount invested in the risky asset is used as the control ($q = pw$). Fully implicit timestepping is applied, using constant timesteps. Parameters are given in Table 4.2, with $\lambda = 0.6$. Values of $E^{q^*}_{t=0,w}[W_T^2]$ are reported at $(W = 1, t = 0)$. Ratio is the ratio of successive changes in the computed values for decreasing values of the discretization parameter h. Analytic solution is $E^{q^*}_{t=0,w}[W_T^2] = 42.6873$. CPU time is normalized. We take the CPU time used for the first test in this table as one unit of CPU time, which uses* 180×105 *nodes for $W \times Q$ grid and 40 timesteps.*

Nodes $(W \times Q)$	Timesteps	$\text{Std}^{q^*}_{t=0,w}[W_T]$	$E^{q^*}_{t=0,w}[W_T]$	Ratio for $\text{Std}^{q^*}_{t=0,w}[W_T]$	Ratio for $E[W_T]$
180 × 105	40	1.74390	6.32297		
360 × 209	80	1.32762	6.21486		
720 × 417	160	1.28790	6.31013	10.480	-1.135
1440 × 833	320	1.26536	6.36226	1.762	1.828
2880 × 1665	640	1.25392	6.38828	1.970	2.003
5760 × 3329	1280	1.24812	6.40132	1.972	1.995

TABLE 5.3: *Convergence study for the wealth case, allowing bankruptcy. The monetary amount invested in the risky asset is used as the control ($q = pw$). Fully implicit timestepping is applied, using constant timesteps. Parameters are given in Table 4.2, with $\lambda = 0.6$. Values of $Std^{q^*}_{t=0,w}[W_T]$ and $E^{q^*}_{t=0,w}[W_T]$ are reported at $(W = 1, t = 0)$. Ratio is the ratio of successive changes in the computed values for decreasing values of the discretization parameter h. Analytic solution is $(Std^{q^*}_{t=0,w}[W_T], E^{q^*}_{t=0,w}[W_T]) = (1.24226, 6.41437)$.*

We also solve the problem for the no bankruptcy case and the bounded control case. Analytic solutions do not exist for these cases. The efficient frontiers are shown in Figure 5.1, with parameters given in Table 4.2. The straight line is the efficient frontier for the allowing bankruptcy case. This result agrees with the analytic solution (equations (5.5.2)). The curve for the case of no bankruptcy is actually two overlapping curves. One is from the solutions obtained by using the monetary amount invested in the risky asset

as the control, and the other is from the solutions using proportion as the control. The lower curve is for the bounded control case. Clearly, the strategy given by the allowing bankruptcy case is the most efficient, and the strategy given by the bounded control case is the least efficient.

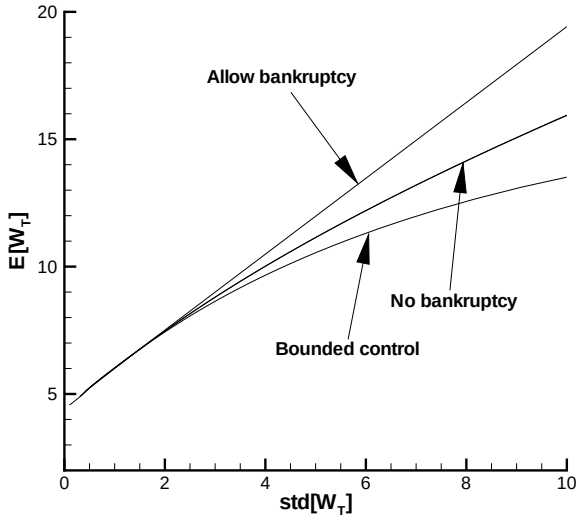

FIGURE 5.1: *Time-consistent efficient frontiers (wealth case) for allowing bankruptcy ($\mathbb{D} = (-\infty, +\infty)$ and $\mathbb{Q} = (-\infty, +\infty)$), no bankruptcy ($\mathbb{D} = [0, +\infty)$ and $\mathbb{Q} = [0, +\infty)$) and bounded control ($\mathbb{D} = [0, +\infty)$ and $\mathbb{Q} = [0, 1.5]$) cases. Parameters are given in Table 4.2. Values are reported at $(W = 1, t = 0)$.*

As mentioned in Section 5.5.1, some error is introduced using the artificial boundaries. However, we can make these errors small by choosing large values for $(|w_{\min}|, w_{\max})$ and $(|q_{\min}|, q_{\max})$. Table 5.4 shows the values of $E^{q^*}_{t=0,w}[W_T^2]$ and $E^{q^*}_{t=0,w}[W_T]$ for different large boundaries. We can see that once $(|w_{\min}|, w_{\max})$ and $(|u_{\min}|, u_{\max})$ are large enough, the values of $E^{q^*}_{t=0,w}[W_T^2]$ and $E^{q^*}_{t=0,w}[W_T]$ are insensitive to the location of these large boundaries.

$(w_{\min}, w_{\max})$	$(q_{\min}, q_{\max})$	$E^{q^*}_{t=0,w}[W_T^2]$	$E^{q^*}_{t=0,w}[W_T]$
(-1000, 1000)	(-1000, 1000)	42.5347	6.40132
(-2000, 2000)	(-2000, 2000)	42.5347	6.40132
(-5000, 5000)	(-5000, 5000)	42.5347	6.40132
(-10000, 10000)	(-10000, 10000)	42.5347	6.40132

TABLE 5.4: *Effect of finite boundary, wealth case, allowing bankruptcy. The monetary amount invested in the risky asset is used as the control ($q = pw$). Parameters are given in Table 4.2, with $\lambda = 0.6$. There are 1280 timesteps for each test. Recall that $q = pw$, which is the monetary amount invested in the risky asset.*

As discussed in Remark 2.1, the wealth case can be reduced to the classic multi-period

portfolio selection problem. The efficient frontier solutions of a particular multi-period portfolio selection problem are shown in Figure 5.2. As for the wealth case, the efficient frontier for the bankruptcy case is a straight line. The curve for the case of no bankruptcy is actually two overlapping curves. One is from the solution obtained using the monetary amount invested in the risky asset as the control, and the other is from the solution computed using the proportion as the control. Again, the strategy given by the allowing bankruptcy case is the most efficient, and the strategy given by the bounded control case is the least efficient.

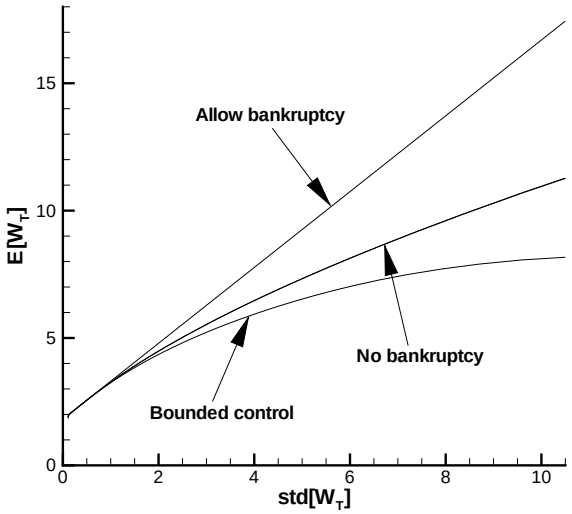

FIGURE 5.2: *Time-consistent efficient frontiers (multi-period portfolio selection problems) for for allowing bankruptcy ($\mathbb{D} = (-\infty, +\infty)$ and $\mathbb{Q} = (-\infty, +\infty)$), no bankruptcy ($\mathbb{D} = [0, +\infty)$ and $\mathbb{Q} = [0, +\infty)$) and bounded control ($\mathbb{D} = [0, +\infty)$ and $\mathbb{Q} = [0, 1.5]$) cases. Parameters are given in Table 4.2 except that the contribution rate $\pi = 0$. Values are reported at $(W = 1, t = 0)$.*

5.6.2 Wealth-to-income Ratio Case

μ_Y	0.	ξ_1	0.2
σ_1	0.2	σ_{Y1}	0.05
σ_{Y0}	0.05	π	0.1
T	20 years	λ	0.25
$\mathbb{Q}$	$[0, 1.5]$	$\mathbb{D}$	$[0, +\infty)$

TABLE 5.5: *Parameters used in the wealth-to-income ratio pension plan examples.*

In this section, we examine the wealth-to-income ratio case (discussed in Section (5.3)). Table 5.5 gives the data used for this example. Table 5.6 and 5.7 show a convergence study

for the bounded control case. We set $x_{\max}, |x_{\min}| = 1000$ in this case. Increasing $x_{\max}$ had no effect on the solution to six digits. Table 5.6 reports the value of $E^{q^*}_{t=0,x}[X_T^2]$, and Table 5.7 reports the values of $E^{q^*}_{t=0,x}[X_T]$ and $\mathrm{Std}^{q^*}_{t=0,x}[X_T]$. The results show that the numerical solutions of $E^{q^*}_{t=0,x}[X_T^2]$ and $E^{q^*}_{t=0,x}[X_T]$ converge at a first order rate as mesh and timestep size tends to zero. No analytic solutions are available in this case.

Nodes $(X \times Q)$	Timesteps	Normalized CPU Time	$E^{q^*}_{t=0,x}[X_T^2]$	Ratio
90×16	40	1.	15.1154	
179×31	80	17.	15.2894	
357×61	160	104.	15.3453	3.113
713×121	320	794.50	15.3696	2.300
1425×241	640	6430.01	15.3814	2.059
2849×481	1280	52513.05	15.3871	2.070

TABLE 5.6: *Convergence study for the wealth-to-income ratio case, bounded control. The proportion of the total wealth invested in the risky asset is used as the control ($q = p$). We set $q = p \in [0, 1.5]$. Fully implicit timestepping is applied, using constant timesteps. Parameters are given in Table 5.5, with $\lambda = 0.25$. Values of $E^{q^*}_{t=0,x}[X_T^2]$ are reported at $(X = 0.5, t = 0)$. Ratio is the ratio of successive changes in the computed values for decreasing values of the discretization parameter h. CPU time is normalized. We take the CPU time used for the first test in this table as one unit of CPU time, which uses 90×16 nodes for $W \times Q$ grid and 40 timesteps.*

Nodes $(X \times Q)$	Timesteps	$\mathrm{Std}^{q^*}_{t=0,x}[X_T]$	$E^{q^*}_{t=0,x}[X_T]$	Ratio for $\mathrm{Std}^{q^*}_{t=0,x}[X_T]$	Ratio for $E[X_T]$
90×16	40	1.37474	3.63669		
179×31	80	1.35197	3.66900		
357×62	160	1.33799	3.68172	1.629	2.540
713×121	320	1.33060	3.68770	1.892	2.127
1425×241	640	1.32688	3.69063	1.987	2.041
2849×481	1280	1.32500	3.69208	1.979	2.021

TABLE 5.7: *Convergence study for the wealth-to-income ratio case, bounded control. The proportion of the total wealth invested in the risky asset is used as the control ($q = p$). We set $q \in [0, 1.5]$. Fully implicit timestepping is applied, using constant timesteps. Parameters are given in Table 5.5, with $\lambda = 0.25$. Values of $Std^{q^*}_{t=0,x}[X_T]$ and $E^{q^*}_{t=0,x}[X_T]$ are reported at $(X = 0.5, t = 0)$. Ratio is the ratio of successive changes in the computed values for decreasing values of the discretization parameter h.*

Efficient frontiers for the wealth case are shown in Figure 5.3, with parameters given in Table 5.5. The curve for bankruptcy case is determined by using the monetary amount invested in the risky asset as the control. As for the wealth case, the curve for the case of no bankruptcy is also two overlapping curves. One is from the solutions using the monetary amount invested in the risky asset as the control, and the other is from the

solutions using the proportion as the control. Again, the strategy given by the allowing bankruptcy case is the most efficient, and the strategy given by the bounded control case is the least efficient.

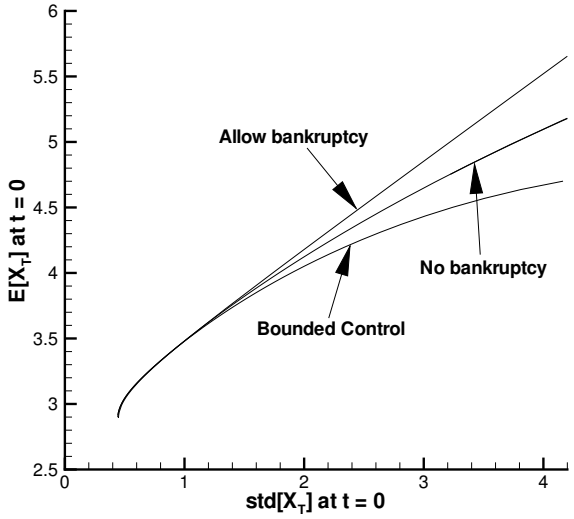

FIGURE 5.3: *Time-consistent efficient frontiers (wealth-to-income ratio case) for allowing bankruptcy ($\mathbb{D} = (-\infty, +\infty)$ and $\mathbb{Q} = (-\infty, +\infty)$), no bankruptcy ($\mathbb{D} = [0, +\infty)$ and $\mathbb{Q} = [0, +\infty)$) and bounded control ($\mathbb{D} = [0, +\infty)$ and $\mathbb{Q} = [0, 1.5]$) cases. Parameters are given in Table 5.5. Values are reported at $(X = 0.5, t = 0)$.*

Remark 5.4. *Similar to the pre-commitment strategy (see Remark 4.5), in the case of bankruptcy prohibition, we have to have $\lim_{z \to 0}(p^* z) = 0$ so that negative wealth is not admissible, where $z = w$ or x. Our numerical tests show that as z goes to zero, $p^* z = O(z^\beta)$. For a reasonable range of parameters, we have $0.9 < \beta < 1$. Hence, this verifies that the boundary conditions (5.5.6) ensure that negative wealth is not admissible under the optimal strategy.*

Figure 5.4 shows the values of the optimal control (the investment strategies) at different times t for a fixed $T = 20$ and $\lambda = 0.25$ for the bounded control case. Under these inputs, if $X(t = 0) = 0.5$, $(\text{Std}^{q^*}_{t=0,x}[X_T], E^{q^*}_{t=0,x}[X_T]) = (1.32500, 3.69208)$ from the finite difference solution. From this figure, we can see that the control q is an increasing function of time t for a fixed X. This behavior of the optimal strategy is also seen in the analytic solution for the wealth case with bankruptcy allowed (Equation 5.5.3). This result is also the same as for the pre-commitment case [74] (see also Chapter 4). In other words, if time goes on, and wealth remains constant, then the investor's optimal strategy is to invest more in the risky asset. Note that the curves for the control are not very smooth in Figure 5.4 (a). This is due to the fact that we have discretized the control in

each interval $[\tau_n, \tau_{n+1}]$. Recall from equation (5.4.5),

$$\begin{aligned} \hat{\mathbb{Q}} = [p_0, p_1, ..., q_m] \quad &, \quad \text{with } p_0 = q_{\min} \ ; \ q_m = q_{\max} \ , \\ \max_{0 \le j \le m-1} (q_{j+1} - q_j) \quad &= \quad C_1 h \ . \end{aligned} \tag{5.6.1}$$

The curves for the control in Figure 5.4 converge to smooth curves as $h \to \infty$. Figure 5.4 (b) is computed by using a finer grid and more timesteps.

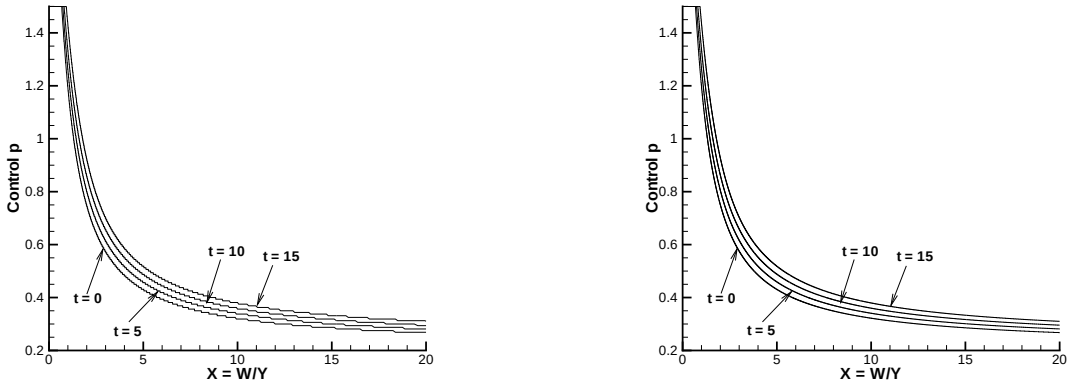

FIGURE 5.4: *Optimal control as a function of* (X, t). *Parameters are given in Table 5.5 with* $\lambda = 0.25$. *Under these inputs, if* $X(t = 0) = 0.5$, $(Std^{q^*}_{t=0,x}[X_T], E^{q^*}_{t=0,x}[X_T]) = (1.32500, 3.69208)$ *from the finite difference solution. Figure (a) uses 4560 nodes for X grid, 433 nodes for the control grid, and 640 timesteps. Figure (b) uses 9120 nodes for X grid, 865 nodes for the control grid, and 1280 timesteps.*

5.6.3 Monte-Carlo Simulation

In this section, we carry out Monte-Carlo simulations. We use the wealth-to-income ratio case with a bounded control as an example. Using the parameters in Table 5.5, we solve the stochastic optimal control problem (equation (5.3.1)) and store the optimal strategies for each $(X = x, t)$. We then carry out Monte-Carlo simulations based on the stored strategies for $X(t = 0) = 0.5$ initially. The value for $(\text{Std}^{q^*}_{t=0,x}[X_T], E^{q^*}_{t=0,x}[X_T])$ is $(1.32500, 3.69208)$ (from the finite difference solution). Table 5.8 shows a convergence study for Monte-Carlo simulations, and Figure 5.5 shows a plot of the convergence study. As the number of simulations increases and the timestep size decreases, the results given by Monte-Carlo simulation converge to the values given by solving the finite difference solution.

Figure 5.6 shows the probability density function computed from the Monte-Carlo simulations (500000 simulations). Figure 5.6 (a) uses $\lambda = 0.15$ ($(\text{Std}^{q^*}_{t=0,x}[X_T], E^{q^*}_{t=0,x}[X_T]) =$

# of Simulations	MC Timestep	$E^{q^*}_{t=0,x}[X_T]$	$\text{Std}^{q^*}_{t=0,x}[X_T]$
1000	0.25	3.7234	1.2753
4000	0.125	3.6705	1.2892
16000	0.0625	3.6815	1.3053
64000	0.03125	3.6883	1.3161
256000	0.015625	3.6913	1.3202

TABLE 5.8: *Convergence study for the Monte-Carlo Simulations (bounded control). Parameters are given in Table 5.5. Values for* $E^{q^*}_{t=0,x}[X_T]$ *and* $Std^{q^*}_{t=0,x}[X_T]$ *are reported at* $(X = 0.5, t = 0)$*. The finite difference values are:* $E^{q^*}_{t=0,x}[X_T] = 3.69208$ *and* $Std^{q^*}_{t=0,x}[X_T] = 1.32500$*.*

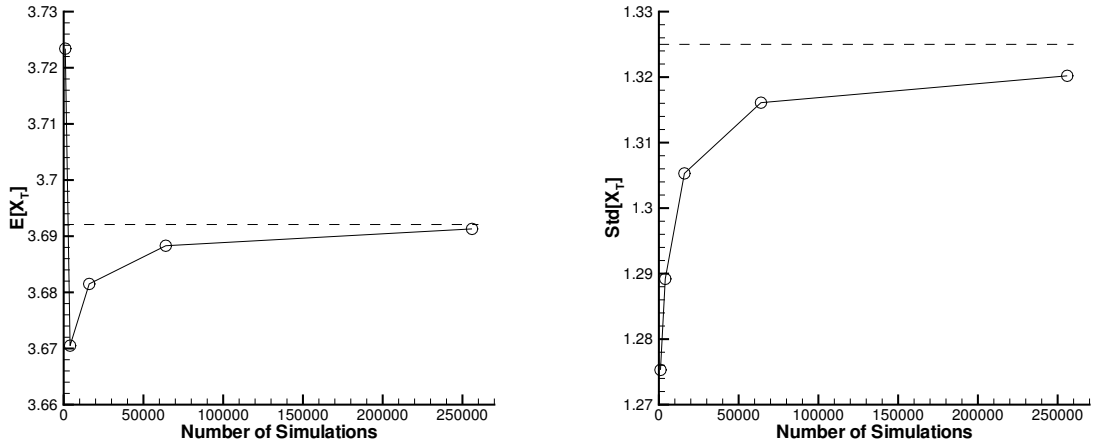

(a) **(b)**

FIGURE 5.5: *Convergence study for Monte-Carlo Simulation (bounded control). Parameters are given in Table 5.5. Figure (a) shows the plot of* $E^{q^*}_{t=0,x}[X_T]$*. Figure (b) shows the plot for* $Std^{q^*}_{t=0,x}[X_T]$*.* $E^{q^*}_{t=0,x}[X_T]$ *and* $Std^{q^*}_{t=0,x}[X_T]$ *are written as* $E[X_T]$ *and* $Std[X_T]$ *in the figure. Values for* $E^{q^*}_{t=0,x}[X_T]$ *and* $Std^{q^*}_{t=0,x}[X_T]$ *are reported in Table 5.8. The finite difference values are* $(Std^{q^*}_{t=0,x}[X_T], E^{q^*}_{t=0,x}[X_T]) = (1.32500, 3.69208)$*.*

$(1.91306, 4.01011)$), while Figure 5.6 (b) uses $\lambda = 0.25$ $((\text{Std}^{q^*}_{t=0,x}[X_T], E^{q^*}_{t=0,x}[X_T]) = (1.32500, 3.69208))$. The shape of the probability density function depends on input parameters (λ in this example). The double peak in Figure 5.6 (a) is due to the same effect as described in [74] (see also Chapter 4).

Figure 5.7 shows the mean and standard deviation for the strategy $q(t, x) = p(t, x)$ as time changes. Figure 5.7 (a) uses $\lambda = 0.15$ $((\text{Std}^{p^*}_{t=0,x}[X_T], E^{p^*}_{t=0,x}[X_T]) = (1.91306, 4.01011))$, while Figure 5.7 (b) uses $\lambda = 0.25$ $((\text{Std}^{p^*}_{t=0,x}[X_T], E^{p^*}_{t=0,x}[X_T]) = (1.32500, 3.69208))$. Both of these Figures show that the mean of $p(t, x)$ is a decreasing function of time t, i.e., as time goes on, the investor switches into the less risky strategy (on average). Since the

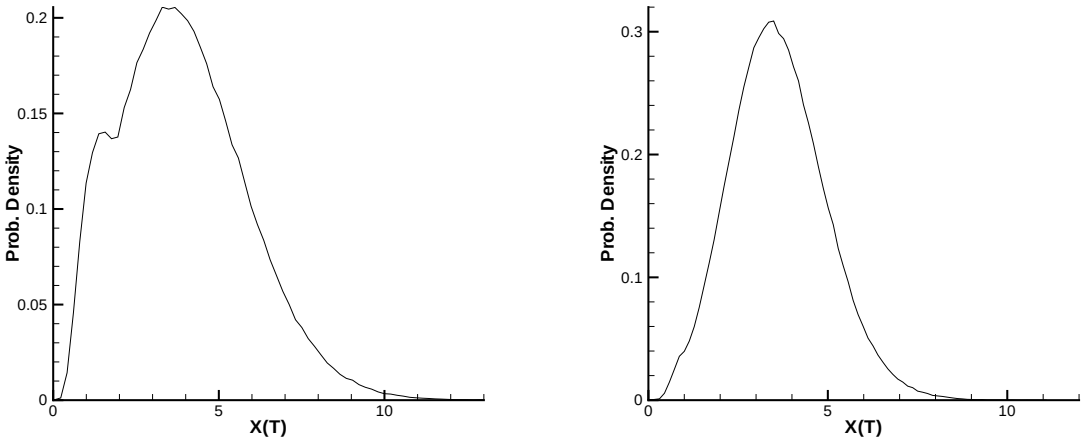

(a) $\lambda = 0.15$ **(b)** $\lambda = 0.25$

FIGURE 5.6: *Probability density function for Monte-Carlo Simulation, bounded control,* $500,000$ *simulations and 1280 simulation timesteps. Parameters are given in Table 5.5. Values for* $(E^{q^*}_{t=0,x}[X_T], Std^{q^*}_{t=0,x}[X_T])$ *are reported at* $(X = 0.5, t = 0)$*. Figure (a) uses* $\lambda = 0.15$*, while Figure (b) uses* $\lambda = 0.25$*. For Figure (a),* $(Std^{q^*}_{t=0,x}[X_T], E^{q^*}_{t=0,x}[X_T]) = (1.91306, 4.01011)$ *from the finite difference solution; For Figure (b),* $(Std^{q^*}_{t=0,x}[X_T], E^{q^*}_{t=0,x}[X_T]) = (1.32500, 3.69208)$ *from the finite difference solution.*

value of $E^{p^*}_{t=0,x}[X_T]$ in Figure 5.7 (b) is higher than the one in Figure 5.7 (a), the mean strategy in Figure 5.7 (b) is more risky compared to Figure 5.7 (a).

5.7 Summary

The main results of this chapter are

- We develop a fully numerical scheme for determining the optimal time-consistent mean variance strategy. Any type of constraint can be applied to the optimal policy.
- The method is based on the piecewise constant policy technique in [45]. In our case, since the time-consistent problem can be formulated as a system of HJB differential algebraic equations, this falls outside the viscosity solution theory in [45]. Hence we have no formal proof of convergence of our method. Nevertheless, our technique does converge to analytic solutions where available.
- Although we have given examples in this chapter with constant λ, the numerical schemes can handle non-constant λ as proposed in [16] (see Appendix C).

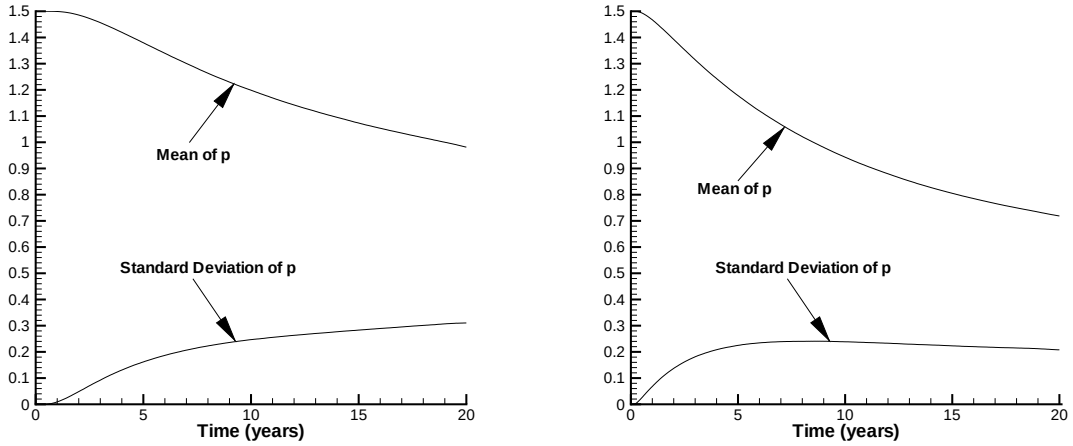

(a) $\lambda = 0.15$ **(b)** $\lambda = 0.25$

FIGURE 5.7: *Mean and standard deviation for the control* $q(t,x) = p(t,x)$*. There are 64000 simulations and 1280 simulation timesteps. Parameters are given in Table 5.5. Figure (a) uses* $\lambda = 0.15$*, while Figure (b) uses* $\lambda = 0.25$*. For Figure (a),* $(Std^{p^*}_{t=0,x}[X_T], E^{p^*}_{t=0,x}[X_T]) = (1.91306, 4.01011)$ *from the finite difference solution; For Figure (b),* $(Std^{p^*}_{t=0,x}[X_T], E^{p^*}_{t=0,x}[X_T]) = (1.32500, 3.69208)$ *from the finite difference solution.*

Chapter 6

Mean Quadratic Variation

We have discussed pre-commitment and time-consistent mean variance strategies in the previous chapters. As discussed in Section 2.3.3, a criticism of both pre-commitment and time-consistent strategies is that the risk is only measured in terms of the standard deviation at the end of trading. In an effort to provide a more direct control over risk during the investment period, a mean quadratic variation objective function has been proposed in [18, 35]. In this chapter, we will study the mean quadratic variation strategy.

6.1 Mean Quadratic Variation Wealth Case

In this section, we give the mathematical model for the optimal mean quadratic variation investment strategy. Let,

$$\begin{aligned} \mathbb{D} &:= \text{the set of all admissible wealth } W(t), \text{ for } 0 \le t \le T; \\ \mathbb{P} &:= \text{the set of all admissible controls } p(t,w), \text{ for } 0 \le t \le T \text{ and } w \in \mathbb{D}. \end{aligned} \tag{6.1.1}$$

In this chapter, we use p (the proportion of the total wealth invested in the risky asset) as the control. Recall that the mean quadratic optimization problem (2.3.11) is

$$J(w,t) = \sup_{p(t,w)} \{E^p_{t,w}[W_T] - \lambda \int_t^T (e^{r(T-u)}\sigma_1 p w)^2 du\}. \tag{6.1.2}$$

We define

$$V(w,t) = \sup_{p\in\mathbb{P}} E^p_{t,w}[W_T - \lambda \int_t^T (e^{r(T-u)}\sigma_1 p w)^2 du] \ . \tag{6.1.3}$$

Let $\tau = T - t$. Then using equation (2.2.2) and Ito's Lemma, we have that $V(w,\tau)$ satisfies the HJB equation

$$V_\tau \ = \ \sup_{p\in\mathbb{P}}\{\mu^p_w V_w + \frac{1}{2}(\sigma^p_w)^2 V_{ww} - \lambda(e^{r\tau}\sigma_1 p w)^2\} \ \ ; \ \ w \in \mathbb{D}, \tag{6.1.4}$$

with terminal condition

$$V(w, \tau = 0) = w \ , \tag{6.1.5}$$

and where

$$\begin{aligned} \mu_w^p &= \pi + w(r + p\sigma_1\xi_1) \\ (\sigma_w^p)^2 &= (p\sigma_1 w)^2 \ . \end{aligned} \tag{6.1.6}$$

In order to trace out the efficient frontier solution (in terms of mean and quadratic variation of the wealth) of problem (6.1.2), we proceed in the following way. Pick an arbitrary value of λ and solve problem (6.1.2), which determines the optimal control $p^*(t, w)$. We also need to determine $E_{t=0,w}^{p^*}[W_T]$.

Let $U = U(w, \tau) = E[W_T | W(t = T - \tau) = w, p(t = T - \tau, w) = p^*(t = T - \tau, w)]$. Then U is given from the solution to

$$U_\tau = \{\mu_w^p U_w + \frac{1}{2}(\sigma_w^p)^2 U_{ww}\}_{p(t=T-\tau,w)=p^*(t=T-\tau,w)} \ \ ; \ \ w \in \mathbb{D} \ , \tag{6.1.7}$$

with the payoff

$$U(w, \tau = 0) = w \ . \tag{6.1.8}$$

Since the most costly part of the solution of equation (6.1.4) is the determination of the optimal control p^*, solution of equation (6.1.7) is very inexpensive, since p^* is known.

Note that $E_{t=0,w}^{p^*}[const.] = const.$. Then

$$\begin{aligned} V(\hat{w}_0, \tau = T) &= E_{t=0,w}^{p^*}[W_T] - \lambda \int_0^T (e^{r(T-t)}\sigma_1 p^* w)^2 dt \ , \\ U(\hat{w}_0, \tau = T) &= E_{t=0,w}^{p^*}[W_T] \ . \end{aligned} \tag{6.1.9}$$

Then, the quadratic variation $\int_0^T (e^{r(T-t)}\sigma_1 p^* w)^2 dt = U(\hat{w}_0, \tau = T) - V(\hat{w}_0, \tau = T)$.

It is useful to know the variance of the terminal wealth, $Var_{t=0,w}^{p^*}[W_T]$, under the optimal strategy in terms of mean quadratic variation. Let $C = C(w, \tau) = E[W_T^2 | W(t = T - \tau) = w, p(t = T - \tau, w) = p^*(t = T - \tau, w)]$. Then C is given from the solution to

$$C_\tau = \{\mu_w^p C_w + \frac{1}{2}(\sigma_w^p)^2 C_{ww}\}_{p(t=T-\tau,w)=p^*(t=T-\tau,w)} \ \ ; \ \ w \in \mathbb{D} \ , \tag{6.1.10}$$

with the payoff

$$C(w, \tau = 0) = w^2 \ . \tag{6.1.11}$$

Assuming $C(\hat{w}_0, \tau = T), U(\hat{w}_0, \tau = T)$ are known, For a given λ, we can then compute the pair $(Var_{t=0,w}^{p^*}[W_T], E_{t=0,w}^{p^*}[W_T])$ from $Var_{t=0,w}^{p^*}[W_T] = C(\hat{w}_0, \tau = T) - U^2(\hat{w}_0, \tau = T)$ and $E_{t=0,w}^{p^*}[W_T] = U(\hat{w}_0, \tau = T)$.

6.2 Localization

Let,

$$\hat{\mathbb{D}} \;:=\; \text{a finite computational domain which approximates the set } \mathbb{D}. \tag{6.2.1}$$

In order to solve the PDEs (6.1.4), (6.1.7) and (6.1.10), we need to use a finite computational domain, $\hat{\mathbb{D}} = [w_{\min}, w_{\max}]$. When $w \to \pm\infty$, we assume that

$$\begin{aligned} V(w \to \pm\infty, \tau) &\simeq H_1(\tau) w^2 \ , \\ U(w \to \pm\infty, \tau) &\simeq J_1(\tau) w \ , \\ C(w \to \pm\infty, \tau) &\simeq I_1(\tau) w^2 \ , \end{aligned} \tag{6.2.2}$$

then, ignoring lower order terms and taking into account the initial conditions (6.1.5), (6.1.8), (6.1.11),

$$\begin{aligned} V(w \to \pm\infty, \tau) &\simeq \frac{\lambda e^{r\tau} k_2}{2k_1 + k_2} (1 - e^{(2k_1+k_2)\tau}) w^2 \ , \\ U(w \to \pm\infty, \tau) &\simeq e^{k_1 \tau} w \ , \\ C(w \to \pm\infty, \tau) &\simeq e^{(2k_1+k_2)\tau} w^2 \ , \end{aligned} \tag{6.2.3}$$

where $k_1 = r + p\sigma_1\xi_1$ and $k_2 = (p\sigma_1)^2$. We consider three cases.

6.2.1 Allowing Bankruptcy, Unbounded Controls

We have defined this case in Section 4.3.1. Our numerical problem uses

$$\hat{\mathbb{D}} \;=\; [w_{\min}, w_{\max}] \ , \tag{6.2.4}$$

where $\hat{\mathbb{D}} = [w_{\min}, w_{\max}]$ is an approximation to the original set $\mathbb{D} = (-\infty, +\infty)$.

When allowing bankruptcy, the solution for the mean quadratic variation strategy is identical to the time-consistent mean variance policy (5.2.2) [16]. Recall that the analytic solution for the time-consistent strategy (equation (5.5.3)) shows that p^*w is constant. Suppose we discretize W into the grid $[w_0, w_1, ..., w_{imax}]$, where $w_0 = w_{min}$ and $w_{imax} = w_{max}$. Then, since p^*w is constant, $p^*(t, w_{min}) = \frac{p^*(t,w_1)w_1}{w_{min}}$, where $p^*(t, w_1)$ can be determined by solving PDE (6.1.4) with the method given in Section 6.4. Similarly, $p^*(t, w_{max}) = \frac{p^*(t,w_{imax-1})w_{imax-1}}{w_{max}}$.

An alternative way to determine $p^*(t, w_{min})$ and $p^*(t, w_{max})$ is to use the method of discretization of the control (see Section 3.4.1 and 3.7.4). Define a discrete set $\hat{\mathbb{P}} = \{p_{min}, ..., p_{max}\}$ for the control. At $w \to \pm\infty$, recall that

$$V(w \to \pm\infty, \tau) \simeq \frac{\lambda e^{r\tau} k_2}{2k_1 + k_2} (1 - e^{(2k_1+k_2)\tau}) w^2 \ , \tag{6.2.5}$$

then,

$$p^*(w \to \pm\infty, \tau) \in \arg\max_{p\in\hat{\mathbb{P}}}\{\mu_w^p V_w + \frac{1}{2}(\sigma_w^p)^2 V_{ww} - \lambda(e^{r\tau}\sigma_1 pw)^2\} \ . \tag{6.2.6}$$

Note that we apply this method only at the boundary nodes w_{min} and w_{max} to determine $p^*(t, w_{min})$ and $p^*(t, w_{max})$.

6.2.2 No Bankruptcy, No Short Sales

We have defined this case in Section 4.3.2. Our numerical problem uses,

$$\hat{\mathbb{D}} \ = \ [0, w_{\max}] \ . \tag{6.2.7}$$

The boundary conditions for V, U, C at $w = w_{\max}$ are given by equations (6.2.3). We make the assumption that as $w \to +\infty$, $p^*(t, w)w$ is constant (as for the allowing bankruptcy case). This is clearly an approximation, but the error in regions of interest can be make small by choosing w_{max} sufficiently large. We can use the same method to determine $p^*(t, w_{max})$ as for the allowing bankruptcy case.

Similar to the pre-commitment strategy, we prohibit the possibility of bankruptcy ($W(t) < 0$) by requiring that (see Remark 4.5) $\lim_{w\to 0}(pw) = 0$, so that equations (6.1.4), (6.1.7) and (6.1.10) reduce to (at $w = 0$)

$$\begin{aligned} V_\tau(0,\tau) &= \pi V_w \ , \\ U_\tau(0,\tau) &= \pi U_w \ . \\ C_\tau(0,\tau) &= \pi C_w \ . \end{aligned} \tag{6.2.8}$$

6.2.3 No Bankruptcy, Bounded Control

We have defined this case in Section 4.3.3. Our numerical problem uses,

$$\hat{\mathbb{D}} \ = \ [0, w_{\max}] \ , \tag{6.2.9}$$

where $w_{\max}$ is an approximation to the infinity boundary. We still make the assumption that as $w \to +\infty$, $p^*(t, w)w$ is constant. Alternatively, we can also determine $p^*(t, w_{min})$ and $p^*(t, w_{max})$ using the method of discretization of the control as for the allowing bankruptcy case. Both methods give similar results. Other assumptions and the boundary conditions for V and U are the same as those of the no bankruptcy case introduced in Section 6.2.2.

We summarize the various cases in Table 6.1

Case	$\hat{\mathbb{D}}$	$\mathbb{P}$
Bankruptcy	$[w_{\min}, w_{\max}]$	$(-\infty, +\infty)$
No Bankruptcy	$[0, w_{\max}]$	$[0, +\infty)$
Bounded Control	$[0, w_{\max}]$	$[0, p_{\max}]$

TABLE 6.1: *Summary of cases.*

6.3 Mean Quadratic Variation Wealth-to-income Ratio Case

We next consider the wealth-to-income ratio case introduced in Section 2.2.2. The stochastic models for the underlying asset S, the plan holder's year salary Y, the wealth W and her wealth-to-income ratio X have been given in equations (2.2.4 - 2.2.7).

The mean quadratic variation control problem is then to determine the strategy $q(t, X(t) = x)$ such that $q(t, x)$ maximizes

$$J(x,t) = \sup_{p(t,x)} (E^p_{t,x}[X_T] - \lambda \int_t^T e^{2r'(T-u)} (\sigma^p_x)^2 du), \tag{6.3.1}$$

subject to stochastic process (2.2.7), where $r' = -\mu_Y + \sigma^2_{Y_0} + \sigma^2_{Y_1}$ and recall that

$$\begin{aligned} \mu^p_x &= \pi + x(-\mu_Y + p\sigma_1(\xi_1 - \sigma_{Y_1}) + \sigma^2_{Y_0} + \sigma^2_{Y_1}) \\ (\sigma^p_x)^2 &= x^2(\sigma^2_{Y_0} + (p\sigma_1 - \sigma_{Y_1})^2) \ . \end{aligned} \tag{6.3.2}$$

Note that we have posed the problem in terms of the future value of the quadratic variation using r' as the discount factor. For the wealth case, with no constraints on the controls, the analytic solution for the time-consistent mean variance policy is identical to the mean quadratic variation strategy (6.1.2) [16]. However, there does not appear to an analytic solution available for the wealth-to-income ratio case. By analogy with the allowing bankruptcy case, we use r' as the effective drift rate, i.e. the drift when there is no investment in the risky asset. There are clearly other possibilities here.

Similar to problem (6.1.2), we define

$$V(x,t) = \sup_{p \in \mathbb{P}} E^p_{t,x}[W_T - \lambda \int_t^T e^{2r'(T-u)} (\sigma^p_x)^2 du] \ . \tag{6.3.3}$$

Let $\tau = T - t$. Then $V(x, \tau)$ satisfies the HJB equation

$$V_\tau = \sup_{p \in \mathbb{P}} \{\mu^p_x V_x + \frac{1}{2}(\sigma^p_x)^2 V_{xx} - \lambda e^{2r'\tau} (\sigma^p_x)^2\} \ ; \ x \in \mathbb{D}, \tag{6.3.4}$$

with terminal condition

$$V(x, \tau = 0) = x \ . \tag{6.3.5}$$

We still use $\mathbb{D}$ and $\mathbb{P}$ as the sets of all admissible wealth-to-income ratio and control. As before, we let $\hat{\mathbb{D}}$ be the localized computational domain.

We also solve for $U(x,\tau) = E[X_T | X(t=T-\tau)=x, p(t=T-\tau,x) = p^*(t=T-\tau,x)]$ and $C(x,\tau) = E[W_X^2 | X(t=T-\tau)=x, p(t=T-\tau,x) = p^*(t=T-\tau,x)]$ using

$$U_\tau = \{\mu_x^p U_x + \frac{1}{2}(\sigma_x^p)^2 U_{xx}\}_{p(t=T-\tau,x)=p^*(t=T-\tau,x)} \;\; ; \;\; x \in [0,+\infty) \; , \tag{6.3.6}$$

$$C_\tau = \{\mu_x^p C_x + \frac{1}{2}(\sigma_x^p)^2 C_{xx}\}_{p(t=T-\tau,x)=p^*(t=T-\tau,x)} \;\; ; \;\; x \in \mathbb{D} \; , \tag{6.3.7}$$

with terminal condition

$$U(x,\tau=0) = x \; . \tag{6.3.8}$$

$$C(x,\tau=0) = x^2 \; . \tag{6.3.9}$$

We can then use the method described in Section 6.1 to trace out the efficient frontier solution of problem (6.3.1).

We consider the cases: allowing bankruptcy ($\mathbb{D} = (-\infty,+\infty)$, $\mathbb{P} = (-\infty,+\infty)$), no bankruptcy ($\mathbb{D} = [0,+\infty)$, $\mathbb{P} = [0,+\infty)$), and bounded control ($\mathbb{D} = [0,+\infty)$, $\mathbb{P} = [0, p_{\max}]$). For computational purposes, we localize the problem to to $\hat{\mathbb{D}} = [x_{\min}, x_{\max}]$, and apply boundary conditions as in Section 6.2. More precisely, if $x = 0$ is a boundary, with $X < 0$ prohibited, then $\lim_{w\to 0}(px) = 0$, and hence

$$\begin{aligned} V_\tau(0,\tau) &= \pi V_x \; , \\ U_\tau(0,\tau) &= \pi U_x \; , \\ C_\tau(0,\tau) &= \pi C_x \; . \end{aligned} \tag{6.3.10}$$

The boundary conditions at $x \to \pm\infty$ are given in equation (6.2.3), but using x instead of w and r' instead of r with $k_1 = -\mu_Y + p\sigma_1(\xi_1 - \sigma_{Y_1}) + \sigma_{Y_0}^2 + \sigma_{Y_1}^2$ and $k_2 = \sigma_{Y_0}^2 + (p\sigma_1 - \sigma_{Y_1})^2$.

At $x \to \pm\infty$, similarly to the wealth case (see Section 6.2.1), we can use the method of discretization of the control to determine the optimal controls for the boundary nodes.

6.4 Discretization of the HJB PDE

Similar to the pre-commitment strategy in Chapter 4, we can directly apply the numerical scheme developed in Chapter 3 for solving equations (6.1.4)/(6.3.4), (6.1.7)/(6.3.6), (6.1.10)/(6.3.7). The pension plan asset allocation model is a special case of the general HJB equation (3.2.2), if we make the identification

$$\begin{aligned} &Q = (p) \; , \quad \hat{Q} = \mathbb{P} \; , \quad d(z,\tau,0) = -\lambda e^{2r'\tau}(\sigma_x^p)^2 \; , \\ &a(z,\tau,Q) = \frac{1}{2}(\sigma_z^p)^2 \; , \quad b(z,\tau,Q) = \mu_z^p, \quad c(z,\tau,Q) = 0 \; , \end{aligned} \tag{6.4.1}$$

where $z = w$ for the wealth case, $z = x$ for the wealth-to-income ratio case, and $Q,\ a,\ b,\ c$ are defined in equation (3.2.2). Then,

$$V_\tau = \sup_{Q \in \hat{Q}} \{\mathcal{L}^Q V + d(z, p, \tau)\} \ , \tag{6.4.2}$$

and

$$U_\tau = \{\mathcal{L}^Q U\}_{Q=Q^*} \ , \tag{6.4.3}$$
$$C_\tau = \{\mathcal{L}^Q C\}_{Q=Q^*} \ . \tag{6.4.4}$$

Given node $z = z_i$, with specified solution estimate $\hat{V}^k = [\hat{v}_0^k, ..., \hat{v}_{imax}^k]'$, the objective function which is maximized at each node in Algorithm (3.5.1) is

$$\begin{aligned} [F^{n+1}(Q, \hat{V}^k)]_i &= [A^{n+1}(Q, \hat{V}^k)\hat{V}^k + D(Q)]_i \\ &= [\mu_z^p]_i[(\hat{v}^k)_z]_i + \frac{1}{2}([\sigma_z^p]_i)^2[(\hat{v}^k)_{zz}]_i^{n+1} + [d(z, Q, \tau)]_i \ , \end{aligned} \tag{6.4.5}$$

where $\hat{V}^k$ is the vector containing the current estimate of the discrete solution values. Similar to the passport option case in Chapter 3, if we want to apply central differencing as much as possible, Algorithm (3.6.13) is used to decide which differencing scheme is used (which depends on Q and $\hat{V}^k$).

Given an initial value $\hat{z}_0$, we can use Algorithm (4.6.1) in Chapter 4 to obtain the efficient frontier.

6.4.1 Convergence to the Viscosity Solution

PDEs (6.4.3) and (6.4.4) are linear, since the optimal control is pre-computed. We can then obtain classical solutions of the linear PDEs (6.4.3) and (6.4.4). However, PDE (6.4.2) is highly nonlinear, so the classical solution may not exist in general. In this case, we are seeking the viscosity solution [5, 29].

As for the numerical scheme for the pre-commitment strategy, following the same proof given in Chapter 3, we can show that our numerical scheme converges to the viscosity solution of equation (6.4.2), assuming that (6.4.2) satisfies a strong comparison principle (Assumption 4.10).

6.5 Numerical Results

In this section we examine the numerical results for the strategy of minimizing the quadratic variation. We consider two risk measures when we construct efficient frontiers. One measure is the usual standard deviation, and the other measure is the quadratic variation, $\int_0^T (e^{r(T-t)}dw)^2$. We use the notation $Q\_std_{t=0,w}^{p^*}[W_T]$ to denote the square root of $\int_0^T (e^{r(T-t)}dw)^2$, i.e. $Q\_std_{t=0,w}^{p^*}[W_T] = \sqrt{\int_0^T (e^{r(T-t)}dw)^2}$.

6.5.1 Wealth Case

When bankruptcy is allowed, as pointed out in [16], the mean quadratic variation strategy has the same solution as the time-consistent strategy. The analytic solutions for the time-consistent strategy are given in Section 5.5.1. Given the parameters in Table 4.2, if $\lambda = 0.6$, the exact solution is $(\text{Std}^{p^*}_{t=0,w}[W_T], E^{p^*}_{t=0,w}[W_T]) = (1.24226, 6.41437)$. Table 6.2 and 6.3 show the numerical results. Table 6.2 reports the value of $V = E^{p^*}_{t=0,w}[W_T - \lambda \int_0^T (e^{r(T-t)} dw)^2]$, which is the viscosity solution of the nonlinear HJB PDE (6.1.4). Table 6.2 shows the our numerical solution converges to the viscosity solution at a first order rate. Table 6.3 reports the value of $E^{p^*}_{t=0,w}[W_T]$, which is the solution of the linear PDE (6.1.7). We also computed the values of $E^{p^*}_{t=0,w}[W_T^2]$ (not shown in tables), which is the the solution of PDE (6.1.10). Given $E^{p^*}_{t=0,w}[W_T^2]$ and $E^{p^*}_{t=0,w}[W_T]$, the standard deviation can now be easily computed, which is also reported in Table 6.3. The results show that the numerical solutions of $\text{Std}^{p^*}_{t=0,w}[W_T]$ and $E^{p^*}_{t=0,w}[W_T]$ converge to the analytic values at a first order rate as mesh and timestep size tends to zero.

Nodes (W)	Timesteps	Nonlinear iterations	Normalized CPU Time	$V(w = 1, t = 0)$	Ratio
1456	320	640	1.	5.49341	
2912	640	1280	4.13	5.49092	
5824	1280	2560	16.31	5.48968	2.008
11648	2560	5120	66.23	5.48906	2.000
23296	5120	10240	268.53	5.48875	2.000
46592	10240	20480	1145.15	5.48860	2.067

TABLE 6.2: *Convergence study, wealth case, allowing bankruptcy. Fully implicit timestepping is applied, using constant timesteps. Parameters are given in Table 4.2, with* $\lambda = 0.6$. *Values of* $V = E^{p^*}_{t=0,w}[W_T - \lambda \int_0^T (e^{r(T-t)} dw)^2]$ *are reported at* $(W = 1, t = 0)$. *Ratio is the ratio of successive changes in the computed values for decreasing values of the discretization parameter* h. *CPU time is normalized. We take the CPU time used for the first test in this table as one unit of CPU time, which uses 1456 nodes for* W *grid and 320 timesteps.*

We also solve the problem for the no bankruptcy case and the bounded control case. The efficient frontiers are shown in Figure 6.1, with parameters given in Table 4.2 and $(W(t = 0) = 1, t = 0)$. Figure 6.1 (a) shows the results obtained by using the standard deviation as the risk measure, and Figure 6.1 (b) shows the results obtained by using the quadratic variation as the risk measure. Note that, in both figures, the three efficient frontiers pass through the same lowest point. At that point, the plan holder simply invests all her wealth in the risk free bond all the time, so the risk (standard deviation/quadratic variation) is zero. For both risk measures, the efficient frontiers for the allowing bankruptcy case are straight lines. This result agrees with the results from the pre-commitment strategy (see Chapter 4) and the time-consistent strategy (see Chapter 5). The strategy given by the allowing bankruptcy case is the most efficient, and the strategy given by the bounded control case is the least efficient.

Nodes (W)	Timesteps	$\text{Std}^{p^*}_{t=0,w}[W_T]$	$E^{p^*}_{t=0,w}[W_T]$	Ratio for $\text{Std}^{p^*}_{t=0,w}[W_T]$	Ratio for $E[W_T]$
1456	320	1.30652	6.41986	1.960	
2912	640	1.27466	6.41711	1.972	
5824	1280	1.25853	6.41574	1.975	2.007
11648	2560	1.25041	6.41505	1.986	1.986
23296	5120	1.24634	6.41471	1.995	2.029
46592	10240	1.244300	6.41454	2.000	1.995

TABLE 6.3: *Convergence study for the wealth case, allowing bankruptcy. Fully implicit timestepping is applied, using constant timesteps. The parameters are given in Table 4.2, with* $\lambda = 0.6$. *Values of* $Std^{q^*}_{t=0,w}[W_T]$ *and* $E^{q^*}_{t=0,w}[W_T]$ *are reported at* $(W = 1, t = 0)$. *Ratio is the ratio of successive changes in the computed values for decreasing values of the discretization parameter* h. *Analytic solution is* $(Std^{p^*}_{t=0,w}[W_T], E^{p^*}_{t=0,w}[W_T]) = (1.24226, 6.41437)$.

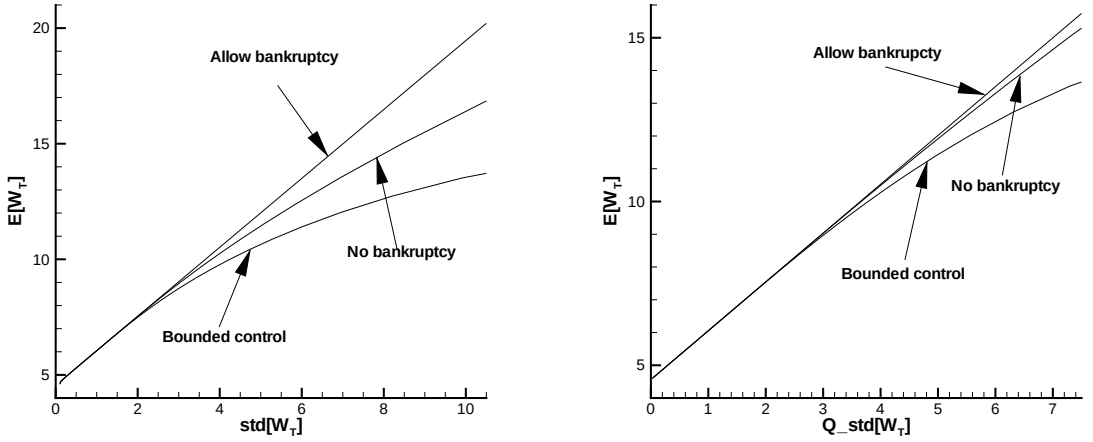

(a) Risk measure: std **(b) Risk measure:** Q_std

FIGURE 6.1: *Mean quadratic variation efficient frontiers (wealth case) for allowing bankruptcy (*$\mathbb{D} = (-\infty, +\infty)$ *and* $\mathbb{P} = (-\infty, +\infty)$*), no bankruptcy (*$\mathbb{D} = [0, +\infty)$ *and* $\mathbb{P} = [0, +\infty)$*) and bounded control (*$\mathbb{D} = [0, +\infty)$ *and* $\mathbb{P} = [0, 1.5]$*) cases. Parameters are given in Table 4.2. Values are reported at* $(W = 1, t = 0)$. *Figure (a) shows the efficient frontiers with risk measure of standard deviation. Figure (b) shows the efficient frontiers with risk measure of quadratic variation.*

Figure 6.2 shows the values of the optimal control (the investment strategies) at different time t for a fixed $T = 20$. The parameters are given in Table 4.2, with bounded control ($p \in [0, 1.5]$) and $\lambda = 0.604$. Under these inputs, if $W(t = 0) = 1$, $(\text{Std}^{p^*}_{t=0,w}[W_T], E^{p^*}_{t=0,w}[W_T]) = (1.23824, 6.40227)$ and $Q\_std^{p^*}_{t=0,w}[W_T] = 1.52262$ from the finite difference solution. From this Figure, we can see that the control p is a increasing function of time t for a fixed w. This agrees with the results from the pre-commitment

[74] (see also Chapter 4) and time-consistent strategies [73] (see also Chapter 5).

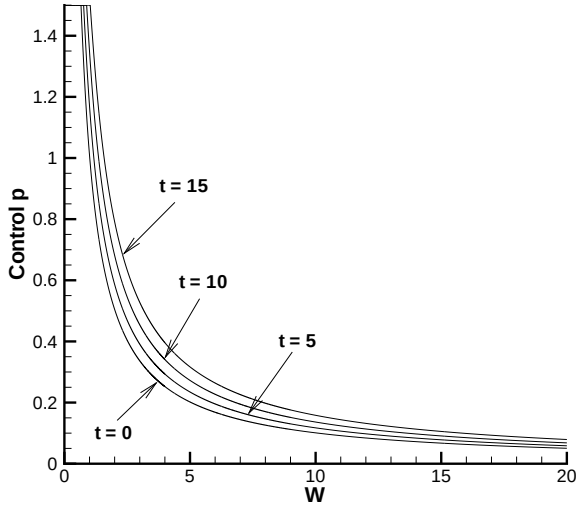

FIGURE 6.2: *Optimal control as a function of* (W, t). *Parameters are given in Table 4.2, with* $\lambda = 0.604$. *Under these inputs, if* $W(t=0) = 1$, $(Std^{p^*}_{t=0,w}[W_T], E^{p^*}_{t=0,w}[W_T]) = (1.23824, 6.40227)$ *and* $Q\_std^{p^*}_{t=0,w}[W_T] = 1.52262$ *from the finite difference solution.*

Remark 6.1. *Similar to the pre-commitment strategy (see Remark 4.5), in the case of bankruptcy prohibition, we have to have* $\lim_{w\to 0}(p^*w) = 0$ *so that negative wealth is not admissible. Our numerical tests show that as* w *goes to zero,* $p^*w = O(w^\beta)$. *For a reasonable range of parameters, we have* $0.9 < \beta < 1$. *Hence, this verifies that the boundary conditions (6.2.8) ensure that negative wealth is not admissible under the optimal strategy. This property also holds for the wealth-to-income ratio case.*

6.5.2 Multi-period Portfolio Selection

As discussed in Remark 2.1, the wealth case can be reduced to the classic multi-period portfolio selection problem. Efficient frontier solutions for a particular multi-period portfolio selection problem are shown in Figure 6.3, with parameters in Table 4.2 but with $\pi = 0$. Again, we consider three cases: allowing bankruptcy, no bankruptcy, and bounded control cases. Figure 6.3 (a) shows the results obtained by using the standard deviation as the risk measure, and Figure 6.3 (b) shows the results obtained by using the quadratic variation as the risk measure. As for the wealth case, in both figures, the efficient frontiers for the allowing bankruptcy case are straight lines.

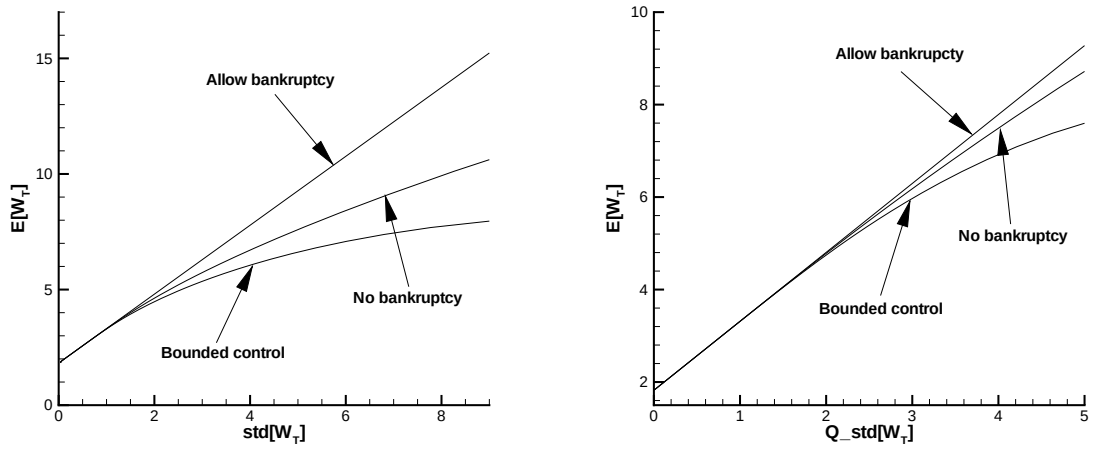

(a) Risk measure: std **(b) Risk measure:** Q_std

FIGURE 6.3: *Efficient frontiers (multi-period portfolio selection) for allowing bankruptcy ($\mathbb{D} = (-\infty, +\infty)$ and $\mathbb{P} = (-\infty, +\infty)$), no bankruptcy ($\mathbb{D} = [0, +\infty)$ and $\mathbb{P} = [0, +\infty)$) and bounded control ($\mathbb{D} = [0, +\infty)$ and $\mathbb{P} = [0, 1.5]$) cases. Parameters are given in Table 4.2 but with $\pi = 0$. Values are reported at $(W = 1, t = 0)$. Figure (a) shows the efficient frontiers with risk measure of standard deviation. Figure (b) shows the efficient frontiers with risk measure of quadratic variation.*

μ_Y	0.	ξ_1	0.2
σ_1	0.2	σ_{Y1}	0.05
σ_{Y0}	0.05	π	0.1
T	20 years	λ	0.25
$\mathbb{Q}$	$[0, 1.5]$	$\mathbb{D}$	$[0, +\infty)$

TABLE 6.4: *Parameters used in the pension plan examples.*

6.5.3 Wealth-to-income Ratio Case

In this section, we examine the wealth-to-income ratio case. Tables 6.5 and 6.6 show the numerical results for the bounded control case, using the parameters in Table 6.4. Table 6.5 reports the value of $V = E^{p^*}_{t=0,x}[X_T - \lambda \int_0^T (e^{r(T-t)} dx)^2]$, which is the viscosity solution of nonlinear HJB PDE (6.3.4). Table 6.6 reports the value of $E^{p^*}_{t=0,x}[X_T]$, which is the solution of the linear PDE (6.3.6). We also computed of the values of $E^{p^*}_{t=0,x}[X_T^2]$ (not shown in tables), which is the the solution of PDE (6.3.7). Given $E^{p^*}_{t=0,x}[X_T^2]$ and $E^{p^*}_{t=0,x}[X_T]$, the standard deviation can be easily computed, which is also reported in Table 6.6. The results show that the numerical solutions of V and $E^{p^*}_{t=0,x}[X_T]$ converge at a first order rate as mesh and timestep size tends to zero.

Efficient frontiers are shown in Figure 6.4, using parameters in Table 6.4 with $(X(t = 0) = 0.5; t = 0)$. Figure 6.4 (a) shows the results obtained by using the standard deviation

Nodes (X)	Timesteps	Nonlinear iterations	Normalized CPU Time	$V(x=0.5,t=0)$	Ratio
177	80	160	0.21	3.26653	
353	160	320	1.	3.26534	
705	320	640	3.86	3.26476	2.052
1409	640	1280	15.00	3.26447	2.000
2817	1280	2560	56.79	3.26433	2.071
5633	2560	5120	239.79	3.26426	2.000
11265	5120	10240	966.29	3.26422	2.003

TABLE 6.5: *Convergence study, mean quadratic variation, Bounded Control. Fully implicit timestepping is applied, using constant timesteps. Parameters are given in Table 6.4, with* $\lambda = 0.2873$. *Values of* $V = E^{p^*}_{t=0,x}[X_T - \lambda \int_0^T (e^{r(T-t)}dx)^2]$ *are reported at* $(X = 0.5, t = 0)$. *Ratio is the ratio of successive changes in the computed values for decreasing values of the discretization parameter* h. *CPU time is normalized. We take the CPU time used for the second test in this table as one unit of CPU time, which uses 353 nodes for* X *grid and 160 timesteps.*

Nodes (X)	Timesteps	$\text{Std}^{p^*}_{t=0,x}[X_T]$	$E^{p^*}_{t=0,x}[X_T]$	Ratio for $\text{Std}^{p^*}_{t=0,x}[X_T]$	Ratio for $E[X_T]$
177	80	1.39064	3.69771		
353	160	1.35723	3.69524		
705	320	1.34035	3.69403	1.979	2.041
1409	640	1.33187	3.69343	1.991	2.017
2817	1280	1.32762	3.69313	1.995	2.000
5633	2560	1.32549	3.69298	1.995	2.000
11265	5120	1.32443	3.69291	2.009	2.143

TABLE 6.6: *Convergence study, wealth-to-income ratio case, bounded control. Fully implicit timestepping is applied, using constant timesteps. Parameters are given in Table 6.4, with* $\lambda = 0.2873$. *Values of* $Std^{p^*}_{t=0,x}[X_T]$ *and* $E^{p^*}_{t=0,x}[X_T]$ *are reported at* $(X = 0.5, t = 0)$. *Ratio is the ratio of successive changes in the computed values for decreasing values of the discretization parameter* h.

as the risk measure, and Figure 6.4 (b) shows the results obtained by using the quadratic variation as the risk measure. Again, for both risk measures, the strategy given by allowing bankruptcy case is the most efficient, and the strategy given by the bounded control case is the least efficient. Note that, although the efficient frontiers in both figures pass through the same lowest point, unlike the wealth case, the minimum standard deviation/quadratic variation for all strategies are no longer zero. Since the plan holder's salary is stochastic (equation (2.2.5)) and the salary risk cannot be completely hedged away, there is no risk free strategy.

Figure 6.5 shows the values of the optimal control (the investment strategies) at different time t for a fixed $T = 20$. The parameters are given in Table 6.4, with $\lambda = 0.2873$. Under these inputs, if $X(t = 0) = 0.5$, $(\text{Std}^{p^*}_{t=0,x}[X_T], E^{p^*}_{t=0,x}[X_T]) = (1.32443, 3.69291)$ and

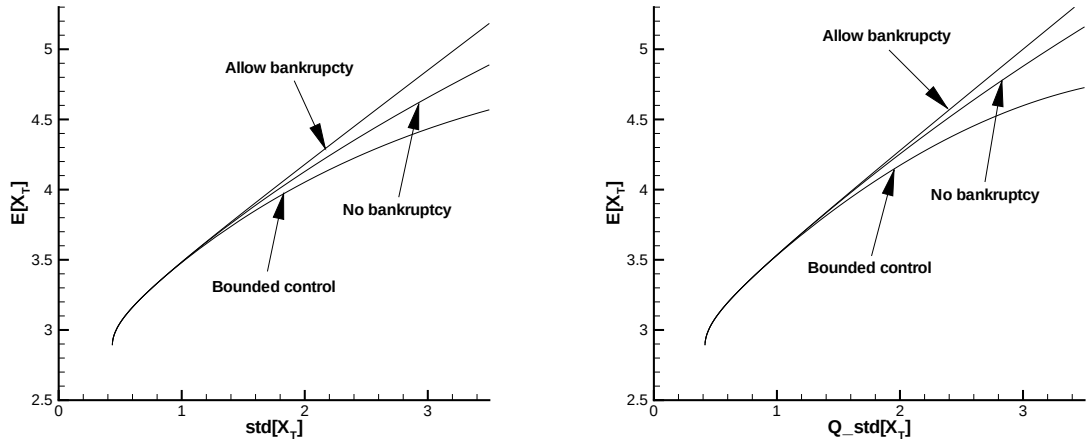

(a) Risk measure: std **(b) Risk measure:** Q_std

FIGURE 6.4: *Mean quadratic variation efficient frontiers (wealth-to-income ratio) for allowing bankruptcy ($\mathbb{D} = (-\infty, +\infty)$ and $\mathbb{P} = (-\infty, +\infty)$), no bankruptcy ($\mathbb{D} = [0, +\infty)$ and $\mathbb{P} = [0, +\infty)$) and bounded control ($\mathbb{D} = [0, +\infty)$ and $\mathbb{P} = [0, 1.5]$) cases. Parameters are given in Table 6.4. Values are reported at $(X = 0.5, t = 0)$. Figure (a) shows the efficient frontiers with risk measure of standard deviation. Figure (b) shows the efficient frontiers with risk measure of quadratic variation.*

$Q\_std^{p^*}_{t=0,w}[X_T] = 1.49213$ from the finite difference solution. Similar to the wealth case, we can see that the control p is a increasing function of time t for a fixed x.

6.6 Summary

In this chapter, we formulate the optimal investment policy for the mean quadratic variation problem as a nonlinear HJB PDE. We extend the numerical methods in [74, 73] (see also Chapters 4 and 5) to handle this case. Our method can handle various constraints on the control policy, and we can prove that our numerical scheme guarantees the convergence to viscosity solutions.

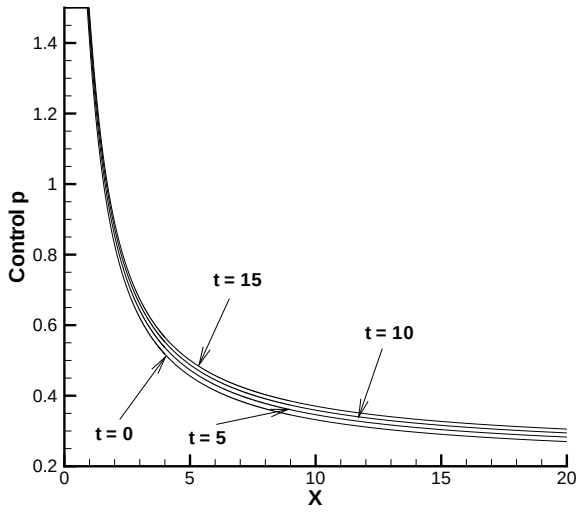

FIGURE 6.5: *Mean quadratic variation optimal control as a function of* (X, t)*, wealth-to-income ratio with bounded control. Parameters are given in Table 6.4, with* $\lambda = 0.2873$*. Under these inputs, if* $X(t = 0) = 0.5$*,* $(Std^{p^*}_{t=0,x}[X_T], E^{p^*}_{t=0,x}[X_T]) = (1.32443, 3.69291)$ *and* $Q\_std^{p^*}_{t=0,x}[X_T] = 1.49213$ *from the finite difference solution.*

Chapter 7

Comparison of Mean-variance Type Strategies

We have studied three mean variance type strategies in previous chapters, including the pre-commitment mean variance (Chapter 4), the time-consistent mean variance (Chapter 5) and the mean quadratic variation (Chapter 6). In this chapter, we compare the three strategies.

7.1 Wealth Case

We first study the wealth case for the three strategies. Figure 7.1 shows the efficient frontiers for the case of allowing bankruptcy for the three strategies. The analytic solution for the pre-commitment strategy is given in [42],

$$\begin{cases} Var^{p^*}_{t=0,w}[W_T] = \frac{e^{\xi_1^2 T}-1}{4\lambda^2} \\ E^{p^*}_{t=0,w}[W_T] = \hat{w}_0 e^{rT} + \pi\frac{e^{rT}-1}{r} + \sqrt{e^{\xi_1^2 T}-1}\text{Std}(W_T) \ , \end{cases} \tag{7.1.1}$$

and the optimal control p^* at any time $t \in [0,T]$ is

$$p^*(t,w) = -\frac{\xi_1}{\sigma_1 w}[w - (\hat{w}_0 e^{rt} + \frac{\pi}{r}(e^{rt}-1)) - \frac{e^{-r(T-t)+\xi_1^2 T}}{2\lambda}] \ . \tag{7.1.2}$$

Extending the results from [11], we can obtain the analytic solution for the time-consistent strategy,

$$\begin{cases} Var_{t=0,\hat{w}_0}[W_T] = \frac{\xi_1^2}{4\lambda^2}T \\ E_{t=0,\hat{w}_0}[W_T] = \hat{w}_0 e^{rT} + \pi\frac{e^{rT}-1}{r} + \xi\sqrt{T}\text{Std}(W_T) \ , \end{cases} \tag{7.1.3}$$

and the optimal control p at any time $t \in [0, T]$ is

$$p^*(t, w) = \frac{\xi_1}{2\lambda\sigma_1 w} e^{-r(T-t)} \ . \tag{7.1.4}$$

Figure 7.1 shows that the efficient frontiers for the time-consistent strategy and the mean quadratic variation strategy are the same. This result agrees with the result in [16]. Figure 7.1 also shows that the pre-commitment strategy is most efficient strategy. The three efficient frontiers are all straight lines, and pass the same point at $(\text{Std}(W_T), E(W_T)) = (0, \hat{w}_0 e^{rT} + \pi \frac{e^{rT}-1}{r})$. At that point, the plan holder simply invests all her wealth in the risk free bond, so the standard deviation is zero. The slope $(= \sqrt{e^{\xi_1^2 T} - 1})$ for the pre-commitment strategy is larger than the slope $(= \xi_1 \sqrt{T})$ for the time-consistent/mean quadratic variation strategy. But note that $\sqrt{e^{\xi_1^2 T} - 1} \to \xi_1 \sqrt{T}$ as $T \to 0$, so the three strategies are the same as $T \to 0$. This is easy to understand, since as $T \to 0$, finding the global optimal strategy (pre-commitment case) is the same as finding the local optimal strategy (time-consistent case).

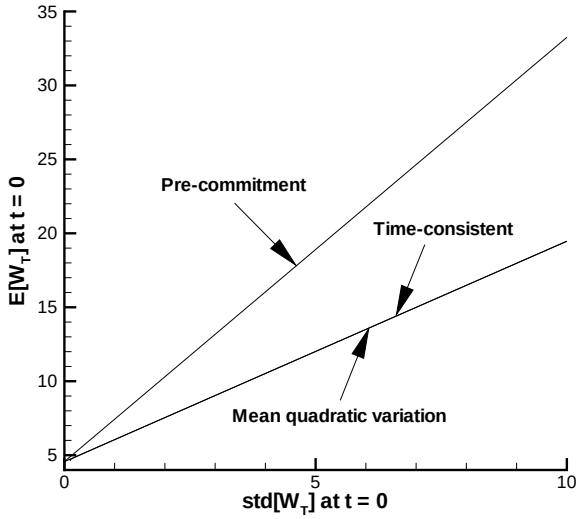

FIGURE 7.1: *Comparison of three strategies: wealth case, allowing bankruptcy. Parameters are given in Table 4.2.*

Figure 7.2 (a) shows a comparison for the three strategies for the no bankruptcy case, and Figure 7.2 (b) is for the bounded control case. We can see that the pre-commitment strategy is the most efficient strategy, and the mean quadratic variation strategy is more efficient than the time-consistent strategy. For the bounded control case, the three efficient frontiers have the same end points. The lower end corresponds to the most conservative strategy, i.e. the whole wealth is invested in the risk free bond at any time. The higher end corresponds to the most aggressive strategy, i.e. choose the control p to be the upper bound $p_{max}(= 1.5)$ at any time. Figure 7.1 and 7.2 show that the difference between the

efficient frontier solutions for the three strategies becomes smaller after adding constraints.

Since the efficient frontiers for the time-consistent strategy and the mean quadratic variation strategy are very close for the bounded control case, we want to make sure that the small difference is not due to computational error. In Table 7.1, we show a convergence study for both time-consistent strategy and mean quadratic variation strategy. The parameters are given in Table 4.2. We fix $\text{Std}^{p^*}_{t=0,w}[W_T] = 5$. Table 7.1 shows that the two strategies converge at a first order rate to different expected terminal wealth.

Refine	Time-consistent $E^{p^*}_{t=0,w}[W_T]$	Mean Quadratic Variation $E^{p^*}_{t=0,w}[W_T]$
0	10.3570	10.4337
1	10.4508	10.5537
2	10.5055	10.6035
3	10.5319	10.6273
4	10.5448	10.6390
5	10.5514	10.6447

TABLE 7.1: *Convergence study, wealth case, bounded control. Fully implicit timestepping is applied, using constant timesteps. The parameters are given in Table 4.2. We fix* $Std^{p^*}_{t=0,w}[W_T] = 5$ *for both time-consistent and mean quadratic variation strategies. Values of* $Std^{p^*}_{t=0,w}[W_T]$ *and* $E^{p^*}_{t=0,w}[W_T]$ *are reported at* $(W = 1, t = 0)$*. On each refinement, a new node is inserted between each two coarse grid nodes, and the timestep is divided by two. Initially (zero refinement), for time-consistent strategy, there are 41 nodes for the control grid, 182 nodes for the wealth grid, and 80 timesteps; for mean quadratic variation strategy, there are 177 nodes for the wealth grid, and 80 timesteps.*

It is not surprising that the pre-commitment strategy is the most efficient strategy, since the pre-commitment strategy is the strategy which optimizes the objective function at the initial time ($t = 0$). However, as discussed in previous chapters, in practice, there are many reasons to choose a time-consistent strategy or a mean quadratic variation strategy.

In Figure 7.3, we compare the control policies for the three strategies. The parameters are given in Table 4.2, and we use the wealth case with bounded control ($p \in [0, 1.5]$). We fix $\text{Std}^{p^*}_{t=0,x}[W_T] \simeq 8.17$ for this test. Figure 7.3 shows that the control policies given by the three strategies are significantly different. This is true even for the bounded control case, where the expected values for the three strategies are similar for fixed standard deviation (see Figure 7.2 (b)). Figure 7.3 (a) shows the control policies at $t = 0^+$.

We can interpret Figure 7.3 as follows. Suppose initially $W(t = 0) = 1$. If at the instant right after $t = 0$, the value for W jumps to $W(t = 0^+)$, Figure 7.3 (a) shows the control policies for all $W(t = 0^+)$. We can see that once the wealth W is large enough, the control policy for the pre-commitment strategy is to invest all wealth in the risk free bond. The reason for this is that for the pre-commitment strategy, there is an effective investment target given at $t = 0$, which depends on the value of λ. Once the target is reached, the investor will not take any more risk and switch all wealth into bonds. However, there is

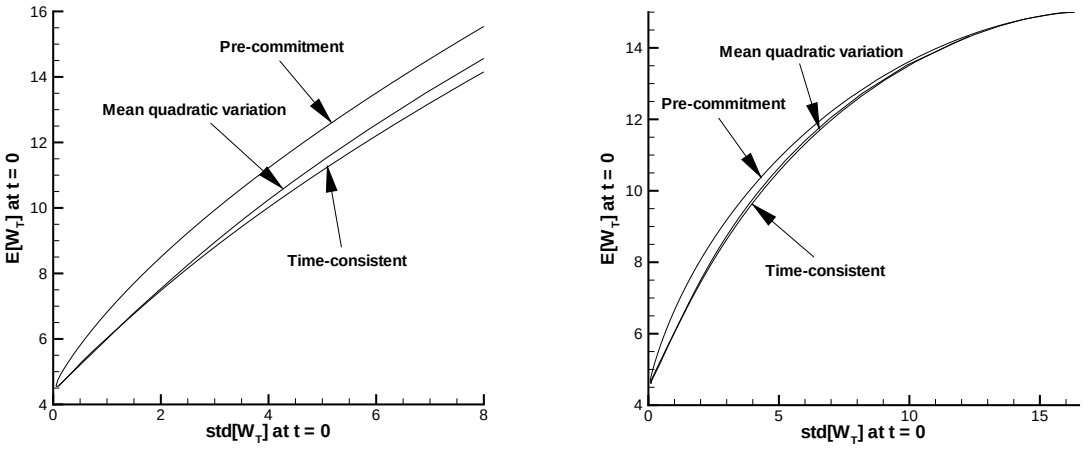

(a) No Bankruptcy **(b) Bounded Control**

FIGURE 7.2: *Comparison of three strategies: wealth case. (a): no bankruptcy case; (b): bounded control case. The parameters are given in Table 4.2.*

no similar effective target for the time-consistent or the mean quadratic variation cases, so the control never reaches zero (for finite W). Figure 7.3 (b) shows the mean of the control policies versus time $t \in [0, T]$. The mean of all policies are decreasing functions of time, i.e. all strategies are less risky (on average) as we approach maturity. We use Monte-Carlo simulations to obtain Figure 7.3 (b). Using the parameters in Table 4.2, we solve the stochastic optimal control problem (2.3.11) with the finite difference scheme introduced in Section 6.4, and store the optimal strategies for each $(W = w, t)$. We then carry out Monte-Carlo simulations based on the stored strategies with $W(t = 0) = 1$ initially. At each time step, we can obtain the control p for each simulation. We then can obtain the mean of p for each time step.

7.2 Wealth-to-income Ratio Case

Figure 7.4 and 7.5 shows a comparison for the three strategies of the wealth-to-income ratio case. Figure 7.4 is for bankruptcy case, Figure 7.5 (a) is for no bankruptcy case, and Figure 7.5 (b) is for the bounded control case. Similar to the allowing bankruptcy case, the pre-commitment strategy is the most efficient strategy for all cases. Note that unlike the wealth case, the efficient frontiers for the three strategies do not have the common lower end point. As discussed in Section 6.5.3, no risk free strategy exists in this case because of the salary risk. Further more, since the salary is correlated with the stock index ($\sigma_{Y_1} \neq 0$), in order to (partially) hedge the salary risk, the most conservative policy is not to invest all money in the bond ($p = 0$) all the time. The three strategies have different views of risk, hence their most conservative investment policies would be different. Therefore, their minimum risks (in terms of standard deviation) are different. Also note that, the efficient

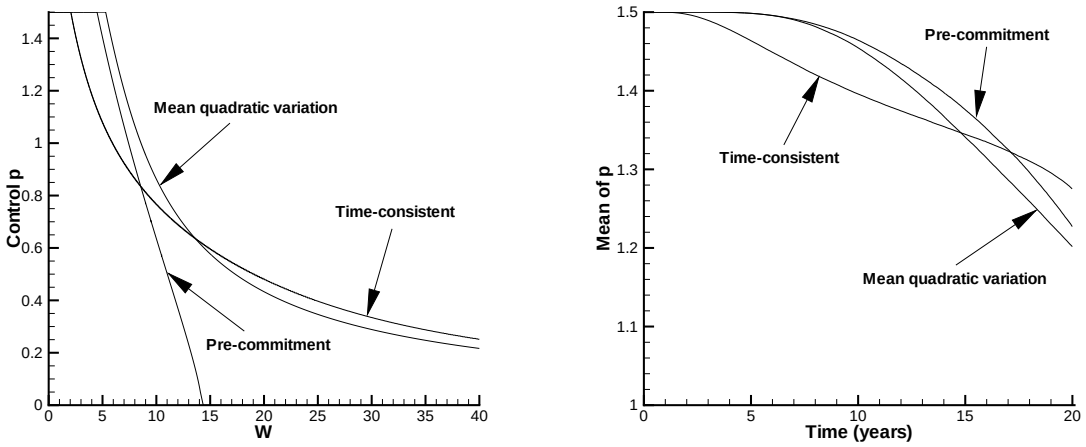

(a) **(b)**

FIGURE 7.3: *Comparison of the control policies: wealth case with bounded control ($p \in [0, 1.5]$). Parameters are given in Table 4.2. We fix $std^{p^*}_{t=0,w}[W_T] \simeq 8.17$ for this test. More precisely, from our finite difference solutions, $(Std^{p^*}_{t=0,w}[W_T], E^{p^*}_{t=0,w}[W_T]) = (8.17479, 12.7177)$ for the mean quadratic variation strategy; $(Std^{p^*}_{t=0,w}[W_T], E^{p^*}_{t=0,w}[W_T]) = (8.17494, 12.6612)$ for the time-consistent strategy; and $(Std^{p^*}_{t=0,w}[W_T], E^{p^*}_{t=0,w}[W_T]) = (8.17453, 12.8326)$ for the pre-commitment strategy. Figure (a) shows the control policies at $t = 0^+$; Figure (b) shows the mean of the control policies versus time $t \in [0, T]$.*

frontiers given by time-consistent strategy and the mean quadratic variation strategy are very close, almost on top of each other.

Similar to the wealth case, Figure 7.6 shows a comparison of the control policies for the three strategies. Parameters are given in Table 6.4, and we use the wealth case with bounded control ($p \in [0, 1.5]$). We fix $\text{Std}^{p^*}_{t=0,x}[X_T] \simeq 3.24$ for this test. The comparison shows that although the three strategies have a similar pair of expected value and standard deviation, the control policies are significantly different.

7.3 Summary

In this chapter, we study the three mean variance type strategies: pre-commitment mean variance, time-consistent mean variance, and mean quadratic variation. For the allowing bankruptcy case, analytic solutions exist for all strategies. Furthermore, in this case, the time-consistent strategy and the mean quadratic variation strategy have the same solution. However, when additional constraints are applied to the control policy, analytic solutions do not exist for all strategies, and the solutions for various strategies are different. After realistic constraints are applied, the efficient frontiers for all three strategies are very

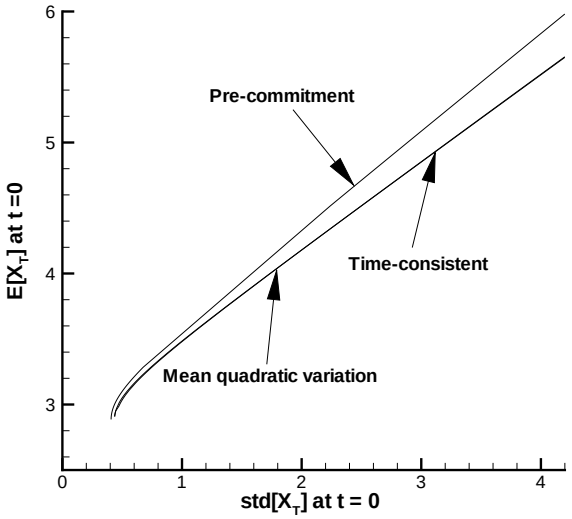

FIGURE 7.4: *Comparison of three strategies: wealth-to-income ratio case, allowing bankruptcy. Parameters are given in Table 6.4.*

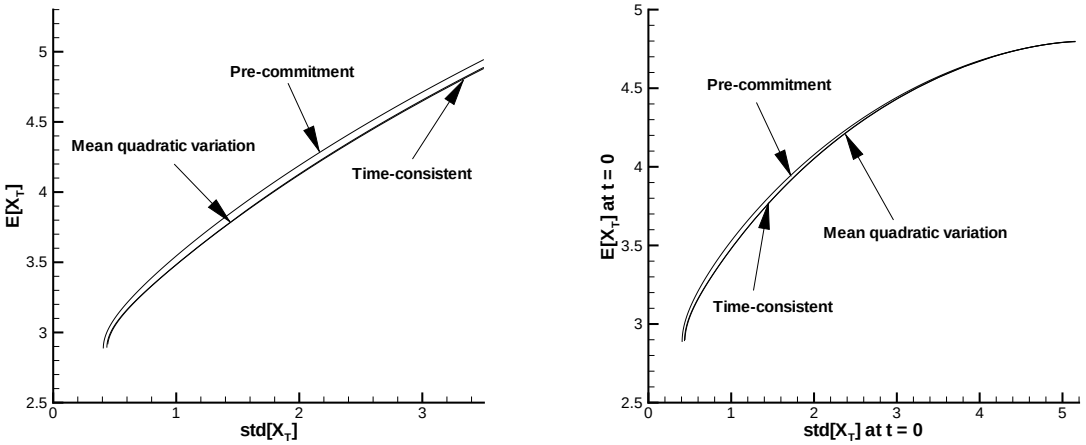

(a) No Bankruptcy **(b) Bounded Control**

FIGURE 7.5: *Comparison of the control policies: wealth-to-income ratio case. (a): no bankruptcy case; (b): bounded control case. Parameters are given in Table 6.4.*

similar. However, the investment policies are quite different. This suggests that the choice among various strategies cannot be made by only examining the efficient frontier, but rather should be based on the qualitative behavior of the optimal policies.

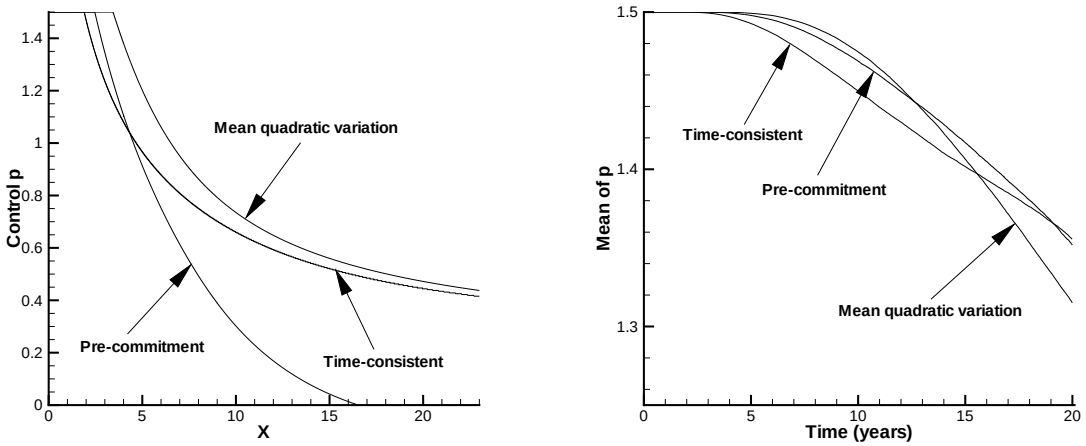

(a) **(b)**

FIGURE 7.6: *Comparison of the control policies: wealth-to-income ratio case with bounded control ($p \in [0, 1.5]$). Parameters are given in Table 6.4. We fix $std^{p^*}_{t=0,x}[X_T] \simeq 3.24$ for this test. More precisely, from our finite difference solutions, $(Std^{p^*}_{t=0,x}[X_T], E^{p^*}_{t=0,x}[X_T]) = (3.24214, 4.50255)$ for the mean quadratic variation strategy; $(Std^{p^*}_{t=0,x}[X_T], E^{p^*}_{t=0,x}[X_T]) = (3.24348, 4.50168)$ for the time-consistent strategy; and $(Std^{p^*}_{t=0,x}[X_T], E^{p^*}_{t=0,x}[X_T]) = (3.24165, 4.50984)$ for the pre-commitment strategy. Figure (a) shows the control policies at $t = 0^+$; Figure (b) shows the mean of the control policies versus time $t \in [0, T]$.*

Chapter 8

Conclusion

Optimal stochastic control problems in finance can usually be formulated in the form of nonlinear HJB PDEs. In general, classical solutions do not exist for these PDEs, and we seek to find the viscosity solutions of the HJB equations.

In this thesis, we first develop a general framework to solve nonlinear HJB PDEs in finance. Our numerical scheme is a fully implicit finite difference scheme, which has the following properties:

- The scheme uses central differencing as much as possible, so that use of locally second order method is maximized.
- There are no timestep limitations due to stability considerations.
- The scheme guarantees the convergence to viscosity solution (assuming the PDEs satisfy a strong comparison result).
- There are no restrictions on the underlying stochastic process, e.g. geometric Brownian motion, jump diffusion, or regime switching can be easily implemented.
- Our method can well handle both bang-bang type of control and non bang-bang type of control.
- The scheme can be easily extended to include features as needed, for example, uncertain volatility, bid-ask spread, transaction costs and so on.

We demonstrate the numerical scheme on two examples: passport option pricing, and an optimal dynamic asset allocation problem for a defined contribution pension plan.

We then use the mean variance approach to solve the optimal dynamic asset allocation problem. Although utility function approach is commonly used for this problem, this has at least two disadvantages. First, it is not clear how to decide which utility function an individual or an institution would prefer. Second, the tradeoff between the risk and the expected return is implicitly contained in the utility function, so the optimal investment decision lacks intuitive interpretation. In contrast, the results given by the mean variance

approach can be easily interpreted in terms of an efficient frontier, in which the tradeoff between the risk and the expected return can be clearly demonstrated, so that an investor can intuitively choose her expected return and risk level. We study three mean variance type strategies: pre-commitment mean variance, time-consistent mean variance, and mean quadratic variation. The key points for these mean variance type strategies are as follows:

- For the pre-commitment strategy, we first embed the original optimization problem into a class of auxiliary stochastic LQ problems, so that dynamic programming can be applied. We then use our fully implicit scheme to solve this problem.
- For the time-consistent strategy, our method is based on the piecewise constant policy technique. Since the time-consistent problem can be formulated as a system of HJB differential algebraic equations, this falls outside present day viscosity solution theory. Nevertheless, our technique does converge to analytic solutions where available.
- For the mean quadratic variation strategy, we can directly apply our fully implicit scheme with a maximum use of central differencing for solving the problem numerically.
- For each strategy, by solving the HJB PDE and related linear PDEs, we develop a numerical method for constructing the mean variance efficient frontier (in continuous time). Any type of constraint can be applied to the investment policy.

Finally, we make a comparison of the three mean variance type strategies.

8.1 Future Work

Some directions for future research are:

- It is desirable to have a numerical method which guarantees convergence for the time-consistent strategy. A major problem here is that, formulated as a system of nonlinear DAEs, the scheme falls outside the current scope of viscosity solution theory.
- It would be a challenge to develop a robust and efficient numerical scheme for optimal stochastic control problems with multi-factor stochastic processes.
- There are also interesting economic issues involved concerning the appropriate choice of pre-commitment, time-consistent, or mean quadratic variation policies. This thesis has focused on developing robust numerical methods for solving for the optimal strategies. We leave the issue of the choice of the appropriate objective function to economists and finance practitioners.

Appendix A

Discrete Equation Coefficients

Let Q_i^n denote the vector of optimal controls at node i, time level n and set

$$a_i^{n+1} = a(S_i, \tau^n, Q_i^n),\ b_i^{n+1} = b(S_i, \tau^n, Q_i^n),\ c_i^{n+1} = c(S_i, \tau^n, Q_i^n)\ . \tag{A.1}$$

Then, we can use central, forward or backward differencing at any node.

Central Differencing:

$$\begin{aligned} \alpha_{i,central}^n &= \left[\frac{2a_i^n}{(S_i - S_{i-1})(S_{i+1} - S_{i-1})} - \frac{b_i^n}{S_{i+1} - S_{i-1}}\right] \\ \beta_{i,central}^n &= \left[\frac{2a_i^n}{(S_{i+1} - S_i)(S_{i+1} - S_{i-1})} + \frac{b_i^n}{S_{i+1} - S_{i-1}}\right]\ . \end{aligned} \tag{A.2}$$

Forward/backward Differencing: $(b_i^n > 0 /\ b_i^n < 0)$

$$\begin{aligned} \alpha_{i,forward/backward}^n &= \left[\frac{2a_i^n}{(S_i - S_{i-1})(S_{i+1} - S_{i-1})} + \max(0, \frac{-b_i^n}{S_i - S_{i-1}})\right] \\ \beta_{i,forward/backward}^n &= \left[\frac{2a_i^n}{(S_{i+1} - S_i)(S_{i+1} - S_{i-1})} + \max(0, \frac{b_i^n}{S_{i+1} - S_i})\right]\ . \end{aligned} \tag{A.3}$$

Appendix B

Proof of Theorem 4.2

In this section, we show that problem (4.2.6) is equivalent to problem (4.2.1).

It is well-known that the points on the variance minimizing frontier can be characterized as solutions to the problem

$$\begin{aligned} &\min Var^{p}_{t=0,w}[W_T] = E^{p}_{t=0,w}[(W_T)^2] - d^2 \\ &\text{subject to } \begin{cases} E^{p}_{t=0,w}[W_T] = d \\ p \in \mathbb{P} \end{cases} . \end{aligned} \tag{B.1}$$

Problem (B.1) is a convex optimization problem, and hence has a unique solution. We can eliminate the constraint in problem (B.1) by using a Lagrange multiplier [51, 15, 77, 4, 37], which we denote by γ. Problem (B.1) can then be posed as [17]

$$\sup_{\gamma} \inf_{p(t,w)\in\mathbb{P}} E^{p}_{t=0,w}[(W_T)^2 - d^2 - \gamma(E^{p}_{t=0,w}[W_T] - d)] . \tag{B.2}$$

For fixed γ, d, this is equivalent to finding the control $p(t,w)$ which solves

$$\inf_{p(t,w)\in\mathbb{P}} E^{p}_{t=0,w}[(W_T - \frac{\gamma}{2})^2] , \tag{B.3}$$

which is the problem (4.2.6). Note that if for some fixed γ, $p^*(t,w)$ is the optimal control of problem (B.3), then $p^*(t,w)$ is also the optimal control of problem (B.1) with $d = E^{p}_{t=0,w}[W_T]$ [51, 15]. Conversely, if there exists a solution to problem (B.1), with $E^{p}_{t=0,w}[W_T] = d$, then there exists a γ which solves problem (B.3) with control $p^*(t,w)$. Hence, problem (B.1) and problem (B.3) are equivalent (i.e. they have the same optimal control).

Since it is well-known that problem (4.2.1) is equivalent to problem (B.1) by choosing the proper value for λ, problem (4.2.1) and problem (B.3) are also equivalent.

Remark B.1 (Efficient Frontier)**.** *The efficient frontier, as normally defined, is a portion of the variance minimizing frontier. That is, given a point* $(E_{p^*}[W_T], \sqrt{Var_{p^*}[W_T]})$ *on the efficient frontier, corresponding to control* p^**, then there exists no other control* $\bar{p}^*$ *such*

that $Var_{\bar{p}^*}[W_T] = Var_{p^*}[W_T]$ *with* $E_{\bar{p}^*}[W_T] > E_{p^*}[W_T]$. *Hence the points on the efficient frontier are Pareto optimal. From a computational perspective, once a set of points on the variance minimizing frontier are determined, then the efficient frontier can be constructed by a simple sorting operation.*

Appendix C

Numerical Test for $\lambda(w)$

In Remark 5.3, we mentioned that [16] suggests using a function $\lambda = \lambda(w)$ for the risk aversion coefficient instead of a constant λ. One simple choice is

$$\lambda(w) = \frac{\theta}{w} \ , \tag{C.1}$$

where θ is a given constant (as suggested in [16]). The efficient frontier can be traced out by varying θ.

For this choice of $\lambda(w)$, the efficient frontiers are shown in Figure C.1, with parameters given in Table 4.2. The top three curves in Figure C.1 are the same efficient frontiers in Figure 5.1 (from the solutions by using constant λ's), and the lower two efficient frontiers are from the solutions by using $\lambda(w) = \frac{\theta}{w}$. Note that we do not include the allowing bankruptcy case when using $\lambda(w) = \frac{\theta}{w}$, since $\frac{\theta}{w}$ is meaningless for a risk aversion coefficient when $w < 0$. Even if we use $\lambda(w) = \frac{\theta}{|w|}$, this does not have much economic justification.

Figure C.1 shows that it is less efficient to use $\lambda(w) = \frac{\theta}{w}$ compared to constant λ as the risk aversion coefficient. Hence, $\lambda(w) = \frac{\theta}{w}$ is not a good choice for this case. Moreover, when we use $\lambda(w) = \frac{\theta}{w}$, the bounded control case is more efficient than the no bankruptcy case. This seems absurd. However, recall the discussion in Remark 2.3, the solution of problem (5.2.2) may not be the efficient frontier solution as normally defined. Therefore, there is no guarantee for which case should be more efficient than the others.

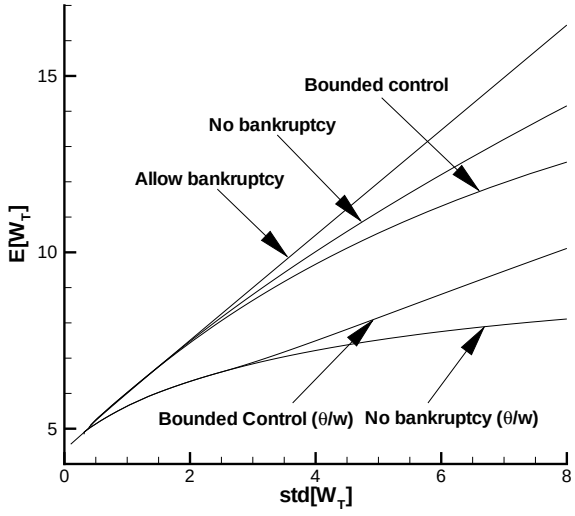

FIGURE C.1: *Time-consistent efficient frontiers (wealth case) for allowing bankruptcy ($\mathbb{D} = (-\infty, +\infty)$ and $\mathbb{Q} = (-\infty, +\infty)$), no bankruptcy ($\mathbb{D} = [0, +\infty)$ and $\mathbb{Q} = [0, +\infty)$) and bounded control ($\mathbb{D} = [0, +\infty)$ and $\mathbb{Q} = [0, 1.5]$) cases. Parameters are given in Table 4.2. Values are reported at $(W = 1, t = 0)$. The top three curves are the same efficient frontiers in Figure 5.1 (from the solutions by using constant λ's), and the lower two efficient frontiers are from the solutions by using $\lambda(w) = \frac{\theta}{w}$.*

References

[1] A. L. Amadori. Nonlinear integro-differential evolution problems arising in option pricing: A viscosity solution approach. *Journal of Differential and Integral Equations*, 16:787–811, 2003. 1

[2] L. Andersen, J. Andreasen, and R. Brotherton-Ratcliffe. The passport option. *Journal of Computational Finance*, 1:15–36, 1998. 1, 7, 16, 24, 25, 28, 29, 34

[3] M. Avellaneda, A. Levy, and A. Parás. Pricing and hedging derivative securities in markets with uncertain volatilities. *Applied Mathematical Finance*, 2:73–88, 1995. 1

[4] L. Bai and H. Zhang. Dynamic mean-variance problem with constrained risk control for the insurers. *Mathematical Methods for Operations Research*, 68:181–205, 2008. 11, 115

[5] G. Barles. Convergence of numerical schemes for degenerate parabolic equations arising in finance. In L. C. G. Rogers and D. Talay, editors, *Numerical Methods in Finance*, pages 1–21, Cambridge University Press, Cambridge, 1997. 1, 15, 20, 95

[6] G. Barles and J. Burdeau. The Dirichlet problem for semilinear second-order degenerate elliptic equations and applications to stochastic exit time control problems. *Communications in Partial Differential Equations*, 20:129–178, 1995. 20

[7] G. Barles, C. Daher, and M. Romano. Convergence of numerical scheme for parabolic equations arising in finance theory. *Mathematical Models and Methods in Applied Sciences*, 5:125–143, 1995. 17, 44, 77

[8] G. Barles and E. Jakobsen. Error bounds for monotone approximation schemes for parabolic Hamilton-Jacobi-Bellman equations. *Mathematics of Computation*, 76:1861–1893, 2007. 1, 2, 15, 20, 21, 37

[9] G. Barles and E. Rouy. A strong comparison result for the Bellman equation arising in stochastic exit time control problems and its applications. *Communications in Partial Differential Equations*, 23:1995–2033, 1998. 17, 20, 49, 50

[10] G. Barles and P. Souganidis. Convergence of approximation schemes for fully nonlinear equations. *Asymptotic Analysis*, 4:271–283, 1991. 1, 15, 20

[11] S. Basak and G. Chabakauri. Dynamic mean-variance asset allocation. *Review of Financial Studies*, forthcoming, 2009. 10, 11, 12, 67, 68, 77, 103

[12] E. Bayraktar and V. Young. Pricing options in incomplete equity markets via the instantaneous Sharpe Ratio. *Annals of Finance*, 4(4):399–429, 2008. 1

[13] F. E. Benth, K. Karlsen, and K. Reikvam. Optimal portfolio management rules in a non-Gaussian market with durability and intertemporal substitution. *Finance and Stochastics*, 5:447–467, 2001. 1

[14] Y. Bergman. Option pricing with differential interest rates. *Review of Financial Studies*, 8:475–500, 1995. 1

[15] T. Bielecki, H. Jin, S. Pliska, and X. Zhou. Continuous time mean-variance portfolio selection with bankruptcy prohibition. *Mathematical Finance*, 15:213–244, 2005. 8, 9, 11, 39, 40, 46, 56, 57, 58, 76, 115

[16] T. Bjork and A. Murgoci. A theory of time inconsistent optimal control. AMAMEF 3rd General Conference, Pitesti, 2008. 11, 12, 67, 68, 77, 86, 91, 93, 96, 104, 117

[17] S. Boyd and L. Vendenberghe. *Convex Optimization*, Cambridge University Press, 2008. 115

[18] P. Brugiere. Optimal portfolio and optimal trading in a dynamic continuous time framework. 6'th AFIR Colloquium, Nurenberg, Germany, 1996. 12, 89

[19] A. Budhiraja and K. Ross. Convergent numerical scheme for singular stochastic control with state constraints in a portfolio selection problem. SIAM Journal on Control and Optimization, 45(6):2169-2206, 2007. 1

[20] J. Cai and H. Yang. Ruin in the perturbed compound Poisson risk process under interest force. *Advances in Applied Probability*, 37(3):819–835, 2005. 1

[21] A. Cairns, D. Blake, and K. Dowd. Stochastic lifestyling: optimal dynamic asset allocation for defined contribution pension plans. *Journal of Economic Dynamics and Control*, 30:843–877, 2006. 7, 16, 30, 31, 32, 34, 39, 40

[22] R. Carmona and M. Ludkovski. Optimal switching and application to tolling contracts. Preprint, Working paper, 2005. 1

[23] J. P. Chancellor, B. Oksendal, and A. Sulem. Combined stochastic control and optimal stopping and application to numerical approximation of combined stochastic and impulse control. *Stochastic Financial Mathematics*, 237:149–173, 2002. 1

[24] S. Chaumont. A strong comparison result for viscosity solutions to Hamilton-Jacobi-Bellman equations with Dirichlet conditions on a non-smooth boundary. Working paper, Institute Elie Cartan, Université Nancy I, 2004. 17, 20, 49

[25] T. Chellathurai and T. Draviam. Dynamic portfolio selection with fixed and/or proportional transaction costs using non-singular stochastic optimal control theory. *Journal of Economic Dynamics and Control*, 31:2168–2195, 2007. 39

[26] A.H.Y Chen, F.C. Jen, and S. Zionts. The optimal portfolio revision policy. *Journal of Business* 44:51–61, 1971. 3

[27] Z. Chen and P. A. Forsyth. A semi-Lagrangian approach for natural gas storage valuation and optimal operation. *SIAM Journal on Scientific Computing*, 30:339–368, 2007. 1

[28] Chiu, M. and D. Li. Asset and liability management under a continuous time mean variance optimization framework. *Insurance: Mathematics and Economics*, 39:330–355, 2006. 10, 39

[29] M. G. Crandall, H. Ishii, and P. L. Lions. User's guide to viscosity solutions of second order partial differential equations. *Bulletin of the American Mathematical Society*, 27:1–67, 1992. 1, 15, 20, 95

[30] A. Damgaard. Computation of reservation prices of options with proportional transaction costs. *Journal of Economic Dynamics and Control*, 30:415–444, 2006. 39

[31] S. Deng and S. S. Oren. Incorporating operational characteristics and start-up costs in option-based valuation of power generation capacity. *Probability in the Engineering and Informational Sciences*, 17:151181, 2003. 1

[32] Duffie, D. and H. Richardson. Mean variance hedging in continuous time. *Annals of Applied Probability*, 1:1–15, 1991. 9

[33] B. Dumas and E. Liucinao An exact solution to a dynamic portfolio choice problem under transaction costs. *Journal of Finance* 46:577-595, 1991. 3

[34] C. Barrera-Esteve, F. Bergeret, C. Dossal, E. Gobet, A. Meziou, R. Munos, and D. Reboul-Salze. Numerical methods for the pricing of swing options: a stochastic control approach. Methodology and Computing in Applied Probability, 8(4):517-540, 2006. 1

[35] P. A. Forsyth, J.S. Kennedy, S.T. Tse, and H. Windcliff. Optimal trade execution: a mean quadratic variation approach. Working paper, submitted to *Quantitative Finance*, 2009. 12, 89

[36] P. Forsyth and G. Labahn. Numerical methods for controlled Hamilton-Jacobi-Bellman pdes in finance. *Journal of Computational Finance*, 11:1–44, 2008. 1, 2, 15, 20, 23

[37] C. Fu, A. Lari-Lavassani, and X. Li. Dynamic mean-variance portfolio selection with borrowing constraint. *European Journal of Operational Research*, 200(1):312–319, 2010. 11, 115

[38] R. Gerrard, S. Haberman, and E. Vigna. Optimal investment choices post retirement in a defined contribution pension scheme. *Insurance: Mathematics and Economics*, 35:321–342, 2004. 10

[39] R.R. Grauer and N.H Hakansson. On the use of mean-variance and quadratic approximations in implementing dynamic investment strategies: a comparison of returns and investment policies. *Management Science*, 39:856-871, 1993. 3

[40] N.H. Hakansson. Multi-period mean-variance analysis: toward a general theory of portfolio choice. *Journal of Finance* 26:857-884, 1971. 3

[41] H. He and H. Mamaysky. Dynamic trading with price impact. *Journal of Economic Dynamics and Control*, 29:891-930, 2005. 3, 8

[42] B. Hojgaard and E. Vigna. Mean variance portfolio selection and efficient frontier for defined contribution pension schemes. Working Paper, Aalborg University, 2007. 10, 40, 45, 103

[43] T. Hyer, A. Lipton-Lifschitz, and D. Pugachevsky. Passport to success. *Risk Magazine*, 10(9):127–131, 1997. 25

[44] Kahl, C., M. Gunther, and T. Rossberg. Structure preserving stochastic integration schemes in interest rate derivative modelling. *Applied Numerical Mathematics*, 58:284–295, 2008. 59

[45] N.V. Krylov. Approximating value functions for controlled degenerate diffusion processes by using piece-wise constant policies. *Electronic Journal of Probability*, 4(2):1–19, 1999. 4, 70, 71, 72, 86

[46] H. Kushner and P. Dupuis. Numerical Methods for Stochastic Control Problems in Continuous Time. *Springer-Verlag*, New York. 1991. 1, 2, 15, 23

[47] M. Leippold, F. Trojani, and P. Vanini. A geometric approach to multiperiod mean variance optimization of assets and liabilities. *Journal of Economic Dynamics and Control*, 28:1079–1113, 2004. 9

[48] H. E. Leland. Option pricing and replication with transaction costs. *Journal of Finance*, 40:1283–1301, 1985. 1

[49] D. Li and W.-L. Ng. Optimal dynamic portfolio selection: Multiperiod mean variance formulation. *Mathematical Finance*, 10:387–406, 2000. 3, 4, 8, 9, 11, 39, 40, 41

[50] X. Li and X. Y. Zhou. Continuous time mean variance efficiency and the 80% rule. *Annals of Applied Probability*, 16:1751–1763, 2006. 8, 11, 40, 57, 58, 65

[51] X. Li, X. Y. Zhou, and E. B. Lim. Dynamic mean variance portfolio selection with no-shorting constraints. *SIAM Journal on Control and Optimization*, 40:1540–1555, 2002. 8, 39, 40, 115

[52] J. Lorenz and R. Almgren. Adaptive arrival price. in Algorithmic Trading III: Precision, Control, Execution, Brian R. Bruce, editor, Institutional Investor Journals, 2007. 10

[53] H. Markowitz. Portfolio Selection. *Journal of Finance* 7(1):77-91, 1952. 3

[54] H. Markowitz. Portfolio Selection: Efficient Diversification of Investment. Wiley, New York, 1959. 3

[55] R. Merton. Optimum consumption and portfolio rules in a continuous time model. *Journal of Economics Theory*, 3:373–413, 1971. 8

[56] M. Milevsky, S. Promislow, and V. Young. Financial valuation of mortality risk via the instantaneous Sharpe ratio. *Journal of Economic Dynamics and Control*, 33(3):676–691, 2009. 1

[57] J. Mossin. Optimal multiperiod portfolio policies. *Journal of Business* 41:215-229, 1968. 3

[58] M. Mnif and A. Sulem. Optimal risk control under excess of loss reinsurance. *French National Institute for Research in Computer Science and Control*, 2001. 1

[59] C. Munk. Optimal consumption/investment policies with undiversifiable income risk and liquidity constraints. *Journal of Economic Dynamics and Control*, 24:1315–1343, 2000. 39

[60] K. Muthuraman. A computational scheme for optimal investment - consumption with proportional transaction costs. *Journal of Economic Dynamics and Control*, 31:1132–1159, 2007. 39

[61] P. Nguyen and R. Portrai. Dynamic asset allocation with mean variance preferences and a solvency constraint. *Journal of Economic Dynamics and Control*, 26:11–32, 2002. 9, 39

[62] B. Oksendal and A. Sulem. Applied Stochastic Control of Jump Diffusions. *Springer Verlag*, Berlin, 2005. 2, 15

[63] H. Pham. On some recent aspects of stochastic control and their applications. *Probability Surveys* 2:506–549, 2005. 1

[64] D. Pooley, P. Forsyth, and K. Vetzal. Numerical convergence properties of option pricing PDEs with uncertain volatility. *IMA Journal of Numerical Analysis*, 23:241–267, 2003. 1, 20, 23

[65] D. M. Pooley. Numerical Methods for Nonlinear Equations in Option Pricing. PhD thesis, School of Computer Science, University of Waterloo, 2003. 2, 23, 24, 28, 29, 34

[66] P.A. Samuelson. Lifetime portfolio selection by dynamic stochastic programming. *Review of Economics and Statistics* 51:239-246, 1969. 3

[67] H. Schmidli. On minimizing the ruin probability by investment and reinsurance. *Annals of Applied Probability*, 12:890–907, 2002. 1

[68] S. Shreve and J. Vecer. Options on a traded account: vacation calls, vacation puts, and passport options. *Finance and Stochastics*, 4:255–274, 2000. 1, 7

[69] M. Thompson, M. Davison, and H. Rasmussen. Natural gas storage valuation and optimization: a real options application. *Naval Research Logistics*, 56(30):226-238, 2009. 1

[70] J. Topper. A finite element implementation of passport options. MSc. Thesis, Oxford, 2003. 24

[71] V. Ly Vath, M. Mnif, and H. Pham. A model of optimal portfolio selection under liquidity risk and price impact. *Finance and Stochastics*, 11:5190, 2007. 3, 8

[72] J. Wang and P. Forsyth. Maximal use of central differencing for Hamilton-Jacobi-Bellman PDEs in finance. *SIAM Journal on Numerical Analysis*, 46:1580–1601, 2008. 1, 60

[73] J. Wang and P.A. Forsyth. Continuous time mean variance asset allocation: a time-consistent strategy. Working paper, submitted to *European Journal of Operational Research*, 2009. 11, 67, 98, 101

[74] J. Wang and P.A. Forsyth. Numerical solution of the Hamilton-Jacobi-Bellman formulation for continuous time mean variance asset allocation. *Journal of Economic Dynamics and Control*, 34:207–230, 2010. 77, 83, 85, 98, 101

[75] Z. Wang, J. Xia, and L. Zhang. Optimal investment for the insurer: The martingale approach. *Insurance: Mathematics and Economics*, 40:322–334, 2007. 10, 39

[76] H. Windcliff, J. Wang, P. Forsyth, and K. Vetzal. Hedging with a correlated asset: Solution of a nonlinear pricing PDE. *Journal of Computational and Applied Mathematics*, 200:86–115, 2007. 1

[77] Xia, J. Mean-variance portfolio choice: Quadratic partial hedging. *Mathematical Finance*, 15:533–538, 2005. 115

[78] X. Zhou and D. Li. Continuous time mean variance portfolio selection: A stochastic LQ framework. *Applied Mathematics and Optimization*, 42:19–33, 2000. 3, 4, 8, 9, 11, 39, 40, 41, 57, 58

[79] Y.L. Zhu and J. Li. Multi-factor financial derivatives on finite domains. *Communications in Mathematical Sciences*, 1:343–359, 2003. 17